


2013

Adsorption of Hydrogen Sulfide on Fine Rubber Particle Media (FRPM)

Ning Wang

Iowa State University

Follow this and additional works at: <https://lib.dr.iastate.edu/etd>

 Part of the [Civil Engineering Commons](#), and the [Environmental Engineering Commons](#)

Recommended Citation

Wang, Ning, "Adsorption of Hydrogen Sulfide on Fine Rubber Particle Media (FRPM)" (2013). *Graduate Theses and Dissertations*. 13110.

<https://lib.dr.iastate.edu/etd/13110>

This Dissertation is brought to you for free and open access by the Iowa State University Capstones, Theses and Dissertations at Iowa State University Digital Repository. It has been accepted for inclusion in Graduate Theses and Dissertations by an authorized administrator of Iowa State University Digital Repository. For more information, please contact digirep@iastate.edu.

**Adsorption of hydrogen sulfide on fine rubber
particle media (FRPM)**

by

Ning Wang

A thesis submitted to the graduate faculty
in partial fulfillment of the requirements for the degree of
DOCTOR OF PHILOSOPHY

Major: Civil Engineering (Environmental Engineering)

Program of Study Committee:
Timothy G. Ellis, Major Professor
Shihwu Sung
Hans van Leeuwen
Young-Jin Lee
Andreja Bakac

Iowa State University
Ames, Iowa
2013

Copyright ©Ning Wang, 2013. All rights reserved.

TABLE OF CONTENTS

LIST OF FIGURES	iv
LIST OF TABLES	vi
EXECUTIVE SUMMARY	viii
CHAPTER 1 GENERAL INTRODUCTION.....	1
CHAPTER 2 WASTE TIRE MEDIA PRODUCTS ADSORBING BIOGAS HYDROGEN SULFIDE AND THE CHARACTERISTICS OF THE RUBBER SAMPLES	6
Introduction	6
Materials and Methods	8
Results and Discussion	14
Conclusions	30
References	32
CHAPTER 3 THE MECHANISM OF HYDROGEN SULFIDE ADSORPTION ON FINE RUBBER PARTICLE MEDIA (FRPM).....	35
Introduction	35
Methods and Materials	38
Result and Discussion	41
Conclusions	54
Reference	55
CHAPTER 4 THE IMPROVEMENT OF HYDROGEN SULFIDE ADSORPTION ON FINE RUBBER PARTICLE MEDIA (FRPM).....	58
Introduction	58
Materials and Methods	59
Results and Discussion	63
Conclusions	79
References	80

CHAPTER 5 REGENERATION OF SPEND FINE RUBBER	
PARTICLE MEDIA (FRPM).....	82
Introduction.....	82
Materials and Methods	84
Results and Discussion	86
Conclusions	93
References	94
CHAPTER 6 CONCLUSIONS.....	96
Engineering Significance	98
REFERENCES.....	105
APPENDICES	109
ACKNOWLEDGEMENT	125

LIST OF FIGURES

Figure 2-1 Scheme of H ₂ S adsorption on FRPM samples	9
Figure 2-2 TGA plots of FRPM sample A (a) and FRPM sample B (b).....	19
Figure 2-3 Surface pH of FRPM sample A and sample B.....	23
Figure 2-4 SEM map of FRPM sample A undergoing surface element analysis	24
Figure 2-5 Surface element analysis using scanning electron microscopy	24
Figure 2-6 Infrared result of FRPM.....	26
Figure 2-7 Adsorption capacity of FRPM sample A and B	29
Figure 3-1 Breakthrough curve of H ₂ S adsorbed by FRPM	41
Figure 3-2 TGA curve of FRPM.....	43
Figure 3-3 Adsorption capacity of H ₂ S on preheated FRPM.....	45
Figure 3-4 Schematic representation of the interaction between zinc stearate and tire rubber (Segre et al., 2002).....	46
Figure 3-5 SEM image of FRPM (scale 150:1).	47
Figure 3-6 Adsorption capacity of H ₂ S on dry FRPM.....	49
Figure 3-7 Reaction between zinc stearate and H ₂ S.....	50
Figure 3-8 XPS spectra of zinc element on FRPM (a. original FRPM; b. 0.1 N HNO ₃ extracted FRPM; c. 0.1 N HCl FRPM; d. 0.5 N NaOH extracted FRPM).	51
Figure 3-9 Adsorption capacity of zinc-extracted FRPM	53
Figure 4-1 Schematic of FRPM H ₂ S adsorption experiments.	60

Figure 4-2 Hydrogen sulfide breakthrough curve (analysis was stopped at 200 ppmv to protect sensor).....	64
Figure 4-3 Effect of FRPM packing quantity on adsorption capacity.....	65
Figure 4-4 Effect of temperature on adsorption capacity.	68
Figure 4-5 Size distribution of and FRPM (Ellis et al., 2008).....	69
Figure 4-6 Adsorption capacity of different size of FRPM.	70
Figure 4-7 Relationship between H ₂ S adsorbed and water concentration (subtracting Dry FRPM H ₂ S adsorption capacity).....	73
Figure 4-8 Relationship between H ₂ S adsorbed and Zn concentration.....	75
Figure 4-9 Adsorption capacity of zinc-extracted FRPM.	77
Figure 5-1 H ₂ S adsorption capacity regeneration by ZnCl ₂ solutions.....	88
Figure 5-2 FRPM moisture balance trend after filtration.	90
Figure 5-3 FRPM repacking tests at room temperature.	91
Figure 5-4 Adsorption capacity recovery following thermal regeneration at 80°C.	92
Figure 5-5 Adsorption capacity difference before raw FRPM and heated FRPM.	93

LIST OF TABLES

Table 2-1 Density and moisture of FRPM sample A and sample B samples	16
Table 2-2 Typical ultimate analysis result (Ucar et al., 2005).....	17
Table 2-3 Ultimate analysis of FRPM.....	17
Table 2-4 Metal test result of FRPM sample A and sample B.....	20
Table 2-5 BET surface area and pore size of FRPM sample A and sample B	22
Table 2-6 Atomic concentration table	25
Table 2-7 Oxidation functionalities concentrations of FRPM sample A and sample B by Boehm titrations	27
Table 2-8 Comparison between FRPM sample A/FRPM sample B and activated carbon	30
Table 3-1 Composition of vehicle tire rubber (Lehmann et al., 1998).	42
Table 3-2 Ultimate analysis result of FRPM compared with previous reports	44
Table 3-3 AAS/AES analysis results of FRPM.....	47
Table 3-4 XPS result of FRPM	48
Table 3-5 Zinc extraction efficiency of FRPM.....	50
Table 4-1 Analysis of variance of packing quantity by JMP 10.0 (Statistical software, SAS institute).	67
Table 4-2 Analysis of variance of temperature by JMP 10.0 (Statistical software, SAS institute).	69
Table 4-3 Analysis of variance of particle size by JMP 10.0 (Statistical software, SAS institute).	71
Table 4-4 Adsorption capacity of FRPM with different moisture contents.....	72

Table 4-5 Zinc extraction results of FRPM.	76
Table 4-6 X-ray photoelectron spectroscopy (XPS) test results.....	77
Table 4-7 Analysis of variance of zinc extraction by JMP 10.0 (Statistical software, SAS institute).	79
Table 6-1 Parameters for cash flow analysis: dry-scrubbing systems.	99
Table 6-2 Cash flow analysis for FRPM system.....	100
Table 6-3 Cash flow analysis for activated carbon system.	101

EXECUTIVE SUMMARY

A commercial rubber waste product, fine rubber particle media (FRPM), was found to adsorb hydrogen sulfide gas (H_2S) from biogas. Compared with traditional H_2S adsorbents, economic advantages make FRPM a potentially attractive alternative. A number of experiments were conducted to investigate fundamental information, surface properties, and breakthrough characteristics of these innovative adsorbents. The physical properties, composition and surface chemistry were investigated and compared with commonly available commercial H_2S adsorbents, such as activated carbon and metal oxide, in order to compare performance and to assess the possible adsorption mechanism. The components of FRPM samples were similar to conventional tire rubber. The specific surface area was less than 1% of activated carbon. The data supported that FRPM samples were particulate in nature with limited porosity. Infrared analysis and metal analysis experiments showed no direct evidence that the adsorption was a pure physical process. Analysis of experimental results and comparison to scientific literature suggest that two components contribute to the H_2S adsorption-- carbon black and zinc.

Fine rubber particle media (FRPM) derived from consumer waste sources, such as discarded vehicle tires, has been found to adsorb hydrogen sulfide (H_2S) from biogas. The challenge for FRPM reuse in biogas scrubbing applications is to increase its adsorption capacity so that it competes well with traditional

adsorbents in terms of effectiveness and life cycle cost. In this research, zinc content, particle size, moisture content, temperature, and packing density were varied during H₂S breakthrough tests. High zinc concentration and lower particle size increased the adsorption capacity of FRPM significantly while moisture content played an important role in the process. Additionally, H₂S removal by FRPM was optimized at a packing density of 75% of the column volume, and the adsorption capacity increased with reactor temperature in a low range (20°C~85°C).

Two regeneration methods of spent FRPM were developed and tested. One efficient solution regeneration method using ZnCl₂ solutions was evaluated in this research for its ability to recover FRPM's H₂S adsorption capacity. Adsorption capacity recovery of FRPM following washing with a zinc solution (1g ZnCl₂/L) yielded an adsorption capacity of 120% of the original. A half strength solution (0.5g ZnCl₂/L) recovered 110% of the adsorption capacity after the first wash and 80% after the second wash. Thermal regeneration at a temperature of 80°C worked well in the first three regeneration cycles and reached approximately 100% recovery. However, the regeneration capacity decreased with additional cycling. During thermal regeneration, at least 30% of H₂S adsorption capacity was attributed to physical adsorption, which occurred at room temperature.

CHAPTER 1 GENERAL INTRODUCTION

Tire Reuse and Adsorption Ability of Rubber

Each year, millions of scrap or used tires are generated in the US. While the majority of these are properly disposed or turned into recycled rubber material, some used tires are improperly disposed creating an environmental hazard. Compared with landfilling and incineration, reuse and recycling tire rubber is an environmentally sustainable option. The steel or other metal parts could be separated with relatively simple mechanical methods and reused. The rubber components need further processing, such as shredding or milling, which is not only necessary for reuse purposes, but also to save space. In Iowa since 1991, whole waste tires have been banned from landfills by House Rule 753, (1989). Rubber can be made into rubber chips or particles with mechanical or chemical methods.

The high carbon concentration makes waste tire rubber a potential new energy source. It is a beneficial reclamation method to transform waste tires into fuel oil and gas through pyrolysis (Ucar et al., 2005) and flammable gases (Leung et al., 2002). However, the energy cost and potential environmental problems should also be considered. Civil engineering material applications are another important reuse option. Tire rubber-additive concrete is widely used in building construction and shows improved quality in strength, resistance and aggregation (Segre et al., 2004; Siddique and Naik, 2004; Li, et al., 2004; Pierce

and Blackwell, 2003). Tire rubber could also be made into asphalt (Putman and Amirghanian, 2004).

In the environmental field, used tire rubber could serve as pollutant control material. Due to the high concentration of carbon, tire rubber is a good potential raw material for activated carbon production. There are many studies focused on the pyrolysis of tire rubber to produce activated carbon (Lehmann et al., 1998). An energy-saving alternative is employing the raw rubber chips or particles directly to deal with pollutants, such as Mercury (II) in contaminated soil (Meng et al., 1998), aqueous Cr (III) (Entezari et al., 2005), BETX compounds (benzene, toluene, ethyl benzene, and m-, p-,o-xylenes) (Park, 2004; Kim et al., 1997; Lisi et al., 2004), anionic surfactants--sodium dodecyl sulfate (Purakayastha et al., 2005; 2002), nitrate leachate in sand-based roots zone of plant growing region (Lisi et al., 2004), and oil spills (Lin et al., 2008). All these applications are based on the adsorption capacity, although the mechanisms are varied and sometimes unclear.

Hydrogen Sulfide Control

H₂S is a notorious by-product in biogas, a type of renewable biofuel, which originates from the biological decomposition of organic matter under anaerobic conditions. At high concentrations, H₂S prevents the usage of biogas in internal combustion engines and micro turbines due to corrosion concerns. H₂S is also found in confined spaces in waste collection and treatment systems, such as digesters, landfills and wastewater collection systems. Besides the corrosion problems caused, it threatens the health of operators and can cause death.

Typically, there are two ways to generate H₂S: anaerobic digestion and biomass gasification. Common biomass feedstock for the former includes sewage, domestic waste and agricultural residues, while wood or other biomass is used for the latter. Sulfur is one of the important inorganic elements in living cells. In digestion, anaerobic microorganisms use sulfate as an electron acceptor for metabolic activities during the digestion process, which results in H₂S production. In gasification (pyrolysis), H₂S is also generated because sulfur is reduced to S²⁻ in the incomplete combustion process in the absence of oxygen.

Many strategies have been developed to control H₂S, including inhibition of H₂S formation, chemical scrubbers, biological scrubbers, membranes, and adsorption. To reduce H₂S production in anaerobic bioreactors, chemical or biological inhibitors, such as sodium molybdate (Ranade et al., 1999), sulfur bacterial (Van der Zee et al., 2007), and iron-oxidizing bacteria (Sugio, et al., 1992), compete with sulfate as the terminal electron acceptor. A chemical scrubber could be a dry sorption process or a liquid process. Iron oxides (Truong and Abatzoglou, 2005) and ZnO powder (Novochinskii et al., 2004) adsorbed H₂S in steam, while in aqueous solutions, ZnO and CuO also worked to remove H₂S (Haimour et al., 2005). Biological scrubbing methods also take advantage of the oxidation of H₂S, but in this case, microorganisms perform the oxidation. Sulfur oxidizing microorganisms could be fixed on films in an H₂S bioscrubber or biotrickling filter (Potivichayanon et al., 2006, Soreanu et al., 2008).

Adsorption, such as activated carbon adsorption, is often a popular choice. The surface characteristics of activated carbon, such as specific surface

area, pore size, moisture content, pH, and surface chemistry (oxygen containing functionalities), can influence the adsorption of H₂S (Bagreev and Bandosz, 2001, Bandosz, 1999, Tsai et al., 2001, Xiao et al., 2008, Adib et al., 1999, Bagreev and Bandosz, 2000). Sludge-derived H₂S adsorbents have attracted attention recently, especially metal sludge from the galvanizing industry (Yuan and Bandosz, 2007, Seredych et al., 2008). Molecular sieves made from materials, such as lime, silica gel and zeolite, are common high capacity adsorbents because of their small pore sizes (Garcia and Lercher, 1992). Additionally, polyelectrolyte membranes and Poly-vinylbenzyltrimethylammonium fluoride (PVBTAF) membranes have been used to separate acid gases from methane or hydrogen (Chatterjee et al., 1997). However, these membranes cannot handle a high H₂S concentration stream. It has been reported that the two-stage poly membrane process with CO₂-selective membranes in the first stage before H₂S-selective membranes could improve the removal of H₂S in the second stage (Hao et al., 2002).

One simple oxidation method is to pump oxygen or air into biogas to oxidize H₂S into sulfur (Kapdi et al., 2005). This method is suitable for higher H₂S concentrations in biogas. Alternatively, a thin, solid-state membrane electrochemical cell could be used to oxidize H₂S (Mbah et al., 2008)

Study Objective

This research evaluated the H₂S adsorption mechanism behavior of FRPM. The goal was to identify potential reuse alternatives for scrap tire rubber in odor control scrubbers for biogas or other natural gas stream contaminated

with H₂S. An additional objective was to characterize the fundamental properties of FRPM, including surface characteristics, chemical and physical characteristics, and elemental analysis. Furthermore, experiments were designed to seek methods for improving removal efficiency by testing the factors associated with the H₂S adsorption capacity of FRPM. As well as efficient and proper regeneration methods fulfilling the sustainable reuse of FRPM, the lab experiments were conducted to provide sufficient theoretical and data preparation for the application of FRPM in large-scale odor control installations.

Dissertation Organization

This dissertation is organized into three major parts as individual papers. The first paper evaluates the adsorption capacity of H₂S on rubber particle media, including FRPM sample A (derived from tires) and FRPM sample B (derived from other industrial rubber use, such as belts) and characterizes the surface, physical and chemical properties. The second paper demonstrates the adsorption performance of FRPM (FRPM sample A only) operated under varying conditions, such as temperature, moisture, and packing density and investigates the adsorption mechanism. The final paper proposes and evaluates various regeneration methods for spent FRPM (FRPM sample A only).

CHAPTER 2 WASTE TIRE MEDIA PRODUCTS ADSORBING BIOGAS HYDROGEN SULFIDE AND THE CHARACTERISTICS OF THE RUBBER SAMPLES

A paper modified from a presentation at *WEFTEC 2010*

Ning Wang; Eric Evans; Timothy G. Ellis
Department of Civil, Construction, and Environmental Engineering,
Iowa State University, Ames, Iowa, 50011 U.S.A.

Introduction

Biogas is a type of renewable biofuel. Under anaerobic conditions, biogas originates from the biological decomposition of organic matter. Sulfur is an important inorganic element in living cells. Anaerobic microorganisms use sulfur as an electron acceptor for metabolic activities during the digestion process which results in hydrogen sulfide (H_2S) release. Hydrogen sulfide is a harmful and malodorous gaseous compound. Besides negatively affecting human health H_2S increases the cost of fuel gas in distribution system maintenance, causes industrial facility corrosion and oxidizes to SO_2 during combustion, which is regulated by the U.S. EPA for air quality protection. The removal of H_2S from biogas would benefit society, industry and the environment.

Waste tires are a potential threat to the environment. Stockpiling and landfilling of used tires occupies large areas of land and leaches hazardous waste materials. Tire incineration is difficult to control and releases hazardous chemicals such as polycyclic aromatic hydrocarbons (PAH) into the atmosphere

(Miguel et al., 2002, Shah et al., 2006). Approximately 300 million scrap tires are generated in the US each year (EPA, 2008). Methods for reuse and recycling of tires include conversion to fuel, incorporation into civil engineering projects as a construction material, pyrolysis to produce activated carbon, conversion to ground rubber (e.g., for use in asphalt), and application for agricultural as well as miscellaneous other uses.

To develop market alternatives, new applications for the reuse of scrap and used tires have been investigated in previous research. Some preliminary research findings have shown that ground tire rubber acts as an adsorbent. For instance, tire rubber was used in soil and water to adsorb metals or organic chemicals (Lisi et al., 2004, Meng et al., 1998). However, little research has focused on gas cleaning using ground tire rubber as the scrubber media.

Previous work in our research group identified the possibility of hydrogen sulfide removal from biogas by using fine rubber particle media (FRPM sample A) and other rubber material (FRPM sample B) from EnviroESI™ (Lawton, Iowa) (Ellis, et al., 2008). Since the raw materials of FRPM are waste tires, it has a relatively small initial cost compared to other commercial products and this makes the FRPM an economically efficient H₂S sorbent. In the current study, Envirotech provided two types of rubber, FRPM sample A and sample B, for the research. The overall objective was to investigate the adsorption mechanism of hydrogen sulfide on rubber particles by conducting laboratory experiments. Since there was no similar previous studies, this work followed the general theory for sorbent and adsorption material behavior. More specifically, the objectives of this study

were to characterize the chemical, physical and surface properties of FRPM sample A and sample B, to compare the material with other commercial H₂S adsorbents, to analyze the adsorption behavior of H₂S relating to the properties of FRPM, and to investigate the mechanisms of adsorption.

Materials and Methods

Rubber particle products

The FRPM sample A and sample B were provided by EnviroESI™. FRPM sample A was generated from used tires size separation was performed, and it was mixed with additives to improve binding capabilities. FRPM sample B was minimally processed receiving primarily size separation and made from other rubber components of a vehicle except for tires. Both FRPM sample A and sample B underwent analysis and were part of this study.

Hydrogen sulfide adsorption reactor

An adsorption reactor was fabricated using a clear PVC column, an air source, and an H₂S sensor. The PVC column was connected to an H₂S gas cylinder. The H₂S gas flow rates were evaluated by a rotameter (Omega Engineering, Inc. FL-2011). An air sampling pump (SKC Model 222-3) was used to supply air to the gas stream after it flowed from the column to meet the measurement criteria of the sensor. The H₂S sensor used was a Jerome 860 hydrogen sulfide monitor by Arizona Instruments, LLC (Tempe, AZ) with a measurement range of 0-200 ppm hydrogen sulfide, a sensitivity of 0.1 ppm, and data logging capabilities. An H₂S source was 200 ppmv H₂S in nitrogen gas

(Calibration Gas Cylinder obtained from Brandt Instruments, Inc.). The entire adsorption system was installed in a fume hood to ensure safety. The dimensions are shown in Figure 2-1.

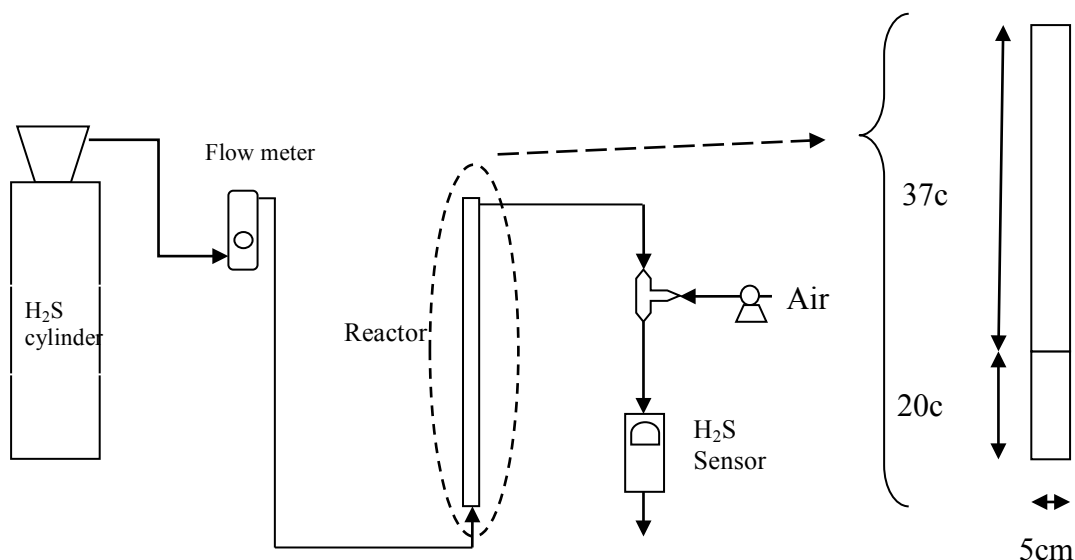


Figure 2-1 Scheme of H₂S adsorption on FRPM samples

Break through curve

Break through curves were used to measure the continuous H₂S adsorption capacity of FRPM sample A and sample B. To obtain the breakthrough curves, first of all, a 10 g FRPM sample A or FRPM sample B sample was packed into the PVC column without compaction. Then, 200 ppmv H₂S was introduced into the column at a flow rate of 0.3 mL/min. As indicated, air was mixed into the column outlet gas before the gas stream was diverted to the sensor. The air flowrate was controlled constantly at 0.22 mL/min. The data read from sensor indicated the concentrations of mixture of outlet gas and added

air. Data measured by the sensor was corrected to the air free H₂S concentration. The data reading was stopped when the H₂S sensor showed 100 ppmv. FRPM sample A and sample B samples were separately tested and analyzed.

Bulk density and particle density

Density information is necessary for packing and porosity calculations. Bulk density testing was completed based on the basic requirements of ASTM D1895B. In this process, a 140 mL beaker was filled with FRPM sample A or FRPM sample B to a setting volume. The weight difference of the beaker before and after filling was recorded. Consequently, the bulk density without compressing could be calculated by the weight difference divided by the volume. To evaluate particle density, water was used to get rid of the air between the rubber particles. A 0.5 g FRPM sample A or FRPM sample B sample was placed into a 50 mL glass tube without shaking. A measured mass of FRPM sample A or FRPM sample B sample was combined with a known volume of water and allowed to sit at room temperature for 24 h to allow the water to enter the pores of the rubber particles. Stoppers were used to avoid the evaporation of water in the glass tubes. After the sample completely settled at the bottom, the tube was filled up with water and the total volume of water was measured. After the tubes were cleaned and dried, the tube volume was measured with water. Consequently, the particle density could be calculated in terms of the weight of rubber particles divided by the volume difference.

Moisture content

The mass of water to mass of FRPM sample A or FRPM sample B ratio resulted in an estimate of the moisture content of the rubber particles. In this measurement, empty beakers were heated at 105 °C for 4 h and then placed in desiccators at room temperature. The beakers were cooled down and weighed. This procedure was repeated until the empty beakers' weight change was less than 0.1 g to avoid any moisture residual. An amount of 10 g FRPM sample A and sample B were separately transferred into the beakers, which were weighed and transferred to an oven at 105°C for 8 h. Finally, the samples were cooled to room temperature and weighed again. The weight differences before and after drying were considered as the mass of water in FRPM sample A or FRPM sample B. The moisture content was calculated with water mass divided by sample mass.

Ultimate analysis

To determine the relative concentrations of the elements (carbon, sulfur and hydrogen), a Perkin-Elmer Model 2400 Series II CHN/S elemental analyzer was used to perform ultimate analysis of FRPM sample A. The experiments were conducted in the Department of Chemistry at Iowa State University.

Inductively-coupled plasma with atomic absorption test

Inductively-Coupled Plasma (ICP) with Atomic Absorption (AA) was used to measure the concentrations of metals in FRPM sample A and sample B samples. FRPM sample A and sample B samples were sent to Minnesota Valley

Testing Laboratories, INC. (MVTL) for digestion and metals analysis. MVTL provided the ICP and AA results including the concentrations of calcium, magnesium, copper, iron, lead, silver, and zinc in FRPM sample A and sample B.

X-ray photoelectron spectroscopy analysis

An x-ray photoelectron spectroscopy (XPS) test was used to identify the relative surface concentrations of elements on FRPM sample A. In this study, carbon, oxygen, sulfur, zinc, and nitrogen were detected by an XPS test in the Ames lab at Iowa State University. The rubber samples included raw FRPM sample A, H₂S-saturated FRPM sample A, HNO₃-rinsing FRPM sample A, and H₂S-saturated HNO₃-rinsed FRPM sample A.

Scanning electron microscope

A scanning electron microscope (Hitachi, S-2460N) was used to measure the elemental concentration in the bulk samples of FRPM sample A and sample B. To perform the test, the rubber samples were applied to a carbon based disc and inserted under the electron stream. The elements were identified in spots or over a larger area of the sample based on refracted waves from the material. The ratio of elements could be estimated by the area sizes in the images.

Thermogravimetric analysis

The thermal stability of FRPM sample A and sample B was estimated in a thermogravimetric analysis (TGA) test. A TGA analyzer by PerkinElmer T6A7™ (Waltham, Massachusetts) was used to conduct the test. Approximately 40 mg FRPM sample A or FRPM sample B sample was used and the temperature program was set from 50 °C to 650 °C at 5 °C/min. A mixture of nitrogen and air

(volume ratio 1:1) was used as the carrier gas. The inflections of mass curve were derived to estimate the composition of FRPM sample A and sample B.

Surface pH

The surface pH of FRPM sample A or FRPM sample B was estimated by measuring the rinse water from rubber particles. 50 mL water was used to rinse 4 g rubber material in a 100 mL glass tube for 12 h in a shake table (200 rpm). After filtering the FRPM sample A and sample B particles, the rinse water pH was tested with an Accumet™/Fisher Scientific XL15 (Pittsburgh, PA) pH meter, which was calibrated in accordance with manufacturer's guidelines.

Nitrogen adsorption

The information of BET surface area and pore size of FRPM sample A and sample B were obtained by a nitrogen adsorption test. The ASAP 2020 BET Micromeritics™ (Norcross, GA) was used to perform the experiment. The process and parameters were described as follows: approximately a 50 g sample was heated to remove volatile compounds in an oven at atmospheric pressure at 120 °C for 48 h; then, the samples were evacuated at 100 °C (temperature rises to 100 °C at a rate of 10 °C/min; Evacuation rate was 30.0 mmHg/s; Evacuation time was 300 min; Vacuum set point was 10 um Hg). Nitrogen adsorption isotherm was obtained at 77 K and the data were analyzed for BET surface area and BJH pore size calculation.

Infrared test

To compare the difference before and after H₂S adsorption on rubber particles, raw and H₂S-saturated FRPM samples were sent to Dr. Steven Martin

for an IR test in the Department of Materials Science and Engineering at Iowa State University.

Boehm titration

Surface oxidation functionalities of FRPM sample A and sample B were evaluated using Boehm Titration. Boehm established a theory to estimate the oxidation group concentration on the surface of carbonous materials (Boehm, 1966). In the theory, NaHCO_3 neutralizes carboxylic groups; Na_2CO_3 neutralizes carboxylic groups and also allows lactonic groups to open and form carboxylic groups, which are then neutralized; NaOH neutralizes carboxylic, lactonic, and phenolic groups. Titrations and differences between titrations allow for estimation of the number of carboxylic, lactonic, and phenolic surface groups. In the experiment, the method “Boehm Titration for carbon black” was employed, and it was assumed that carbon black occupies a large proportion in tire rubber particles. A sample of 0.25 g FRPM sample A or FRPM sample B was added in test tubes, and each tube contained either 0.05 M NaHCO_3 , 0.05 M Na_2CO_3 , or 0.05 M NaOH . After shaking for 24 h, 10 mL samples were filtered and transferred to 100mL beakers. A known excess volume of 0.05 M HCl and 4 drops of Phenolphthalein were then added to the solution. Finally, 0.05 M NaOH was used to titrate the solution until the solution’s color changed to pink.

Results and Discussion

For both FRPM samples, the fundamental characteristics of bulk density, particle density, and moisture content are shown in Table 2-1. It was reported

that the bulk density of tire rubber particles is 0.285 kg/m^3 (Purakayastha et al., 2005), which is similar to the results from these experiments. Low bulk density requires large volumes of FRPM sample A or FRPM sample B to provide a given mass. However, compaction could offset this challenge. Previous research showed that roughly 40 to 50 Newtons of force could provide a compaction of approximately 30%. Compared with bulk density, particle density is essential for model evaluation and prediction of fluid behavior in a biphasic system. The typical particle density of tire rubber ranges from 0.83 to 0.96 g/mL (Hernandez-Olivares, Barluenga et al., 2002; Bignozzi and Sndrolini 2006; Colom, Carrilo et al., 2007). The densities of FRPM sample A and sample B samples are slightly greater than these (0.95 g/mL and 1.28 g/mL, respectively), while FRPM sample A presents a particle density greater than water. It is possible that additives, such as metal and carbon black, contributed to the variability in the density. A phenomenon that FRPM sample A and sample B resist surface wetting initially was found during the particle density test procedure. However, after saturation over a period of 12 to 24 h, both samples would settle down in the containers. Since water does not fill the micropores, a potential limitation of the particle density test may exist. However, there is little micropore structure in both rubber materials, according to the surface area test (shown in Table 2-5). FRPM sample A has higher density than FRPM sample B in terms of both bulk and particle density. The gap between the two kinds of densities indicates the high potential for compaction to achieve a greater density.

Table 2-1 Density and moisture of FRPM sample A and sample B samples

Sample	FRPM sample B	FRPM sample A
Bulk density (kg/m ³)	0.21	0.31
Particle density (kg/m ³)	0.95±0.06	1.28±0.13
Moisture content (%)	1.31±0.004	0.56±0.003

The low background moisture content showed that FRPM sample A or FRPM sample B does not freely sorb or attract water. According to studies on the H₂S adsorption mechanism on the surface of activated carbon, water plays an important role in the oxidation of H₂S (Bouzaza et al., 2004, Bagreev and Badosz, 2001). They showed that the adsorption capacity of H₂S decreased sharply without water. Water may provide a favorable environment for H₂S oxidized by free radicals or reacting with other chemicals. The first step of adsorption is the dissolution of H₂S in water on the surface of the adsorbent. A low moisture content might limit the adsorption of H₂S.

Another fundamental characteristic coming from the ultimate analysis is the relative concentrations of the main elements, such as carbon, sulfur, hydrogen, nitrogen, and oxygen. The typical concentrations in rubber are shown in Table 2-2.

Table 2-2 Typical ultimate analysis result (Ucar et al., 2005)

Ultimate analysis (dry, %)	Passenger car tire	Truck tire
C	74.3	83.20
H	7.2	7.70
N	0.9	1.50
O	15.89	6.16
S	1.71	1.44

The elemental composition of FRPM sample A and sample B from the ultimate analysis are shown in Table 2-3. Carbon is the major element, associated with the black appearance of both rubber materials. High sulfur content was expected since sulfur is used in tire manufacturing. Comparing with the above data, the composition of FRPM sample A is similar to tires while FRPM sample B has a lower carbon concentration, since FRPM sample B was made from other rubber rather than used tires. The saturation of H₂S has no obvious influence on the sulfur concentration because the adsorption capacity is lower.

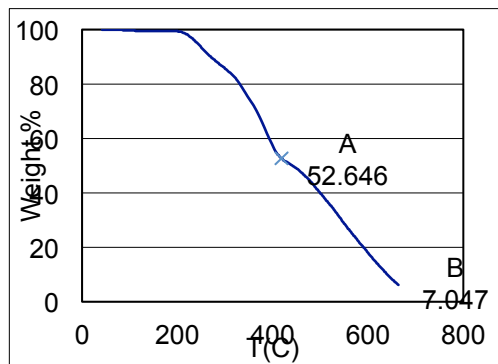
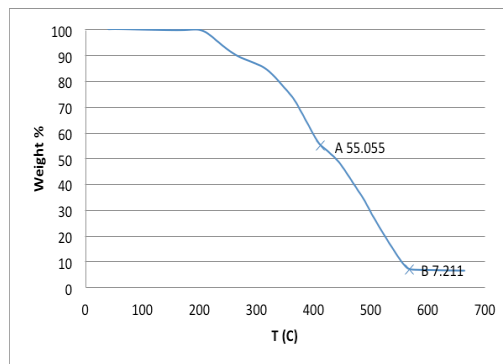
Table 2-3 Ultimate analysis of FRPM

Ultimate analysis (dry, %)	FRPM sample A	H ₂ S saturated FRPM sample A	FRPM sample B	H ₂ S saturated FRPM sample B
C	83.10±1.38	83.01±1.03	62.28±0.74	61.17±0.73
H	8.19±0.04	8.11±0.14	6.54±0.13	5.80±0.31
N	0.45±0.02	0.42±0.03	0.26±0.04	0.23±0.02
S	1.84±0.08	1.85±0.03	1.44±0.08	1.31±0.05
O*	6.44	6.61	29.50	31.49

*The relative of oxygen is calculated by subtracting other four elements from 100%.

Tire rubber typically contains carbon black, polymers, and other trace elements (silicon, sulfur and chlorine) (Williams and Beslers, 1995), which is the raw material of FRPM sample A and sample B. Polymer adsorption was not found in literature or previous work, while carbon black was found to adsorb gases, which may contribute to the H₂S adsorption on FRPM sample A and sample B samples (Rodgers, 2004). Some metal additives, which are involved in the production of both rubber materials, may also benefit the adsorption. TGA analysis not only indicates the temperature resistance, but also estimates the concentrations of carbon black. Some researchers described the common carbon black concentrations as 20–35% weight ratio in tire rubber (Wik and Dave, 2009). The TGA curves demonstrate that concentrations of carbon black were about 45.6% for FRPM sample B and about 47.8% for FRPM sample A (Figure 2-2). These demonstrated the high concentrations of carbon black existing in both rubber materials. Carbon black can provide a large surface area for adsorption and the oxygen containing functionalities on it can attach H₂S. It has been found in prior research that tire derived carbon black inherently

contains a high adsorption capacity (Hamadi, Chen et al., 2001; Pantea, Darmstadt et al., 2003; Manchon-Vizueté, Macias-Garcia et al., 2005). The TGA test results also show FRPM sample A and sample B samples were stable at temperature up to 250 °C. Therefore, FRPM sample A and sample B could work at elevated temperatures in other industrial processes when removing H₂S from waste steams.



(a)

(b)

Figure 2-2 TGA plots of FRPM sample A (a) and FRPM sample B (b)

Another potential active component for H₂S adsorption is the metal composition in FRPM sample A and sample B. The concentrations of metals are

shown in Table 2-4. Among all the metals, zinc, magnesium and iron are present in FRPM sample A and sample B in high concentrations based on the AAS and AES analyses. The metal elements could primarily exist in the form of metal oxides, because the used tire product has undergone a long period of friction in air as vehicle tires. Additionally, this is supported by the high pH measurements (Figure 2-3), and oxygen concentration (Table 2-6). Metal oxide is a traditional adsorbent for sulfide removal from biogas depending on acid-base reaction. In this case, sulfide and metal chemical reactions are important for the H₂S removal mechanism using FRPM sample A and sample B, which are suggested by the measured metal concentration. Besides the measurement results, the theoretical stoichiometric sulfur consumption on a mass basis is also shown in Table 2-4, and this reflects a large reactant reserve.

Table 2-4 Metal test result of FRPM sample A and sample B

Metal	FRPM sample B (mg/kg)	FRPM sample A(mg/kg)	Potential sulfur consumed (mg/kg) ¹
Calcium	1.41	2,398 ± 585	2,038
Magnesium	5,017	462.5 ± 28.9	655.1
Copper	0.451	7.22 ± 0.243	3.893
Iron	269.4	1,183 ± 465	718.3
Lead	<6.77	7.67 ± 1.29	---
Silver	NM ²	<0.4963	---
Zinc	17,950	15,690 ± 2,079	8,207
Total			11,623

¹The values are calculated by assuming the products as metal sulfides for the average given by FRPM.

²NM – Not measured

Commonly, surface properties are relevant to the adsorption capacity for some solid adsorbents, such as activated carbon and molecular sieves. With the

similar appearance of activated carbon, the surface properties of FRPM sample A and sample B samples were also investigated in this study. A nitrogen adsorption test was employed to gather BET surface area and pore size information, and the results are shown in Table 2-5. The measured nominal pore size of FRPM sample A and sample B samples are considered as mesopore (mesoporous materials with a pore size near 10 nm). However, in other studies, the specific surface area of mesoporous materials should be 100-500 m²/g typically (Alonso-Lemus, Verde et al., 2009). The surface area of both samples were approximately 0.2~0.3 m²/g, much less than the definition. This presents an inconsistency between the nominal pore size and the specific surface area measurement. It indicated that the number of mesopores does not dominate on the surface of on FRPM sample A and sample B. This happens when either the material contains minimal pores, or the nominal pore size extends beyond the test range of the ASAP 2020 instrument limitation. It is suggested that FRPM sample A or FRPM sample B are possibly non-porous particles rather than porous materials and physical adsorption is probably not the only reason why H₂S was adsorbed.

Table 2-5 BET surface area and pore size of FRPM sample A and sample B

Samples	FRPM sample B	FRPM sample A
BET Surface Area (m ² /g)	0.2802	0.2257
BJH Desorption average pore diameter Å	143.327	71.128
BJH Adsorption average pore diameter Å	68.028	90.114

High surface pH facilitates H₂S adsorption, which has been demonstrated by activated carbon research (Adib, Bargreev et al., 1999). The surface pH of FRPM sample A and sample B samples were both greater than 7, as shown in Figure 2-3. If a similar adsorption mechanism to activated carbon of FRPM sample A and sample B is exploited, a higher pH would enhance the adsorption of H₂S. One explanation for the higher pH values may be because some alkaline chemicals were added during the FRPM sample A and sample B production process. Another reason may be that some metal element exists in the form of oxides, e.g. ZnO (Smolders and Degryse, 2002), which increase the pH of water when they are dissolved.

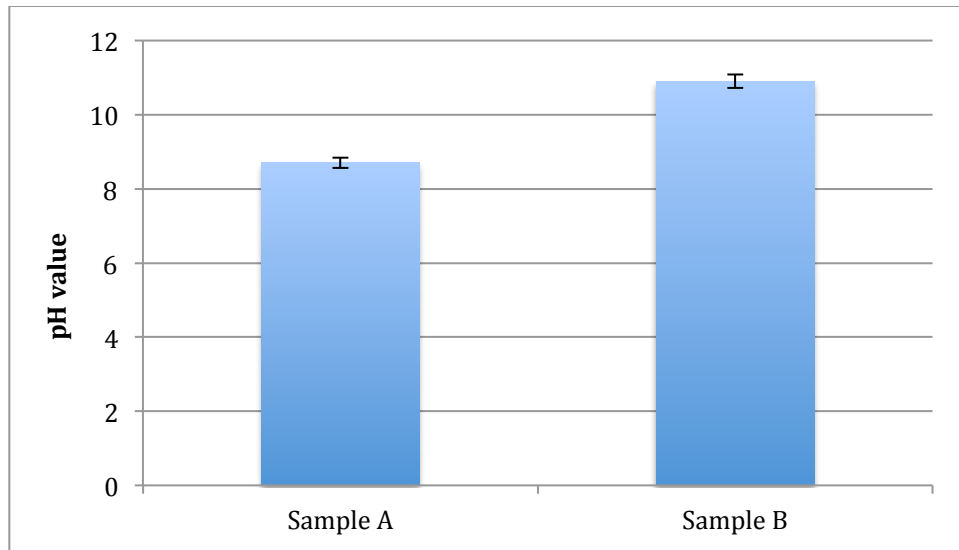


Figure 2-3 Surface pH of FRPM sample A and sample B

Surface element distribution information of FRPM was obtained with SEM (Figure 2-4 and Figure 2-5) and XPS (Table 2-6). The former refers to the bulk volume of the surface while the latter detects the thin layer of the surface (approximately 10 nm). SEM image suggests the presence of zinc, magnesium, and calcium, which would be necessary to react with H_2S . In addition, sulfur, silicon and oxygen were also detected in relatively smaller amounts. The oxygen present may have been associated with metal oxides. The major element is carbon resulting from the higher ratio in FRPM of carbon black.

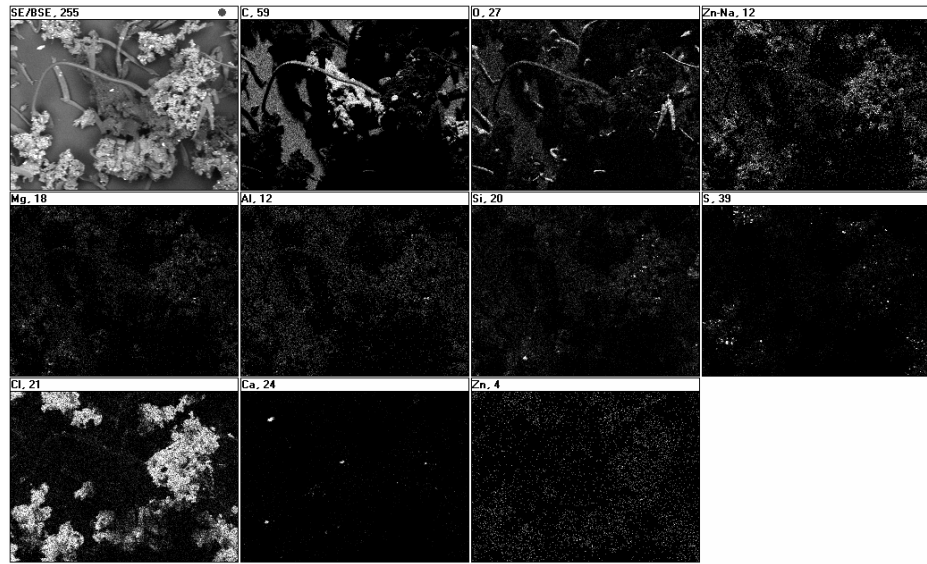


Figure 2-4 SEM map of FRPM sample A undergoing surface element analysis

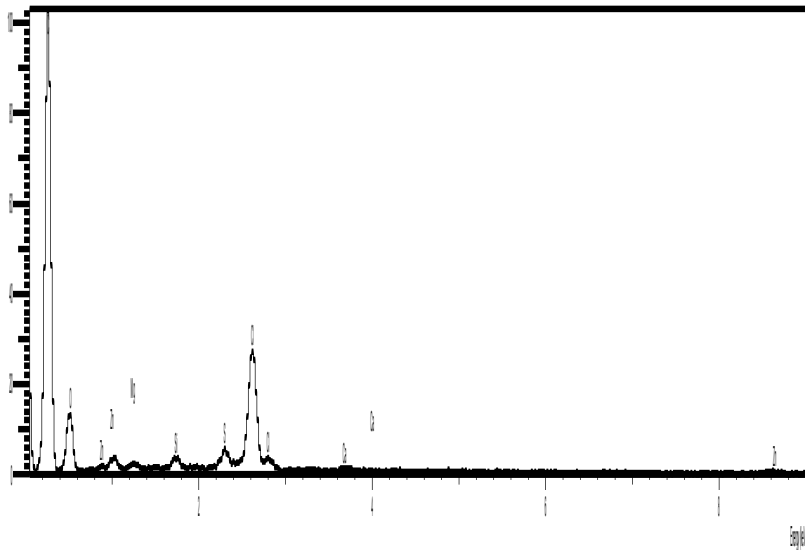


Figure 2-5 Surface element analysis using scanning electron microscopy

XPS experiment results, presented in Table 2-6, illustrate the surface concentration of elements. Zinc was investigated because of the high

concentration as a metal component shown in Table 2-4 and a potential H₂S adsorbent. The results demonstrate that zinc concentrations changed due to extraction. They also suggest that the species of the element zinc on the FRPM sample A surface has an oxidation of +2, which was assumed to be zinc oxide or zinc sulfate. Considering the higher concentration of oxygen compared to sulfur, the presence of zinc oxide is more likely. In addition, this coincides with the fact that ZnO is usually used as an additive in tire rubber manufacture. An unusual observation was that the measured concentration of sulfur before H₂S saturation was larger than after H₂S saturation, as based on the detected area of the XPS. Because the distribution of sulfur is not even, the same observed area (approximately 20 mm radius) may cause considerable variation. Furthermore, the small adsorption capacity of H₂S on FRPM sample A, shown in Figure 2-7, compared to the total sulfur content, makes the difference in the sulfur concentrations relatively small.

Table 2-6 Atomic concentration table

FRPM sample A	C 1s	N 1s	O 1s	S 2p	Zn 2p3	Total
Raw	89.28	0.2	8.53	0.43	1.56	100
After HNO ₃ extraction	91.8	0.78	6.53	0.12	0.77	100
H ₂ S saturated	91	0.4	6.68	0.21	1.71	100
H ₂ S saturated after HNO ₃ extraction	89.07	1.22	8.52	0.19	1.00	100

From the IR spectrum (Shown in Figure 2-6), FRPM sample A and sample B may contain carbon dioxide or carboxyl functional groups based on the peaks measured at 2400 cm^{-1} . After saturation of H_2S , a H_2S peak was not found in IR spectrum for FRPM sample A and sample B samples. Several reasons are considered: It is possible that the H_2S concentration was too low to be detected; H_2S reacted and the sulfur species changed to a form which was not detected by IR spectrometry; H_2S was adsorbed within pores and hidden so that it was inaccessible by the IR beam.

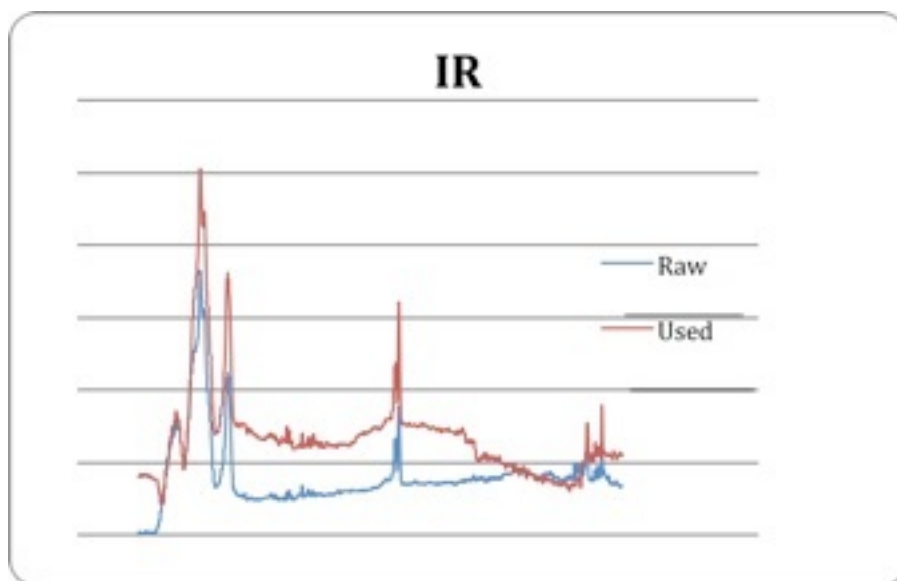


Figure 2-6 Infrared result of FRPM

Boehm Titrations were performed to evaluate the surface functional groups on FRPM sample A and sample B. The titration results do not fit Boehm's theory for surface functional group titration. The data shows an unusual relationship between the titrations. Sodium hydroxide should consume a greater

volume of titrant, because more surface functionalities are affected by sodium hydroxide than the other two chemicals. The mass of FRPM sample A and sample B were increased and to check reproducibility. The titration results show the concentration of oxidation functional groups was still lower, as shown in Table 2-7.

Table 2-7 Oxidation functionalities concentrations of FRPM sample A and sample B by Boehm titrations

Item	FRPM sample B	FRPM sample A
Carboxylic group conc. (mole/g)	0.0018	0.0027
Carboxylic and lactonic groups conc. (mole/g)	0.0029	0.0031
Carboxylic, lactonic and phenolic groups conc. (mole/g)	0.00013	0.000074

Therefore, it is possible that the Boehm theory does not work here. However, it still provides some information. Based on the measured combined concentrations of surface groups (using hydroxide), the concentration of total oxidation functional groups is lower than that for activated carbon. The low concentration matches the higher pH of 8.56 to 11.53 versus 4.04~5.6 of virgin activated carbon (Adib et al., 1999; Boudou et al., 2003). Depending on acid-base theory, a higher surface pH better supports adsorption of H₂S on the surface of FRPM sample A and sample B. The unusual Boehm titration results increase the suspicion that some chemicals interfere with the experiments, e.g. metal oxide. This is supported by the metal analysis above.

The adsorption capacity of for FRPM sample A and sample B was determined by the H₂S breakthrough curve. However, because of the lower adsorption capacity and the small reactor, the adsorption amount was calculated at the point that the breakthrough concentration was 100 ppmv, rather than at the actual breakthrough point. The results (Figure 2-7) show that FRPM sample B contains a higher specific capacity than FRPM sample A. One explanation is that FRPM sample A's surface pH was lower than the sample FRPM sample B. According to previous research (Bandosz, 1999), a lower surface pH environment may resist the H₂S adsorption. The surface pH test results show that the pH of FRPM was lower than FRPM sample B, which matched the H₂S adsorption capacity comparison, although the specific surface area of the FRPM sample A was higher than the FRPM sample B. Another possibility was that the moisture content of FRPM sample A was lower than FRPM sample B. These indicate that the major adsorption mechanism is more likely a chemical reaction rather than physical adsorption. Another possible reason is that the zinc concentration of FRPM sample B was also higher than the zinc concentration of FRPM sample A. According to the metal test results (Table 2-4), the zinc concentration was 14.22 mg/g, and therefore, 7.44 mg/g H₂S could be consumed based on reaction ($ZnO + nH_2O + H_2S \rightarrow ZnS + (n+1) [H_2O]$). During the tire manufacturing process, zinc is added after the vulcanization process and works as an activation catalyst and as a wear matrix (Bandosz, 1999). However, the theoretical H₂S adsorption was much higher than the real amount (1-3 mg/g). It is possible that moisture content contributes to the reaction kinetics and

equilibrium because the reaction takes place in the aqueous phase. Another explanation is that not all the zinc is on the surface of both rubber materials. A portion of the zinc inside the rubber particle may not have participated in the reaction.

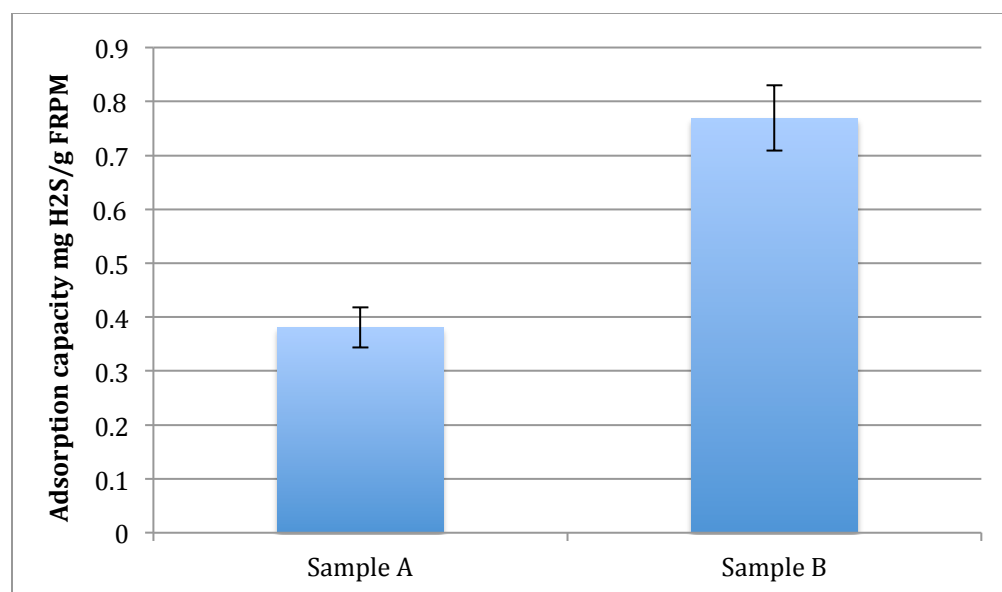


Figure 2-7 Adsorption capacity of FRPM sample A and B

Since there is no previous study to evaluate the H₂S adsorption on rubber particles, activated carbon was used as comparison to investigate the adsorption mechanism. FRPM samples and activated carbon, however, the BET surface area and pore size of activated carbon are 500-3,000 m²/g and 10 Å, respectively, and the breakthrough capacity varies from 2 to 300 mg/g (Adib, Bargreev *et al.*, 1999; Bandosz 1999; Xiao, Wang *et al.*, 2008). These values are significantly larger than FRPM samples. Although the breakthrough capacity

of FRPM sample A and sample B (1-3 mg/g) was less than the capacity listed for activated carbon, it should be noted that the ratio of H₂S adsorption capacity to specific surface area for FRPM sample A and sample B is higher than for activated carbon. This suggests that there exists a different adsorption mechanism for FRPM sample A and sample B than for activated carbon. H₂S is absorbed by activated carbon due to the large surface area and oxidation of the surface functional groups including carboxylic, lactonic and phenolic groups. One explanation is that FRPM sample A and sample B adsorption involves chemical reactions, for instance, metal-hydrogen sulfide reactions.

Table 2-8 Comparison between FRPM sample A/FRPM sample B and activated carbon

Parameter	FRPM sample A	FRPM sample B	Granular Activated Carbon ¹	Impregnated Activated Carbon ¹
BET Surface Area (m ² /g)	0.2257	0.2802	732	715
Pore diameter (Å)	90.114	68.028	10 ²	10 ²
Breakthrough Capacity (mg/g)	0.381	0.769	2.1-3.0	7.7-9.3
H ₂ S adsorption capacity/Specific surface area (mg/m ²)	4.431-13.291	3.569-10.707	0.0029-0.0041	0.011-0.013

¹Based on a study evaluating impact of impregnating activated carbon with soda ash (Xiao, Wang et al., 2008)

²Representative value based on distributed range (Cao, Wang et al., 2002; Purewal, Kabbour et al., 2009)

Conclusions

FRPM sample A and sample B were evaluated for H₂S adsorption capacity. They are potential adsorbents to remove H₂S gas from biogas. The

low adsorption capacity could be offset by the low cost when compared to activated carbon and other adsorbents.

To thoroughly investigate FRPM sample A and sample B, a number of basic physical characteristics were established as part of this work including density, moisture content, carbon black content, surface pH, and surface adsorption properties. While the high surface pH and the carbon content tend to support hydrogen sulfide adsorption in a manner analogous to activated carbon, other properties are starkly different from activated carbon.

It was found that FRPM sample A and sample B are more particulate in nature and not highly porous. This is reasonable, because, there is no activation step to generate pores as there is with activated carbon. The low surface area challenges the hypothesis that FRPM sample A and sample B behaves like activated carbon when adsorbing hydrogen sulfide. A number of other factors support chemisorption on the macrosurface as the mechanism rather than physical adsorption in micropores. Based on the effects of zinc and moisture content, chemical reaction or chemisorption may be the dominant H₂S adsorption mechanism.

Future work is planned to better elucidate the role of metals, particularly zinc, and oxidation functionality groups on the adsorption capacity of FRPM sample A and sample B media. Additional surface characterization of FRPM sample A and sample B is needed to help understand the mechanism for FRPM sample A and sample B adsorption of hydrogen sulfide.

References

- Adib, F.; Bagreev, A.; Bandosz, T. (1999) Effect of Surface Characteristics of Wood-Based Activated Carbons on Adsorption of Hydrogen Sulfide. *Journal of colloid and interface science*, **214** (2), 407-415.
- Alonso-Lemus, I.; Verde, Y.; Álvarez-Contreras, L. (2009) Doped Mesoporous Materials as Pem Fuel Cell Electrocatalyst Support. ECS: p 902-930.
- Bagreev, A.; Bandosz, T. (2001) H₂S Adsorption/Oxidation on Unmodified Activated Carbons: Importance of Prehumidification. *Carbon*, **39** (15), 2303-2311.
- Bandosz, T. (1999) Effect of Pore Structure and Surface Chemistry of Virgin Activated Carbons on Removal of Hydrogen Sulfide. *Carbon*, **37** (3), 483-491.
- Bignozzi, M.; Sandrolini, F. (2006) Tyre Rubber Waste Recycling in Self-Compacting Concrete. *Cement and Concrete Research*, **36** (4), 735-739.
- Boudou, J.; Chehimi, M.; Broniek, E.; Siemieniewska, T.; Bimer, J. (2003) Adsorption of H₂S or SO₂ on an Activated Carbon Cloth Modified by Ammonia Treatment. *Carbon*, **41** (10), 1999-2007.
- Cao, D., W. Wang, *et al.*, (2002). "Determination of pore size distribution and adsorption of methane and CCl₄ on activated carbon by molecular simulation." *Carbon* **40**(13): 2359-2365.
- Colom, X.; Carrillo, F.; Canavate, J. (2007) Composites Reinforced with Reused Tyres: Surface Oxidant Treatment to Improve the Interfacial Compatibility. *Composites Part A*, **38** (1), 44-50.
- Ellis, T. G.; Park, J.; Oh, J. (2008) *A Novel and Cost-Effective H₂S Absorption Technology Using Tire Derived Rubber Particles*. Report
- Hamadi, N.; Chen, X.; Farid, M.; Lu, M. (2001) Adsorption Kinetics for the Removal of Chromium (VI) from Aqueous Solution by Adsorbents Derived from Used Tyres and Sawdust. *Chemical Engineering Journal*, **84** (2), 95-105.
- Hernandez-Olivares, F.; Barluenga, G.; Bollati, M.; Witoszek, B. (2002) Static and Dynamic Behaviour of Recycled Tyre Rubber-Filled Concrete. *Cement and Concrete Research*, **32** (10), 1587-1596.
- Li, H. (2008) Selective catalytic oxidation of hydrogen sulfide from syngas,

Master's Thesis, University of Pittsburgh.

- Lisi, R.; Park, J.; Stier, J. (2004) Mitigating Nutrient Leaching with a Sub-Surface Drainage Layer of Granulated Tires. *Waste Management*, **24** (8), 831-839.
- Manchon-Vizueté, E.; Macías-García, A.; Nadal Gisbert, A.; Fernández-González, C.; Gómez-Serrano, V. (2005) Adsorption of Mercury by Carbonaceous Adsorbents Prepared from Rubber of Tyre Wastes. *Journal of Hazardous Materials*, **119** (1-3), 231-238.
- Meng, X.; Hua, Z.; Dermatas, D.; Wang, W.; Kuo, H. (1998) Immobilization of Mercury (II) in Contaminated Soil with Used Tire Rubber. *Journal of Hazardous Materials*, **57** (1-3), 231-241.
- Miguel, G.; Fowler, G.; Dall'Orso, M.; Sollars, C. (2002) Porosity and Surface Characteristics of Activated Carbons Produced from Waste Tyre Rubber. *Journal of Chemical Technology & Biotechnology*, **77** (1), 1-8.
- Pantea, D.; Darmstadt, H.; Kaliaguine, S.; Roy, C. (2003) Heat-Treatment of Carbon Blacks Obtained by Pyrolysis of Used Tires. Effect on the Surface Chemistry, Porosity and Electrical Conductivity. *Journal of Analytical and Applied Pyrolysis*, **67** (1), 55-76.
- Purakayastha, P.; Pal, A.; Bandyopadhyay, M. (2005) Sorption Kinetics of Anionic Surfactant on Waste Tire Rubber Granules. *Separation and Purification Technology*, **46** (3), 129-135.
- Purewal, J. J., H. Kabbour, *et al.*, (2009). "Pore size distribution and supercritical hydrogen adsorption in activated carbon fibers." *Nanotechnology* **20**(20): 204012.
- Rodgers, B. (2004) *Rubber Compounding – Chemistry and Applications*, Marcel Dekker, Inc.
- Shah, J.; Jan, M.; Mabood, F.; Shahid, M. (2006) Conversion of Waste Tyres into Carbon Black and Their Utilization as Adsorbent. *Journal of the Chinese Chemical Society*, **53** (5), 1085-1089.
- Smolders, E.; Degryse, F. (2002) Fate and Effect of Zinc from Tire Debris in Soil. *Environ. Sci. Technol.*, **36** (17), 3706-3710.
- Ucar, S.; Karagoz, S.; Ozkan, A.; Yanik, J. (2005) Evaluation of Two Different Scrap Tires as Hydrocarbon Source by Pyrolysis. *Fuel*, **84** (14-15), 1884-1892.

- Williams, P.; Besler, S. (1995) Pyrolysis-Thermogravimetric Analysis of Tyres and Tyre Components. *Fuel*, **74** (9), 1277-1283.
- Wik, A. and G. Dave (2009). "Occurrence and effects of tire wear particles in the environment - A critical review and an initial risk assessment." *Environmental Pollution* **157**(1): 1-11.
- Xiao, Y.; Wang, S.; Wu, D.; Yuan, Q. (2008) Experimental and Simulation Study of Hydrogen Sulfide Adsorption on Impregnated Activated Carbon under Anaerobic Conditions. *Journal of Hazardous Materials*, **153** (3), 1193-1200.
- EPA (2008). Wastes - Resource Conservation - Common Wastes & Materials - Scrap Tires. URL:
<http://www.epa.gov/osw/conserve/materials/tires/basic.htm>

CHAPTER 3 THE MECHANISM OF HYDROGEN SULFIDE ADSORPTION ON FINE RUBBER PARTICLE MEDIA (FRPM)

A paper to be submitted to *The Journal of Hazardous Materials*

Ning Wang, Park Jaeyoung, and Timothy G. Ellis

Department of Civil, Construction, and Environmental Engineering,
Iowa State University, Ames, Iowa, 50011 U.S.A.

Introduction

Each year millions of used tires are generated in the US threatening the environment wasting useful land and potentially leaching hazardous chemicals when disposed by incineration and landfilling. Compared with traditional ultimate disposal methods or reclaiming is an environmentally sustainable option, and there have been some recent endeavors in this field. The high carbon element concentration makes waste tire rubber a potential new energy source. It is a beneficial reclamation method to transform waste tires into fuel, such as oils and flammable gases through pyrolysis (Ucar *et al*, 2005; Leung *et al*, 2002). However, the energy cost and potential environmental problems should also be considered. Civil engineering material application is another important reclamation option. Tire rubber-additive concrete is widely used in building construction and shows improved quality in strength, resistance and aggregation (Segre *et al*, 2004; Siddique *et al*, 2004; Li *et al*, 2004). Tire rubber could also be made into asphalt (Putman *et al*, 2004). In the environmental field, used tire

rubber could serve as pollutant control material. Due to the high concentration of carbon element, tire rubber is a good potential activated carbon raw material. There are many studies focusing on the pyrolysis of tire rubber to produce activated carbon (Lehmann *et al*, 1998). An energy-saving alternative idea is employing the raw rubber chips or particles directly to deal with pollutants, such as Mercury (II) in contaminated soil (Meng *et al*, 1998), aqueous Cr (III) (Entezari *et al*, 2005), a variety of VOCs, including BETX compounds (benzene, toluene, ethyl benzene, and m-, p-, o-xylenes) (Park, 2004; Kim *et al*, 1997; Lisi *et al*, 2004), anionic surfactants--sodium dodecyl sulfate (Purakayastha *et al*, 2002; 2005), nitrate leachate in sand-based roots zone of plant growing region (Lisi *et al*, 2004), and oil spills (Lin *et al*, 2008). All these applications are based on the adsorption capacity, though some of the mechanisms might be unknown.

Utilizing the rubber waste as an adsorbent in environmental applications reduces the volume of this material that would otherwise go to landfilling or incineration. The consequence of rubber reuse in terms of sustainability and environmental protection are compelling. However, there is little research referring to the direct cleaning of gaseous media with tire-derived material, such as removal hydrogen sulfide (H₂S) from biogas, which is a harmful and malodorous gaseous compound commonly found in biogas, sewer gas, and other wastewater treatment system off-gasses (Boudou *et al*, 2003). In anaerobic environments, H₂S is generated from the metabolic activities of sulfur-reducing bacteria. H₂S can threaten the health of workers, corrode metal and concrete facilities, attack electrical and electronic components, and damage

conveyance systems in wastewater treatment plants. In addition, biogas from anaerobic digesters contains potentially high concentrations of H₂S. Ideally, the H₂S concentration should be lowered to less than 50 ppmv before entering internal combustion engines. With increased prices of fossil fuels, including oil, coal, and natural gas, biogas, as a bio-renewable alternative, could sustainably alleviate the increasing energy consumption. However, the pressing challenge is to find an efficient and cost-effective way to reduce H₂S concentrations prior to use. Adsorption is an effective and simple method to control H₂S. Traditional commercial H₂S adsorbents, such as activated carbon, molecular sieves, and metal oxides, are widely used. The surface characteristics of activated carbon, such as specific surface area, pore size, moisture content, pH, and surface chemistry (oxygen containing functionalities), influence the adsorption of H₂S (Bagreev *et al*, 2000, 2001; Bandosz *et al*, 1999; Tsai *et al*, 2001; Xiao *et al*, 2008; Adib *et al*, 1999), sludge-derived H₂S adsorbents have attracted research recently, especially metal sludge from the galvanizing industry (Yuan *et al*, 2007; Seredych *et al*, 2008). Molecular sieves, such as lime (mineral), silica gel and zeolite, are a type of common high capacity adsorbent because of their small pores (Garcia *et al*, 1992). Iron oxides (Truong *et al*, 2005) and ZnO powder (Novochinskii *et al*, 2004) adsorb H₂S from steam. Although above adsorbents can effectively remove H₂S, they are relatively expensive, compared with reused rubber particle media.

In this project, a potential rubber-based H₂S scrubber containing fine (less than 1 mm in diameter) rubber particle media (FRPM) was investigated. The

rubber media was derived from consumer waste sources, such as discarded vehicle tires. It could also be derived from manufacturing processes, such as belt and gasket manufacturing and tire retreading operations. Compared with traditional H₂S adsorbents, such as activated carbon, the economic advantage makes FRPM a potentially attractive alternative. In this research, lab-scale tests were conducted to investigate the removal of H₂S on FRPM and to identify the mechanism FRPM adsorption exploits for hydrogen sulfide removal.

Methods and Materials

Materials preparation

FRPM (Fine Rubber Particle Media) was provided by EnviroESI™ and was derived from used tire rubber. The diameter of the particles was approximately 1 mm, the moisture content was 0.5 %, and the bulk and particle densities was 0.3 g/cm³ and 1.3 g/cm³ respectively. A BET surface area of 0.3 m²/g was measured using an ASAP 2020 BET Micromeritics™ (Norcross, GA). 50 g FRPM were heated in an oven at atmospheric pressure at 120°C for 48 h to remove volatile compounds. Then, the samples were evacuated at 100 °C (temperature rises to 100 °C at rate 10 °C; Evacuation rate was 30.0 mmHg/s; Evacuation time was 300 min; Vacuum setpoint was 10 um Hg). The nitrogen adsorption isotherm was evaluated at 77 K.

Ultimate analysis was conducted with Perkin-Elmer Model 2400 Series II CHN/S elemental analyzer, detecting weight composition of carbon, sulfur, nitrogen, and hydrogen. Metal compositions were analyzed with Inductively-

Coupled Plasma (ICP) with Atomic Absorption (AA) operated by Minnesota Valley Testing Laboratories, INC. (MVTL).

Thermogravimetric analysis (TGA) was used to estimate the carbon black concentration of TDRP™ and ORM™. Approximately 40 mg TDRP™ or ORM™ sample was placed into a TGA analyzer by PerkinElmer T6A7™ (Waltham, Massachusetts) and heated from 50 °C to 650 °C at 5 °C/min. Nitrogen and air of volume ratio 1:1 were used as carrier gas. The composition concentration was estimated by the inflections of mass curve.

Breakthrough

A copper cylinder served as the H₂S-FRPM reactor. H₂S gas, from a cylinder containing 500 ppmv in nitrogen, was continuously passed through an FRPM bed with a flow rate of 0.2 L/min controlled by a flow meter. The concentration of H₂S in the outlet gas was detected with a sensor (Jerome 860 H₂S sensor, Arizona Instrument Inc.) which recorded the H₂S concentration data at 2-second intervals. Due to the operational requirement of the sensor that oxygen must be present in the detection process, air was pumped in and diluted the outlet gas at the same flow rate. For safety considerations, the whole test apparatus was put in the fume hood to avoid H₂S venting.

Zinc extraction

To investigate the effect of zinc on H₂S adsorption, zinc distribution on FRPM was changed through extracting with different solutions. Distilled water, 0.1 N hydrochloric acid, 0.1 N nitric acid, and 0.5 N sodium hydroxide solutions were chosen as extractants. 50 g of FRPM sample were rinsed for 24 hours in 1

L solution before the mixture was filtered with Büchner funnel and filter paper. Filtered solutions were gathered and the zinc concentrations in filtrates were analyzed with GBC 932 plus Atomic Absorption Spectrophotometer (GBC Scientific (USA) LLC.) in Environmental Engineering Research Laboratory of Iowa State University. To prevent remaining acid or base influencing the following test, all retentate was washed three times with 300 ml distilled water. The FRPM samples were placed in air for 2 days to equalized the moisture content before testing H₂S adsorption capacity following the above breakthrough method.

Surface analysis

Scanning electron microscopy (SEM) (Hitachi, S-2460N) and X-ray photoelectron spectroscopy (XPS) (Ames Laboratory in Iowa state university) were used to detect the distribution of zinc on the surface. An SEM image referring to zinc distribution was gained by applying FRPM to a carbon based disc and inserted under the electron stream. The elements were identified in specific spots or over a larger area of the sample based on the refracted waves from the material. From XPS, the signal intensity of some elements (carbon, oxygen, sulfur, zinc, and nitrogen) was detected and the atom weight ratio among these elements was obtained by conversion. FRPM samples were press flat for determination.

Zinc stearate reaction with H₂S

A batch test was used to investigate the feasibility of reaction between zinc stearate and H₂S gas. 10 g zinc stearate (Technical grade, Sigma-Aldrich Inc.) was placed in a 1 L container filled with 500 ppmv H₂S in nitrogen. A spike monitoring of H₂S was conducted every 20 min with the help of a pump (Model 222-3, SKC Inc.) and the H₂S sensor (Jerome 860 H₂S sensor, Arizona Instrument Inc.).

Result and Discussion

Figure 3-1 shows one of the breakthrough curves of H₂S on FRPM. The adsorption capacity of H₂S on FRPM was approximately 0.12 mg H₂S/g FRPM by integrating the area above the breakthrough curve.

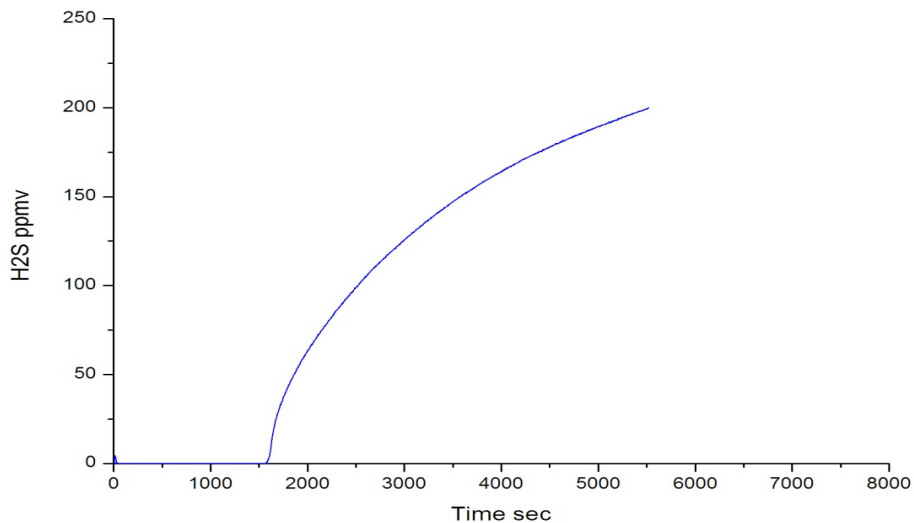


Figure 3-1 Breakthrough curve of H₂S adsorbed by FRPM

Considering the BET surface area of FRPM ($0.3 \text{ m}^2/\text{g}$), the area specific H_2S adsorption capacity was approximately $0.4 \text{ mg}/\text{m}^2$. This value was much larger than activated carbon in lab-scale experiments (approximately $0.003 \text{ mg}/\text{m}^2$) (Xiao, Wang *et al.* 2008). This suggests that the adsorption mechanism of FRPM is different than activated carbon or other carbonaceous materials; although the appearance of both is similar. According to the definition of porous material (Alonso-Lemus, Verde *et al.* 2009), the low BET surface area suggest that FRPD primarily consists of solid particles, although some literature suggests a porous structure. Since FRPM is non-porous with relatively high adsorption capacity, but with low BET surface area, the likely mechanism for adsorption becomes chemisorption, as opposed to physical adsorption.

It is logical to start with analyzing the composition and properties of FRPM to seek what active ingredients resulting in the adsorption ability. The typical composition of tire rubber is shown in Table 3-1.

Table 3-1 Composition of vehicle tire rubber (Lehmann et al., 1998).

Component	wt %
Polymer	62.1
carbon black	31
extender oils	1.9
zinc oxide	1.9
stearic acid	1.2
sulfur	1.1
other additives	0.7

Polymers are a main component of tire rubber. One of the most common is styrene-butadiene copolymer. However, there is no research mentioning the

reaction between H_2S and these polymers, while other two major components, carbon black and zinc oxide, were reported to adsorb H_2S separately (Boehm, 1966; Li, 2008; Hassan, 2010; Samokhvalov and Tatarchuk, 2011). Both of them could contribute to H_2S adsorption to some degree.

Carbon black

As carbonaceous material, carbon black has a similar adsorption mechanism of H_2S as activated carbon. On the surface of carbonaceous media, oxidation functionalities, such as carboxyl, anhydride, lactone, and phenol, would oxidize H_2S into sulfur element (Bagreev and Bandosz, 2001). Carbon black is one of the main components in rubber products, which provides the backbone for rubber fibers to build on (Peng, 2007). Although most of the pores in carbon black have been filled, the BET surface area test of FRPM still showed the existing of mesopore with diameter of 9 nm. TGA curve (Figure 3-2) is usually used to estimate the proportion of carbon black in FRPM.

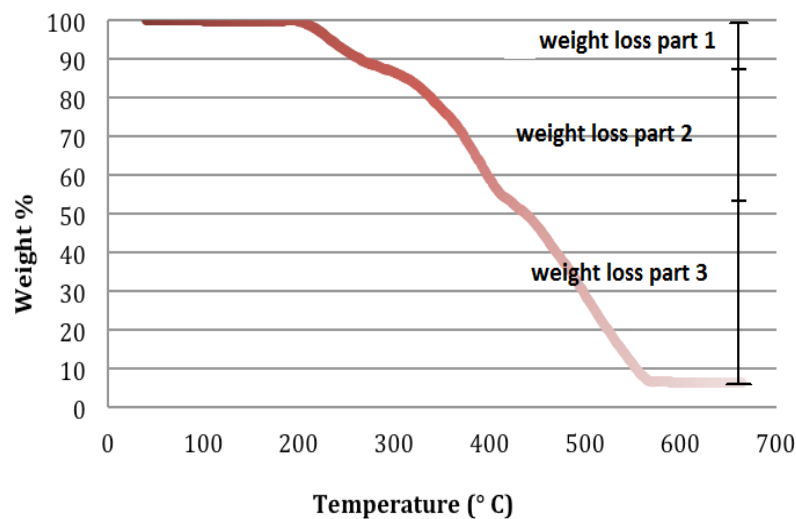


Figure 3-2 TGA curve of FRPM

In the TGA figure, the curve part could be divided into three parts presenting three different major thermal sensitive compositions in tire rubber: the weight loss part one is thought to be the weight percentage of carbon black (Loadman, 1998); the upper part 2 and part 3 attribute to oil and polymer, respectively. The carbon black content in FRPM is approximately 40% weight percentage, which is higher than that reported in Table 3-1. The ultimate analysis (Table 3-2) also shows the large percentage of carbon in FRPM, which also correlates with the high content of carbon black and polymer constituents.

Table 3-2 Ultimate analysis result of FRPM compared with previous reports

Ultimate analysis (dry, %)	FRPM	Passenger car tire ^a	Truck tire ^a
C	83.10	74.3	83.20
H	8.19	7.2	7.70
N	0.45	0.9	1.50
S	1.84	15.89	6.16
O*	6.44	1.71	1.44

* The relative of oxygen is calculated by subtracting other four elements from 100%.

^a (Ucar *et al.*, 2005)

For carbonaceous material, e.g. activated carbon, surface oxidation also increases the adsorption capacity. This suggests that the preheated material has a higher H₂S adsorption capacity. FRPM has similar properties shown in Figure 3-3, in which preheated FRPM's adsorption capacity performs 20% better than the origin, non-preheated material. Although carbon black has a role in the

adsorption of H_2S , quantitative analysis is a big challenge since some activated carbon black pores have been filled with polymers and there is no effective way to figure out the portion of these pores. Although some pores of carbon black are filled by rubber polymer, some could be available for gas adsorption.

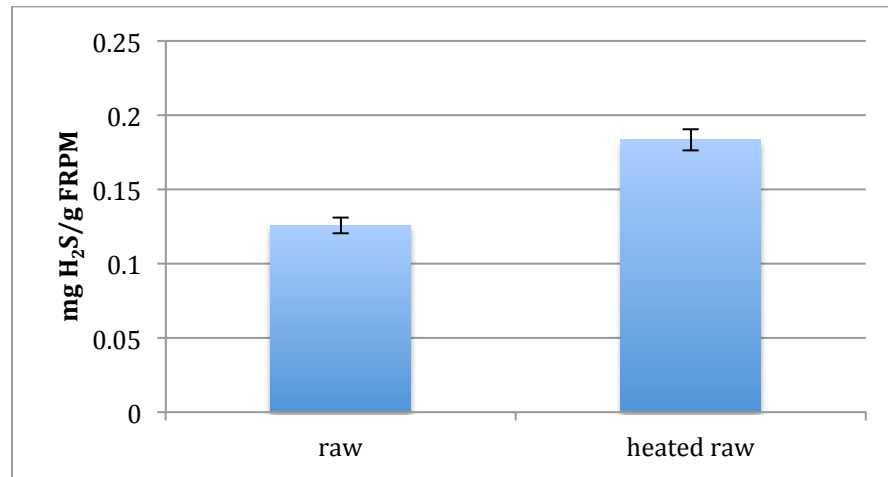


Figure 3-3 Adsorption capacity of H_2S on preheated FRPM

Zinc

The other potential active components in H_2S adsorption are metal compounds (mostly Zn compounds) in FRPM. Usually, excess zinc oxide is added with stearate acid for vulcanization of rubber and some investigators get good vulcanization results by using zinc stearate directly instead of both zinc oxide and stearate acid (Helaly et al, 2011). Zinc stearate generation might result from the solubilization of ZnO in fatty acids during the vulcanization process. Because solubilized ZnO performs better than solid ZnO particles, to gain better dispersion and solubility of zinc ions, zinc stearate might replace ZnO as the activator (Rodgers, 2004). Figure 3-4 shows the relationship between

carbon black and zinc stearate working together to construct a firm rubber structure.

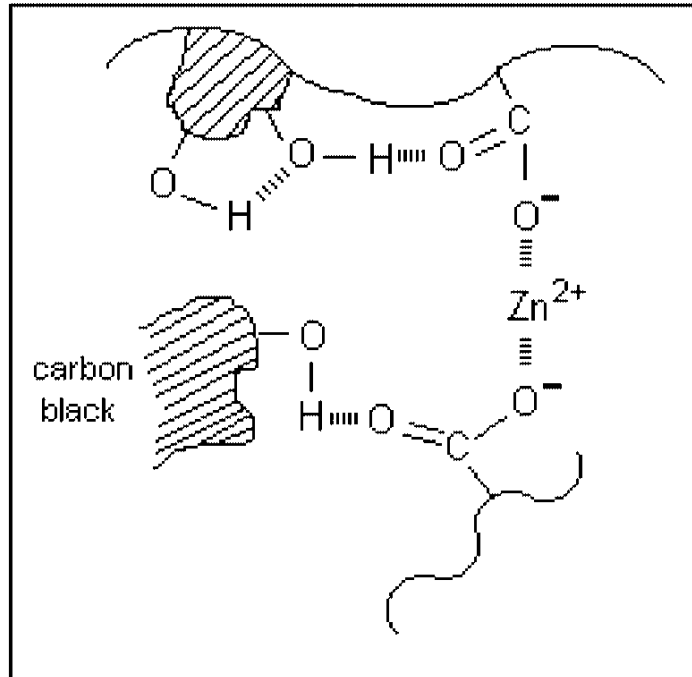


Figure 3-4 Schematic representation of the interaction between zinc stearate and tire rubber (Segre et al., 2002).

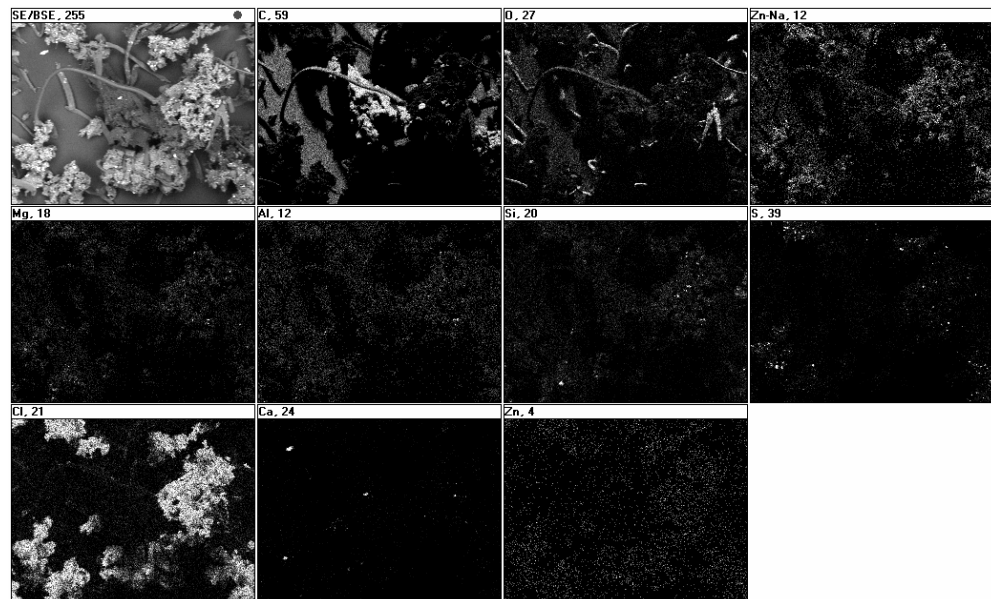
Table 3-3 shows a list of metal elements and their weight concentration in FRPM via AAS and AES methods. The concentration of zinc is much higher than other metals because zinc oxide is one of major components of rubber producing. However, both AAS and AES analyses destroyed the rubber samples. Therefore, the metal surface distribution could not be determined.

Table 3-3 AAS/AES analysis results of FRPM.

Metal	mg/kg	Standard error
Calcium	2,398	± 585
Magnesium	462.5	± 28.9
Copper	7.22	± 0.243
Iron	1,183	± 465
Lead	7.67	± 1.29
Zinc	15,690	± 2,079

A SEM image analysis of FRPM could avoid this problem and shows the surface distribution of metals. The zinc distribution is shown in the Figure 3-5.

The illuminated areas represent the presence of zinc.

**Figure 3-5 SEM image of FRPM (scale 150:1)**

Because the usage of zinc oxide is in excess during manufacturing, excess zinc oxide may remain in the produced tire rubber. Unfortunately, the actual forms of zinc compound within the rubber are still not known (Heideman et al, 2011). Then, it is arbitrary to attribute the adsorption ability to zinc oxide on FRPM, though zinc oxide is a popular H₂S scrubber. It was shown that zinc is involved in the crosslinking reaction through sulfur crosslinks, a Zn atom being necessary to form a two-sulfur-atoms crosslink. Some researchers argue that zinc might exist as a S-Zn-S ionic bond during vulcanization (Heideman et al, 2011; Marzocca et al, 2006). Some excess zinc oxide works as a H₂S controller during the rubber production and forms zinc sulfate. However, according to the XPS analysis of FRPM in Table 3-4, the atom percentages demonstrate that Zn/S ratio is much larger than ½. This suggests the existence of Zn-O ionic bonds besides Zn-S bonds.

Table 3-4 XPS result of FRPM

Element	Atom %	Standard error
C1s	90.14	1.22
N1s	0.30	0.14
O1s	7.61	1.31
S2p	0.32	0.16
Zn2p3/2	1.64	0.11

According to the HSAB (Hard-Soft-Acid-Base) theory, Zn²⁺, as an intermediate acid, prefers to react with sulfur-containing ligands (soft base, such as HS⁻ and S²⁻) to oxygen-containing ones (hard base, such as O²⁻ and R-COO⁻). The mechanism is similar to solid ZnO scrubbing H₂S. In the reaction, an ionic compound ZnO dissociate H₂S into H⁺ and HS⁻, followed by diffusion of HS⁻ into

the oxide lattice and migration of oxide and water out. This reaction could occur without the participation of H_2O . FRPM could also facilitate H_2S removal in a dry environment. Figure 3-6 shows the adsorption capacity.

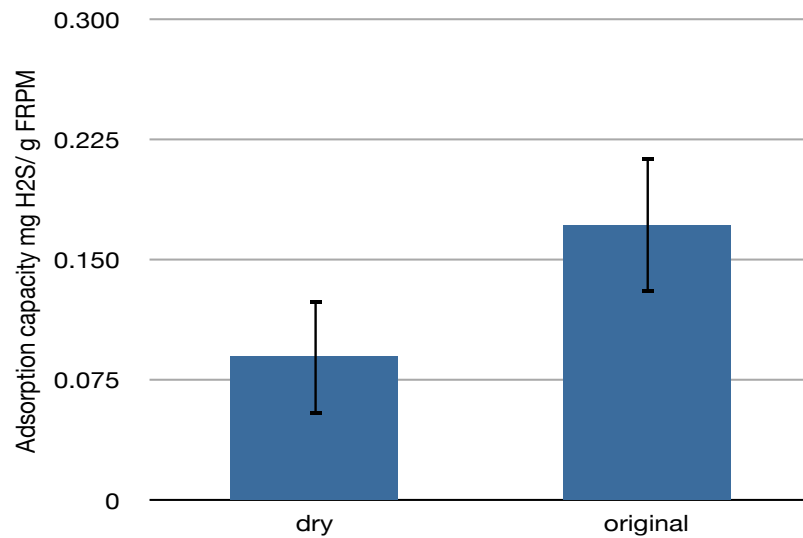


Figure 3-6 Adsorption capacity of H_2S on dry FRPM

Dry FRPM remained half of adsorption capacity of original FRPM. The water's role in the process cannot be ignored even though the moisture content of FRPM is as low as 0.5%wt. Water can promote the ionization of H_2S gas and increase the contact opportunity so as to remove more H_2S molecules during the same operation period. Besides zinc oxide, solid zinc stearate also adsorbs H_2S , which have been shown in this research. Figure 3-7 reflects the result of a batch test between zinc stearate and H_2S gas. A concentration of 500 ppmv of H_2S was totally adsorbed in less than 20 minutes using 20 g of zinc stearate.

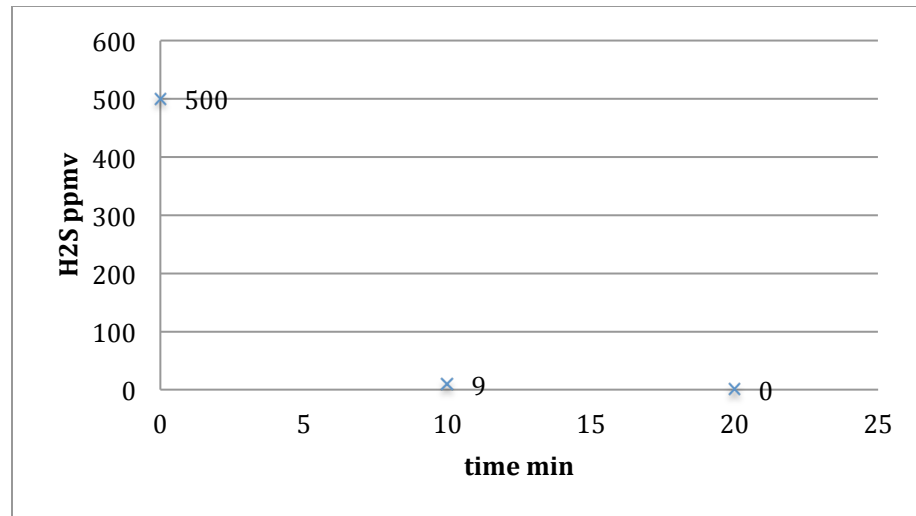


Figure 3-7 Reaction between zinc stearate and H₂S

The zinc surface distribution could be altered by acid or base solution washing since both ZnO and zinc stearate dissolve in these solutions. Table 3-5 shows the weight percentage of zinc after extraction with nitric acid and sodium hydroxide solution.

Table 3-5 Zinc extraction efficiency of FRPM.

	Zinc extraction efficiency %*			
	Primary extraction	Secondary extraction	Tertiary extraction	Individual 5-day extraction
HNO ₃ (0.1 N)	4.0%	0.36%	0.26%	5.52%
HNO ₃ (0.5 N)	4.4%	0.36%	0.36%	4.73%
NaOH (0.1 N)	1.2%	0.33%	---	---
NaOH (0.5 N)	2.1%	0.18%	---	---

* The percentage based on the total zinc amount in FRPM detected.

All one-day primary extraction efficiencies are less than 5%, which might appear low. However, because only zinc existing on or close to the surface of

FRPM could be removed rather than that inside the rubber particle, while the extraction rates were calculated based on the total zinc concentration (Table 3-4) including surface and bulk. The zinc inside the FRPM has no opportunity to contact with extractants. The results showed that extended contact time improved the zinc extraction but primary one-day extraction could remove most of the surface zinc. It favored the higher concentration extractant for both solutions, but the effect was not as dramatic for HNO_3 as it was for NaOH . The surface intensity change of zinc could be detected by an X-ray photoelectron spectroscopy (XPS) experiment before and after HNO_3 extraction, as presented in Figure 3-8, which shows the zinc surface distribution via XPS.

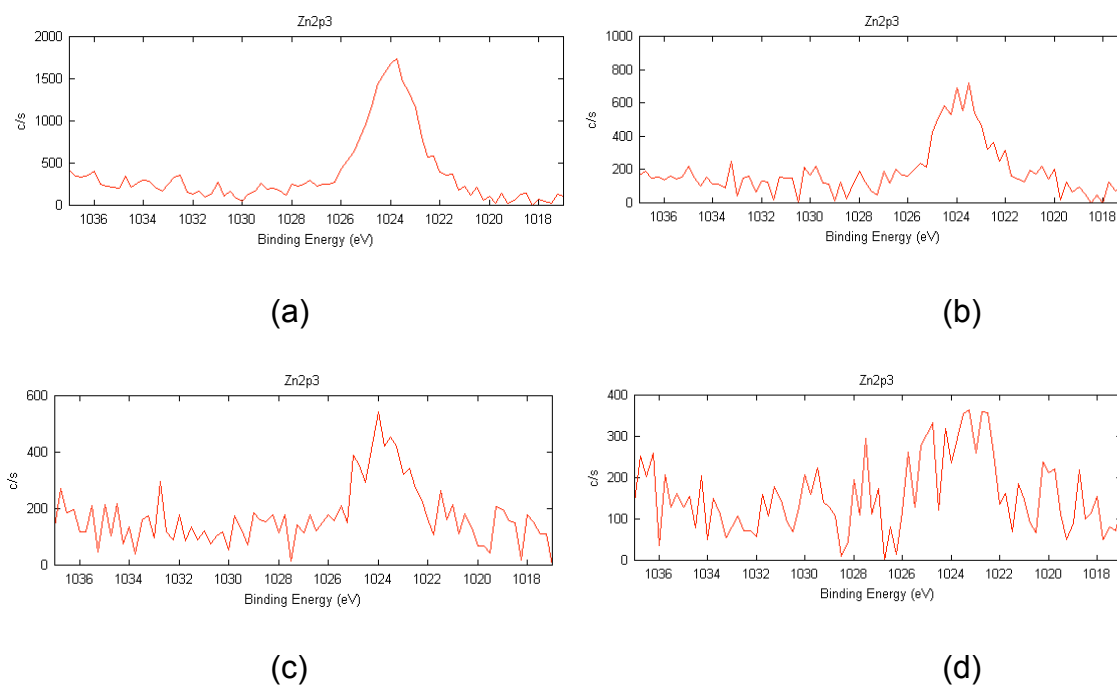


Figure 3-8 XPS spectra of Zinc element on FRPM (a. original FRPM; b. 0.1 N HNO_3 extracted FRPM; c. 0.1 N HCl FRPM; d. 0.5 N NaOH extracted FRPM).

The peak of Zn (2p 3/2) appeared at the binding energy of approximately 1024 eV on the original FRPM, which means that a certain amount of zinc element with valence +2 was distributed on the surface of the rubber particles. The signal intensity of Zn of other treated FPRMs was decreased to a different degree. The peaks could still be recognized in the spectra of HCl and HNO₃ extracted FRPM. However, the signal strength was much lower compared with original and may be hard to distinguish with the background noise. For NaOH treated sample, the peak completely disappeared in the signal noise. These changes of spectra demonstrate that all three treatments decrease the distribution of surface zinc. However, XPS only detected the element distribution to the depth of 10 nm of the surface. Some zinc that exist in the cracks or pores in rubber particles may not be determined. Another concern is that in Table 3-5, HNO₃ solution shows a better extraction efficiency, while the XPS spectra shows that NaOH solution worked well on surface zinc removal. The reason could be the HNO₃ destroyed some fiber structure of the FRPM and released more zinc from bulk particle rather than surface. The adsorption capacity results of the treatment FRPM are shown in Figure 3-9.

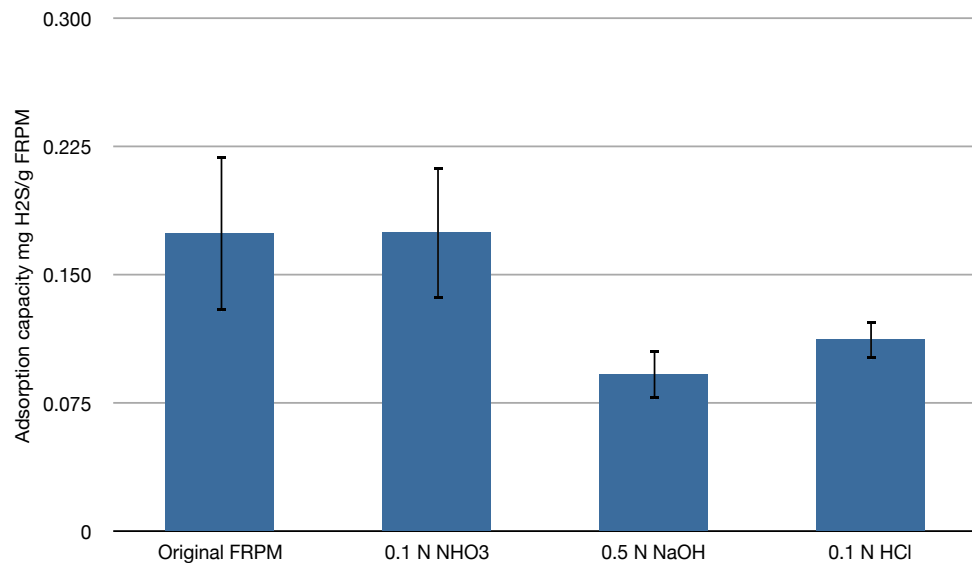


Figure 3-9 Adsorption capacity of zinc-extracted FRPM

From the results, either NaOH or HCl treated FRPM shows a certain loss of adsorption capacity of H₂S. This matches the fact of zinc decrease demonstrated by XPS spectra. However, the interesting observation is that HNO₃ extraction did not shift the capacity much as expected, though its zinc removal effect is similar to HCl. It could be attributed to the increasing surface functional groups caused by the oxidation by HNO₃. Through the previous hypothesis, two possible kinds of active sites result in H₂S adsorption--carbon black and metal ions. Since the zinc concentration differed from the original FRPM, it is possible that the surface properties of carbon black were renovated to compensate the adsorption capacity loss of zinc. HNO₃ solution might increase the number of the functional groups. This is similar to the adsorption property of carbonaceous materials. Many researchers have shown that the

oxidation of carbon material, such as activated carbon and carbon black, by nitric acid can improve the adsorption of H₂S (Bagreev et al, 2001).

Conclusions

Through the investigation of properties and surface characterization of FRPM, some factors affecting adsorption were revealed. The specific surface was much lower than activated carbon and porous materials. Rubber particle materials were more particulate in nature rather than porous. It suggested that physical adsorption could not work alone to remove H₂S. Metal concentrations, especially zinc, were relatively high in FRPM, which benefits the adsorption by reaction between metal oxides and H₂S. Carbon black comprised around 40% of the weight of the rubber particle material, on which the functionality groups also capture H₂S molecules. Consequently, chemisorption may be the primary adsorption mechanism, and both zinc oxide and carbon black could be the active components. Generally speaking, the adsorption mechanism of H₂S on FRPM is complex and involves a combination of zinc compounds and carbon black.

References

- Adib, F.; Bagreev, A.; Bandosz, T. (1999) Effect of Surface Characteristics of Wood-Based Activated Carbons on Adsorption of Hydrogen Sulfide. *Journal of colloid and interface science*, **214** (2), 407-415.
- Bagreev, A.; Bandosz, T. (2001) H₂S Adsorption/Oxidation on Unmodified Activated Carbons: Importance of Prehumidification. *Carbon*, **39** (15), 2303-2311.
- Bagreev, A.; Bandosz, T. (2000) Study of Hydrogen Sulfide Adsorption on Activated Carbons Using Inverse Gas Chromatography at Infinite Dilution. *J. Phys. Chem. B*, **104** (37), 8841-8847.
- Bandosz, T. (1999) Effect of Pore Structure and Surface Chemistry of Virgin Activated Carbons on Removal of Hydrogen Sulfide. *Carbon*, **37** (3), 483-491.
- Boehm, H. (1966) Chemical Identification of Surface Groups. *Advances in catalysis*, **16** 179-274.
- Boudou, J.; Chehimi, M.; Broniek, E.; Siemieniowska, T.; Bimer, J. (2003) Adsorption of H₂S or SO₂ on an Activated Carbon Cloth Modified by Ammonia Treatment. *Carbon*, **41** (10), 1999-2007.
- Entezari, M.; Ghows, N.; Chamsaz, M. (2005) Combination of Ultrasound and Discarded Tire Rubber: Removal of Cr (Iii) from Aqueous Solution. *Journal of Physical Chemistry A*, **109** (20), 4638-4642.
- Garcia, C.; Lercher, J. (1992) Adsorption of Hydrogen Sulfide on Zsm 5 Zeolites. *The Journal of Physical Chemistry*, **96** (5), 2230-2235.
- Hassan, K.H. (2010) Regeneration and Activity Test of Spent Zinc Oxide Hydrogen Sulfide Removal Catalyst, *European Journal of Scientific Research*, **39** (2) 289-295
- Heideman, G.; Datta, R.N. ; Noordermeer, J.W.M.; Van Baarle, B. (2004) Activators in Accelerated Sulfur Vulcanization. *Rubber Chemistry and Technology*, **77**, (3), 512-541.
- Helaly, F.M.;El Sabbagh, S.H.; El Kinawy, O.S. ; El Sawy, S.M. (2011) Effect of synthesized zinc stearate on the properties of natural rubber vulcanizates in the absence and presence of some fillers. *Materials & Design* **32**, (5), 2835–2843
- Kim, J.; Park, J.; Edil, T. (1997) Sorption of Organic Compounds in the Aqueous Phase onto Tire Rubber. *Journal of Environmental Engineering*, **123** (9), 827-835.
- Lehmann, C.; Rostam-Abadi, M.; Rood, M.; Sun, J. (1998) Reprocessing and Reuse of Waste Tire Rubber to Solve Air-Quality Related Problems. *Energy Fuels*, **12** (6), 1095-1099.

- Leung, D.; Yin, X.; Zhao, Z.; Xu, B.; Chen, Y. (2002) Pyrolysis of Tire Powder: Influence of Operation Variables on the Composition and Yields of Gaseous Product. *Fuel Processing Technology*, **79** (2), 141-155.
- Li, G.; Stubblefield, M.; Garrick, G.; Eggers, J.; Abadie, C.; Huang, B. (2004) Development of Waste Tire Modified Concrete. *Cement and Concrete Research*, **34** (12), 2283-2289. [7]Lehmann, C.; Rostam-Abadi, M.; Rood, M.; Sun, J. (1998) Reprocessing and Reuse of Waste Tire Rubber to Solve Air-Quality Related Problems. *Energy Fuels*, **12** (6), 1095-1099.
- Lin, C.; Huang, C.; Shern, C. (2008) Recycling Waste Tire Powder for the Recovery of Oil Spills. *Resources, Conservation & Recycling*, **52** (10), 1162-1166.
- Lisi, R.; Park, J.; Stier, J. (2004) Mitigating Nutrient Leaching with a Sub-Surface Drainage Layer of Granulated Tires. *Waste Management*, **24** (8), 831-839.
- Marzocca, A. J.; Mansilla, M. A. (2006) Vulcanization Kinetic of Styrene-butadiene Rubber by Sulfur/TBBS. *Journal of Applied Polymer Science*. **101**, (1), 35-41.
- Meng, X.; Hua, Z.; Dermatas, D.; Wang, W.; Kuo, H. (1998) Immobilization of Mercury (II) in Contaminated Soil with Used Tire Rubber. *Journal of Hazardous Materials*, **57** (1-3), 231-241.
- Novochinskii, I.; Song, C.; Ma, X.; Liu, X.; Shore, L.; Lampert, J.; Farrauto, R. (2004) Low-Temperature H₂S Removal from Steam-Containing Gas Mixtures with ZnO for Fuel Cell Application. 1. ZnO Particles and Extrudates. *Energy and Fuels*, **18** (2), 576-583.
- Park, J. (2004) Effectiveness of Scrap Tire Chips as Sorptive Drainage Material. *Journal of Environmental Engineering*, **130**, 824.
- Peng, Y.K. (2007) The effect of carbon black and silica fillers on cure characteristics and mechanical properties of breaker compounds, M.S. Thesis
- Purakayastha, P.; Pal, A.; Bandyopadhyay, M. (2002) Adsorption of Anionic Surfactant by a Low-Cost Adsorbent. *Journal of environmental science and health. Part A, Toxic/hazardous substances & environmental engineering*, **37** (5), 925-938.
- Purakayastha, P.; Pal, A.; Bandyopadhyay, M. (2005) Sorption Kinetics of Anionic Surfactant on to Waste Tire Rubber Granules. *Separation and Purification Technology*, **46** (3), 129-135.
- Putman, B.; Amir Khanian, S. (2004) Utilization of Waste Fibers in Stone Matrix Asphalt Mixtures. *Resources, Conservation & Recycling*, **42** (3), 265-274.
- Rodgers, B. (2004) Rubber Compounding – Chemistry and Applications, Marcel Dekker, Inc.

- Samokhvalov, A. and Tatarchuk, B.J. (2011) Characterization of active sites, determination of mechanisms of H₂S, COS and CS₂ sorption and regeneration of ZnO low-temperature sorbents: past, current and perspectives, *Phys. Chem. Chem. Phys.* **13**, 3197–3209
- Segre, N.; Joekes, I.; Galves, A.; Rodrigues, J. (2004) Rubber-Mortar Composites: Effect of Composition on Properties. *Journal of Materials Science*, **39** (10), 3319-3327.
- Seredych, M.; Strydom, C.; Bandosz, T. (2008) Effect of Fly Ash Addition on the Removal of Hydrogen Sulfide from Biogas and Air on Sewage Sludge-Based Composite Adsorbents. *Waste Management*, **28** (10), 1983-1992.
- Siddique, R.; Naik, T. (2004) Properties of Concrete Containing Scrap-Tire Rubber—an Overview. *Waste Management*, **24** (6), 563-569.
- Truong, L.; Abatzoglou, N. (2005) A H₂S Reactive Adsorption Process for the Purification of Biogas Prior to Its Use as a Bioenergy Vector. *Biomass and Bioenergy*, **29** (2), 142-151.
- Tsai, J.; Jeng, F.; Chiang, H. (2001) Removal of H₂S from Exhaust Gas by Use of Alkaline Activated Carbon. *Adsorption*, **7** (4), 357-366.
- Ucar, S.; Karagoz, S.; Ozkan, A.; Yanik, J. (2005) Evaluation of Two Different Scrap Tires as Hydrocarbon Source by Pyrolysis. *Fuel*, **84** (14-15), 1884-1892.
- Xiao, Y.; Wang, S.; Wu, D.; Yuan, Q. (2008) Experimental and Simulation Study of Hydrogen Sulfide Adsorption on Impregnated Activated Carbon under Anaerobic Conditions. *Journal of Hazardous Materials*, **153** (3), 1193-1200.
- Yuan, W.; Bandosz, T. (2007) Removal of Hydrogen Sulfide from Biogas on Sludge-Derived Adsorbents. *Fuel*, **86** (17-18), 2736-2746.

CHAPTER 4 THE IMPROVEMENT OF HYDROGEN SULFIDE ADSORPTION ON FINE RUBBER PARTICLE MEDIA (FRPM)

Introduction

Hydrogen sulfide (H_2S) is a harmful and malodorous gaseous compound commonly found in biogas, sewer gas, and other wastewater treatment system off-gasses (Boudou, et al., 2003). In anaerobic environments, H_2S is generated from the metabolic activities of sulfur-reducing bacteria. H_2S can threaten the health of workers, corrode metal and concrete facilities, attack electrical and electronic components, and damage conveyance systems in wastewater treatment plants. In addition, biogas from anaerobic digestion contains potentially high concentrations of H_2S . Ideally, the H_2S concentration should be lowered to less than 50 ppmv before entering internal combustion engines. With increased prices of fossil fuels, including oil, coal, and natural gas, biogas, as a bio-renewable alternative, could sustainably mediate increasing energy consumption. However, the pressing challenge is to find an efficient and cost-effective way to reduce H_2S concentrations prior to use. Adsorption is an effective and comparatively easy method to control H_2S . Although traditional commercial H_2S adsorbents, such as activated carbon and metal oxides, can effectively remove H_2S , they are expensive. In this project, a cheaper but

efficient adsorbent, fine (less than 1 mm in diameter) rubber particle media (FRPM), was selected and studied.

FPRM has been found to adsorb hydrogen sulfide (H_2S) from biogas in previous research (Ellis, et al., 2008, Evans et al., 2010). It is derived from consumer waste sources, such as discarded vehicle tires. It can also be derived from manufacturing processes, such as belt and gasket manufacturing and tire retreading operations. Utilizing the rubber waste as an adsorbent in environmental applications reduces the volume of this material that would otherwise go to landfilling or incineration. The consequence of rubber reuse in terms of sustainability and environmental protection are compelling. Compared with traditional H_2S adsorbents, such as activated carbon, the economic advantage makes FRPM a potentially attractive alternative. The challenge of FRPM reuse in scrubbing applications concerns how to increase its adsorption capacity so that it competes well with traditional adsorbents in terms of effectiveness and life cycle cost.

In this research, lab-scale tests were conducted to obtain the optimum operating conditions to increase the H_2S adsorption capacity of FRPM. Temperature and packing density were adjusted in the H_2S breakthrough tests.

Materials and Methods

Reactor

A fabricated double-layer copper cylinder served as the H_2S -FRPM reactor, shown in Figure 4-1. H_2S gas, from a cylinder containing 500 ppmv of

nitrogen, was continuously passed through an FRPM bed with a flowrate of 0.2 L/min controlled by a flowmeter. The concentration of H_2S in the outlet gas was detected with a sensor (Jerome 860 H_2S sensor, Arizona Instrument Inc.), which recorded the H_2S concentration data at 2-second intervals. Due to the operational requirement of the sensor that oxygen must be present in the detection process, air was pumped in and diluted the outlet gas at the same flow rate. For safety consideration, the entire test apparatus was put in a fume hood to avoid H_2S escaping into the laboratory.

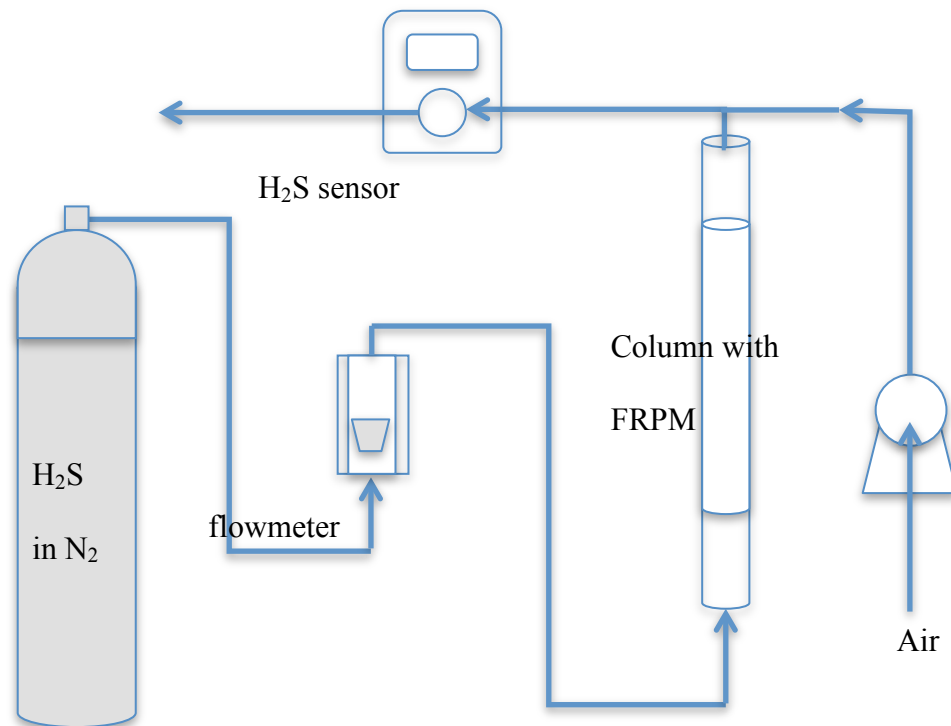


Figure 4-1 Schematic of FRPM H_2S adsorption experiments

Breakthrough curve

The H₂S adsorption capacities on FRPM were calculated based on breakthrough curves, which represented the relationship between outlet H₂S concentration and elapsed time. In this research, the breakthrough curves were obtained by continuously monitoring the concentration of the effluent H₂S flow through a water jacketed metal column packed with FRPM until a concentration of 200 ppmv was reached, which is the recommended accuracy limit of the sensor (with less than 5% error).

Temperature

Using the double-layer structure of the metal column, the operating temperature was controlled by passing water through the water jacket. The desired temperature was maintained by circulating certain temperature water from thermostatic water bath (EX-111, Neslab instrument, inc.). In this research, adsorption capacities of H₂S on FRPM were determined at 20°C, 30°C, 60°C, and 85°C respectively. Before the H₂S adsorption experiments, the reactor was packed with FRPM and pre-heated to the experimental temperature. The adsorption capacities were acquired following the previously mentioned breakthrough curve procedure. To avoid error from the copper metal reactor, the potential influence on H₂S adsorption of the empty column was evaluated under each temperature with the significance determined by analysis of the variance.

Packing amounts

The reactor was packed with different volumes of FRPM: 25, 50, 75 and 100% of the column volume (20 g, 40 g, 60 g, and 80 g) without extra packing

pressure aside from gravity. Following the breakthrough curve procedure, the adsorption capacities were obtained for analysis.

Size distribution effect

FRPM samples were separated by diameter (less than 0.6 mm, between 0.6 mm and 1 mm, and larger than 1 mm) with dry sieves. All three size categories of samples were conducted for adsorption capacity experiments separately.

Moisture content effect

The moisture content of FRPM sample was adjusted by adding water. All water-saturated samples were placed in the oven for different time spans under 90°C. Each sample was cooled down for 24hr under room temperature and moisture contents were analyzed prior to the adsorption capacity tests.

Zinc effect

The high concentration of zinc in FRPM and its potential capacity to react with H₂S required additional investigation of its effect on H₂S adsorption. Zinc was added into and extracted from FRPM to determine the change of the adsorption ability on H₂S. In reference to zinc addition, FRPM samples were rinsed in known-concentration ZnCl₂ solutions and shaken for 12 hr for zinc to fix on the FRPM. Dehydration and moisture content balance were conducted for all the treated samples before testing the H₂S adsorption capacity. Zinc extraction experiments were performed with nitric acid and sodium hydroxide solutions separately. After rinsing and shaking for 24 hr in these solutions, the mixtures were filtered with a Büchner funnel and filter glass paper. A GBC 932 plus

Atomic Absorption Spectrophotometer (GBC Scientific (USA) LLC.) was used for the determination of zinc concentrations in the filtered solutions. After drying and moisture balancing, the separated solids were used for adsorption capacity experiments. The same procedure was repeated for secondary extraction and tertiary extraction. To reveal the zinc extraction rate with nitric acid, a five-day rinse was made to compare with the 24hr extraction.

Results and Discussion

A breakthrough curve of H₂S on FRPM was constructed with data points monitored and measured by the H₂S sensor at two-second intervals (Figure 4-2). H₂S started to breakthrough the scrubber after approximately 30 minutes, which was much later than the empty column contact time (by several minutes). This means that FRPM was able to effectively adsorb H₂S. This positive result suggests possible H₂S removal from biogas produced from an anaerobic digestion process in a wastewater treatment system. The result is supported by previous research by the same research group (Siefers, et al., 2010). Based on breakthrough curves, the average adsorption capacity was approximately 0.2 mg H₂S/g FRPM estimated by the software Origin 8.0 (OriginLab Corporation). Compared with activated carbon, 2~3mg H₂S/g adsorbent (Xiao, et al, 2008), the absorption capacity of the rubber particles was significantly lower. However, considering the manufacturing cost, several dollars per ton for FRPM versus thousands dollars for activated carbon, the financial advantage of the former method is obvious. The adsorption capacity of FRPM was also lower than that in

the pilot-scale experiment, which was conducted at the Ames Water Pollution Control Plant (Siefers, et al, 2010). Although the previous results were generated with a shorter contact time and smaller reactor, it did not impact our investigation, since the main purpose of the current project was to evaluate the absorption capacity under different operating conditions, with the goal of maximizing the adsorption capacity in the lab-scale experiments.

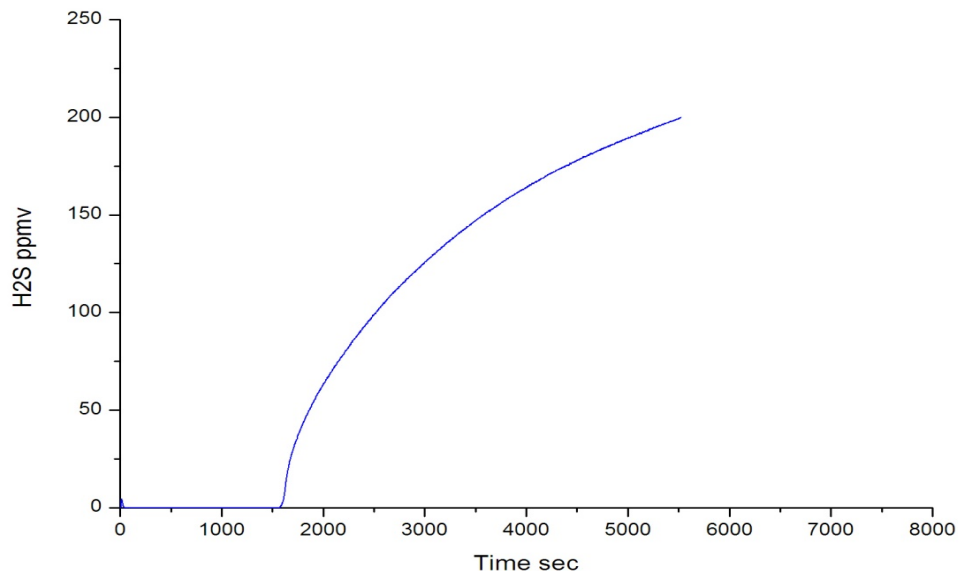


Figure 4-2 Hydrogen sulfide breakthrough curve (analysis was stopped at 200 ppmv to protect sensor)

The effects of packing density of FRPM on H₂S removal are shown in Figure 4-3. Among the different packing densities, FRPM showed the maximum adsorption capacity at a packing density of 75% of the column volume. The adsorption capacities increased with the packing density, which could be caused

by more opportunity for contact between the H₂S molecules and FRPM. In each column, higher packing quantity resulted in larger adsorption bed length and the adsorbate covers a longer distance through the adsorbent. Unlike a liquid phase scrubber, there was a large amount of pore space among the rubber particles, which enabled H₂S to have less opportunity to reach adsorbate-adsorbent equilibrium before exiting. Then, a longer contact time increased the efficiency of the adsorbent. It has been pointed out that the length of reaction bed influences positively the adsorption for some solid adsorbents (Noll, 1992).

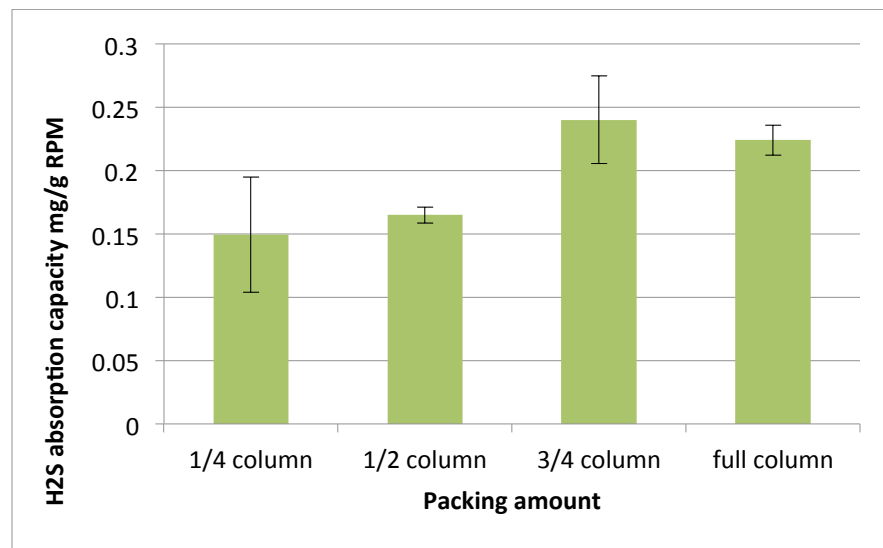


Figure 4-3 Effect of FRPM packing quantity on adsorption capacity

Analysis of variance (Table 4-1) showed packing density had a significant influence on H₂S adsorption capacities on FRPM. Packing densities greater than half the column volume resulted in significant improvements in H₂S removal compared with densities less than half the column volume. However, the

difference between 75% and full column volume was not statistically significant. It is believed that bed length was not the only reason causing the adsorption capacity variance, which may depend on other parameters such as concentration and pressure (Godini and Mowla, 2008).

In ideal conditions, no matter how much the reactor is packed, the H₂S adsorption capacity of FRPM should show no significant difference among those density differences. However, the result, shown in Figure 4-3, demonstrates that the capacity depends on the packing amount. Half full or full packing FRPM can adsorb more H₂S than less packing. This phenomenon could result from the compression of the rubber material. The gravity change caused by packing could increase the bulk density of FRPM and shrink the space between particles. Then H₂S molecules have more opportunity to collide and bond with rubber particles. The fact that the FRPM is not a homogeneous material may also contribute to the observation. Not all FRPM was contacted with H₂S when gas passed through the spaces of the irregular and loose adsorbent before arriving on the surface of FRPM. This perhaps is another reason why the longer adsorbent packing brings higher adsorption capacity by increasing the contacting time.

**Table 4-1 Analysis of variance of packing quantity by JMP 10.0
(Statistical software, SAS institute)**

Alpha =0.05		
t=2.20099		
Packing size	Adsorption capacity mg/g	Difference significance
80 g	0.31	a*
60 g	0.28	a
40 g	0.20	b*
20 g	0.16	b

* Different letter means significant difference while same letter means no significant difference

According to previous research, the adsorption mechanism of H₂S on FRPM attributes mostly to chemisorption in which temperature plays an important role (Wang, et al, 2010). The H₂S adsorption capacity of carbonaceous material varies with the operating temperatures due to the higher surface diffusion and mass transfer. While carbon black is one of the main components of FRPM and plays an important role in the adsorption mechanism (Wang, et al, 2010), it was postulated that temperature would alter H₂S removal efficiency. The results, shown in Figure 4-4, agree with the assumption that the adsorption capacity increases dramatically with temperature. The trend suggests that there is a quadratic relationship between temperature and H₂S removal.

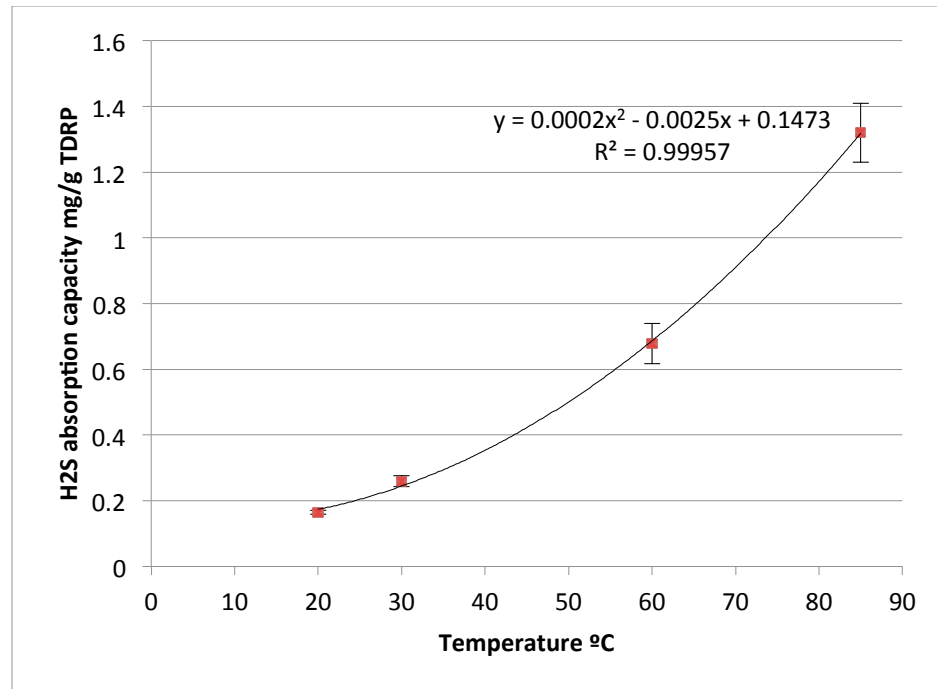


Figure 4-4 Effect of temperature on adsorption capacity

Increased temperature caused significant influence on the adsorption capacity (Table 4-2). Two reasons might help to explain this phenomenon. One is that the chemical reaction rate (i.e., kinetics) between H₂S and active sites within the composition of FRPM, believed to be an acid-base reaction, might be enhanced during higher temperature. The other one is that there was a higher molecular diffusion rate of H₂S, which was trapped or oxidized when it entered the carbon black pores in the same time period. Although higher temperature could improve the performance of FRPM, the effect was, to some extent, dependent on the original biogas composition and source. These results suggest that the adsorption scrubber should be placed in close proximity to the source to minimize cooling. Additionally, the experiments also indicate that FRPM plugging

may occur at temperatures of 100°C or greater and after 12 hours, which may limit the allowable operating temperature.

**Table 4-2 Analysis of variance of temperature by JMP 10.0
(Statistical software, SAS institute)**

Alpha=0.05		LSD=0.104 mg/g
t=2.30600	Adsorption capacity mg/g	Difference significance*
20°C	0.16	c
30°C	0.26	c
60°C	0.68	b
85°C	1.32	a

* Different letter means significant difference while same letter means no significant difference

Previous research shows the size distributions of FRPM in Figure 4-5 (Ellis *et al.*, 2008). According to these results, the rubber material was divided into three size categories (diameter 0~0.6 mm, 0.6~1 mm and 1~ mm).

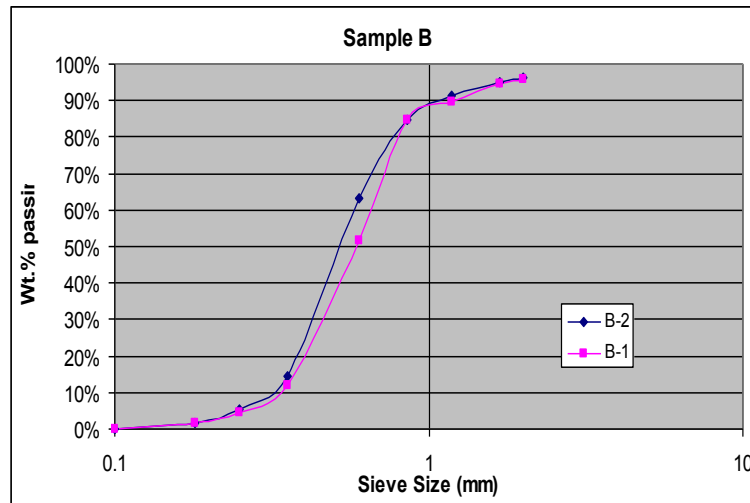


Figure 4-5 Size distribution of and FRPM (Ellis *et al.*, 2008)

The adsorption capacity of FRPM was found as a function of diameter of the rubber particle (shown in Figure 4-5). In this figure, the particle was assumed to be a regular sphere in order to estimate the surface area. From the results, the adsorption capacity favored a higher surface area. This verifies that the adsorption process occurs on the surface rather than throughout the bulk of the particle. A large surface area provides more opportunity for gas-adsorbent contact.

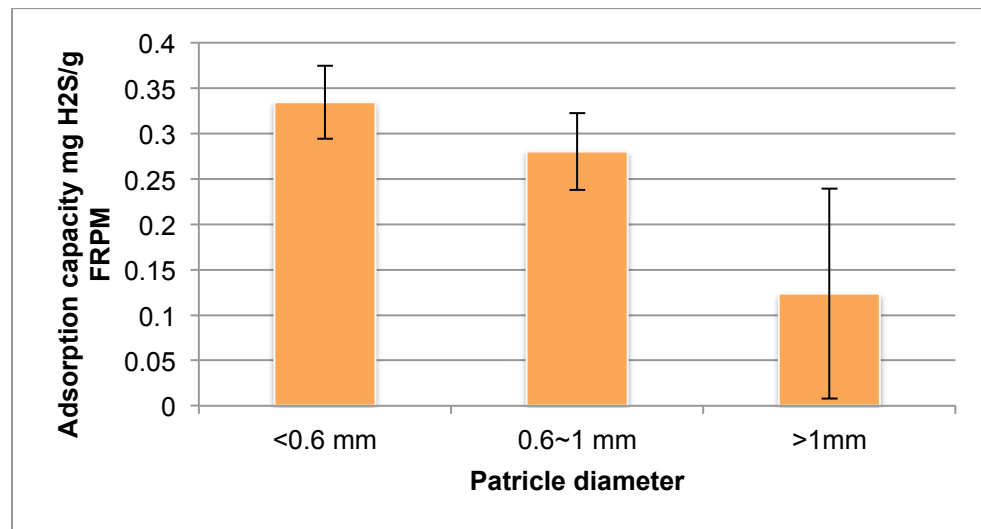


Figure 4-6 Adsorption capacity of different size of FRPM

Particle size selection could be an efficient way to improve FRPM performance. Larger diameter rubber particles have limited adsorption capacity, which is significantly lower than other smaller sizes (Table 4-3). To check the result of size distribution experiments, the theoretical adsorption capacity of the original sample was calculated in terms of the sum of three categories with

proper weight proportion. The result matches with the experimental data in this project.

**Table 4-3 Analysis of variance of particle size by JMP 10.0
(Statistical software, SAS institute)**

t=2.44691		
Alpha=0.05		
LSD=0.12 mg/g		
Diameter	Adsorption capacity mg/g	Difference significance*
<0.6 mm	0.28	a
0.6 mm~1 mm	0.23	a
>1 mm	0.09	b

* Different letter means significant difference while same letter means no significant difference

Studies on H₂S adsorption by activated carbon demonstrated that moisture content played an important role in the removal process. Moisture content decrease caused dramatic reduction of adsorption capacity (Bagreev and Badosz 2001; Bouzaza, Laplanche et al., 2004). A water film provides a favorable environment for H₂S oxidization by free radicals or reacting with other chemicals. An alternative assumption is that the limiting step in adsorption is that the dissolution of H₂S into the water on the surface of the adsorbent. Similar results were obtained from this research, shown in Figure 4-6.

Table 4-4 Adsorption capacity of FRPM with different moisture contents

	<i>Adsorption capacity (mg/g)</i>	<i>Time to 100 ppmv (min)</i>
Dry FRPM	0.13	47.2
Moisture content 1.07%	0.73	163.6
Moisture content 1.30%	0.81	180.4
Moisture content 3.8%	0.98	170.8
Moisture content 11.7%	1.67	196.5
Moisture content 18.9%	2.07	265.2

Table 4-4 shows that the adsorption capacity of an FRPM with a lower moisture content was lower than with a higher moisture content. Adsorption may require a chemical reaction in the aqueous phase, which means it requires water to provide a favorable adsorption environment. The fact that H₂S adsorption capacity of the dry FRPM sample was much lower than other higher moisture content sample suggests the important role water plays in the adsorption process. The solubility of H₂S in water at 25°C is about 3.5 mg/g, which is lower than the slope, 7.54 mg H₂S/g H₂O, of the trend line in Figure 4-7.

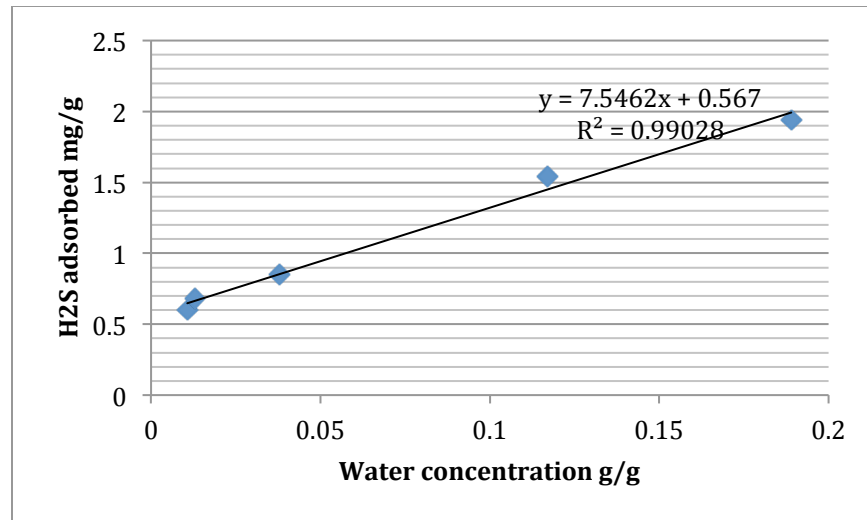


Figure 4-7 Relationship between H₂S adsorbed and water concentration (subtracting Dry FRPM H₂S adsorption capacity)

This means that the increased moisture content was not simply a function of H₂S solubility, but water may engage in the reaction along with other chemicals on the surface of FRPM. For instance, water may be part of the solvation complex, e.g. ZnS \cdot x(H₂O), in precipitation reactions involving H₂S on the surface of FRPM. The zinc concentration in FRPM was approximately 14 mg/g in terms of the metal analysis test (Wang, et al, 2010), while approximately 7 mg/g of H₂S would be consumed stoichiometrically based on the reaction (ZnO + nH₂O + H₂S \rightarrow ZnS \cdot (n+1) [H₂O]). Usually, zinc was added into the rubber precursors during the vulcanization process and works as an activation catalyst and a wear matrix (Bandosz 1999). The theoretical H₂S adsorption was several times larger than the measured amount (approximately 1 mg/g). It was possible that the moisture content contributes to the reaction kinetics and equilibrium if the reaction must take place in the aqueous phase. Furthermore, the zinc

concentration included both the bulk phase and on the surface of FRPM particles. The zinc inside FRPM had no opportunity to contact with H₂S gas, which means that the theoretical adsorption value is smaller. This suggests that the Zn reaction with H₂S may not be the only reason why H₂S is captured on FRPM.

In the zinc-impregnating test, zinc ion was precipitated on the surface of FRPM in order to double or triple the original zinc concentration in FRPM. It is known that rubber particles could adsorb metal ions from aqueous solutions (Alexandre-Franco, et al., 2011). Additionally, previous work has investigated the ability of FRPM to trap zinc ions (Fan, M. 2005). The adsorption capacity results (Figure 4-8) demonstrate that H₂S adsorption capacities are proportional to the zinc concentrations of FRPM samples. The moisture contents of the samples were not abnormal (about 1%) with the original ones. This suggests that the adsorption capacity change was not affected by moisture content but by the zinc addition. The interesting point is the way that the added zinc ion was bound on the surface of FRPM, which made the zinc ion retain the ability to react with H₂S.

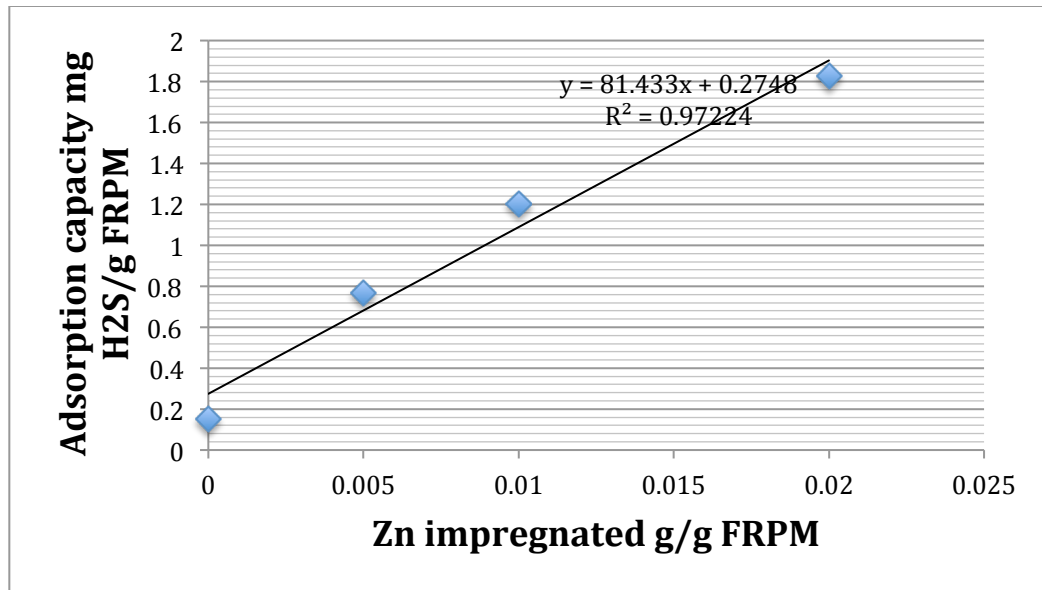


Figure 4-8 Relationship between H₂S adsorbed and Zn concentration

As a supplement, the zinc extraction test from FRPM is necessary to evaluate the zinc effect on H₂S removal by FRPM. The extraction efficiencies of NaOH and HNO₃ were evaluated with atomic adsorption spectrophotometry (AAS) shown in Table 4-5. Both primary extraction efficiencies were less than 5%. The low efficiency was likely due to the fact that only zinc on the surface was removed rather than that inside FRPM while the extraction rates were calculated based on the total zinc concentration including surface and bulk zinc. Most zinc inside FRPM has no opportunity to contact with extractants. The results show that extended contact time improved the zinc extraction while primary extraction could remove most of the surface zinc. These results suggest that the NaOH solution was a more efficient zinc extractant than HNO₃.

Table 4-5 Zinc extraction results of FRPM

	<i>Zinc extraction efficiency %*</i>			
	Primary extraction	Secondary extraction	Tertiary extraction	Individual 5-day extraction
HNO ₃ (0.1 N)	4.0%	0.36%	0.26%	5.52%
HNO ₃ (0.5 N)	4.4%	0.36%	0.36%	4.73%
NaOH (0.1N)	1.2%	0.33%	---	---
NaOH (0.5N)	2.1%	0.18%	---	---

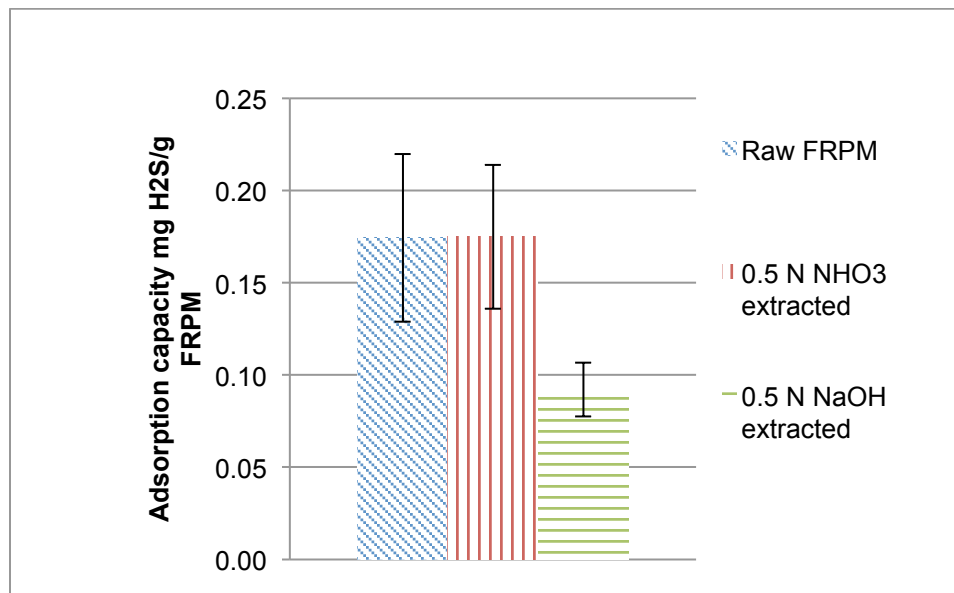
* The percentage based on the total zinc content in FRPM.

The surface concentration change of zinc was detected by an X-ray photoelectron spectroscopy (XPS) experiment before and after HNO₃ extraction, as presented in Table 4-6. Over 50% of surface zinc was transferred into HNO₃ while approximately 25% for NaOH extraction, which was relatively lower. The XPS results in Table 4-6 show that the species of element zinc on the FRPM surface has a valance number +2, which is highly likely to be zinc oxide. The finding corroborates the fact that excessive ZnO is usually used as additive in tire rubber manufacture as mentioned before. Previous research argued that NaOH could change the structure of zinc stearate molecules (Segre, et al., 2002) which might affect adsorption.

Table 4-6 X-ray photoelectron spectroscopy (XPS) test results

FRPM	C 1s	N 1s	O 1s	S 2p	Zn 2p3	Total
Raw	89.28	0.2	8.53	0.43	1.56	100
After HNO ₃ extraction	91.8	0.78	6.53	0.12	0.77	100
H ₂ S saturated	91	0.4	6.68	0.21	1.71	100
H ₂ S saturated after HNO ₃ extraction	89.07	1.22	8.52	0.19	1.00	100

Both HNO₃ and NaOH extracted samples were used in H₂S adsorption capacity tests and the results are shown in Figure 4-9.

**Figure 4-9 Adsorption capacity of zinc-extracted FRPM**

The interesting observation is that HNO₃ extraction did not shift the capacity significantly, while the NaOH treated sample experienced a substantial decrease (Table 4-7). This fact does not meet the surface zinc concentration order (raw sample > HNO₃ treated sample > NaOH treated sample). The HNO₃ treated sample did not decrease as expected. It could be attributed to the

increasing surface functional groups caused by the oxidation of HNO_3 . Based on the previous hypothesis, two possible kinds of active sites result in H_2S adsorption--carbon black and metal ions (Wang, et al., 2010). Since the zinc concentration deferred from the original FRPM, it is possible that the surface properties of carbon black were rejuvenated to compensate for the adsorption capacity loss of zinc. Carbon black is the main component in rubber products, which provides the backbone for rubber fiber to build on (Peng, Y.K., 2007). Although some pores of carbon black are filled by rubber polymer, parts of them could be free for gas adsorption. Additionally, the surface of carbon black has many functional groups on the surface. HNO_3 might either clean the pores or increase the group number, both of which improve the adsorption capacity. Many researchers have shown that the oxidation of carbon material, such as activated carbon and carbon black, by nitric acid can improve the adsorption of H_2S (Bagreev and Bandosz, 2000).

**Table 4-7 Analysis of variance of zinc extraction by JMP 10.0
(Statistical software, SAS institute)**

Alpha=0.05		LSD=0.07 mg/g
t=2.44691		
	Adsorption capacity mg/g	Difference significance
Raw FRPM	0.17	a
0.5 N HNO ₃ extraction	0.18	a
0.5 N NaOH extraction	0.09	b

Conclusions

Higher packing quantity and smaller rubber particle size significantly increase the H₂S removal efficiency by increasing contact time and area between FRPM and gas molecules. Considering these effects, compression and fine grinding would benefit the adsorption process. Since these operations improve the diffusion and interaction opportunities of H₂S molecules, it aids both physical adsorption and chemisorption. Temperature makes a similar effect on FRPM. Although H₂S adsorption favors higher temperature, it has to be controlled below 100°C to avoid the clogging of rubber particles.

Moisture content is essential for H₂S adsorption on FRPM. Higher moisture contents were shown to enhance the adsorption capacity. The variance of zinc concentrations also leads to change. Based on the effects of zinc and moisture content, chemical reaction or chemisorption may be the dominant H₂S adsorption mechanism. Zinc is suggested to be the important active composition in FRPM, while the HNO₃ extraction result supports the observation that carbon black plays a role in the process.

These factors bolster the apparent advantage of reusing rubber waste products as environmental adsorbents, possibly as replacements for costly activated carbon. These data will assist in scrubber design and operation for H₂S removal and also help to elucidate the mechanisms for H₂S adsorption on fine rubber particles.

References

- Alexandre-Franco, M.; Fernández-González, C.; Alfaro-Domínguez, M.; Gómez-Serrano, V. (2011) Adsorption of cadmium on carbonaceous adsorbents developed from used tire rubber. *Journal of Environmental Management*, 2011, **92** (9), 2193-2200
- Boudou, J.; Chehimi, M.; Broniek, E.; Siemieniowska, T.; Bimer, J. (2003) Adsorption of H₂S or SO₂ on an Activated Carbon Cloth Modified by Ammonia Treatment. *Carbon*, **41** (10), 1999-2007.
- Ellis, T. G.; Park, J.; Oh, J. (2008) *A Novel and Cost-Effective H₂S Adsorption Technology Using Tire Derived Rubber Particles*. Final project report to the Grow Iowa Values Fund, Iowa State University.
- Evans, E.A.; Siefers, A.; Wang, N.; and Ellis, T.G. (2010) A novel and cost-effective H₂S removal technology using tire derived rubber particles. *Proceedings of the Water Environment Technical Exposition and Conference*, New Orleans, LA, October 2010.
- Fan, M. (2005) Evaluation of As-Received Tire Derived Rubber Particles in Environmental Engineering Report
- Godini, H.; Mowla, D (2008) Selectivity study of H₂S and CO₂ absorption from gaseous mixtures by MEA in packed beds, *chemical engineering research and design* **86**, 401–409
- Miguel, G.; Fowler, G.; Dall'Orso, M.; Sollars, C. (2002) Porosity and Surface Characteristics of Activated Carbons Produced from Waste Tyre Rubber. *Journal of Chemical Technology & Biotechnology*, **77** (1), 1-8.

- Noll, E.K.; Gounaris, V.; Hou, W. (1992) Adsorption technology for air and water pollution control. *Lewis publishers, INC*, chapter 1.
- Peng, Y.K. (2007) The effect of carbon black and silica fillers on cure characteristics and mechanical properties of breaker compounds, M.S. Thesis
- Shah, J.; Jan, M.; Mabood, F.; Shahid, M. (2006) Conversion of Waste Tyres into Carbon Black and Their Utilization as Adsorbent. *Journal of the Chinese Chemical Society*, **53**, 1085-1089.
- Siefers, A.; Wang, N.; Sindt, A.; Dunn, J.; McElvogue, J.; Evans, E.; Ellis, T. (2010) A Novel and Cost-Effective Hydrogen Sulfide Removal Technology Using Tire Derived Rubber Particles, WEFTEC 2010: Session 61 through Session 70, pp. 4597-4622(26)
- Wang, N.; Evans, E.A.; Ellis, T. G., Biogas Hydrogen Sulfide Adsorption using Waste Tire Media Products, WEFTEC 2010: Session 1 through Session 10 , pp. 39-58(20)
- Xiao, Y.; Wang S. (2008). "Experimental and simulation study of hydrogen sulfide adsorption on impregnated activated carbon under anaerobic conditions." *Journal of Hazardous Materials* **153**(3): 1193-1200.

CHAPTER 5 REGENERATION OF SPEND FINE RUBBER PARTICLE MEDIA (FRPM)

Introduction

Hydrogen sulfide (H_2S) is a common component of biogas from anaerobic digestion of organic substances. Its toxicity and corrosiveness limit the reuse of biogas and increase the cost of facilities and maintenance. Adsorption is a popular option when considering its simple operation and maintenance and high removal efficiency. Proper adsorbent selection is critical for the treatment process. Common adsorbents include activated carbon, metal oxides, and molecular sieves based on their chemical or physical properties to separate H_2S from the target gas (Leuch, et al, 2003; Chiang, et al, 2000; Wang, et al, 2008). Scrubbers can easily reach more than 99% H_2S removal efficiency and researchers have turned their interest to cost-effective alternatives, either increasing adsorption capacity or decreasing material cost. As mentioned in previous work (Wang, et al, 2010), fine rubber particle media (FRPM) is a potential option with low manufactured cost and moderate adsorption capacity. Additionally, it is another option to reuse and recycle used tires, which have become a prominent environmental problem. Five million tons of vehicle tires are discarded every year worldwide (Troca-Torrado, et al, 2011). Both landfilling and incineration are not sustainable treatment, since this solid pollutant occupies

useful land, consumes energy, or releases harmful chemicals (Smolders and Degryse, 2002; Wang, et al, 2011; Shakya, et al, 2008).

With respect to economical and environmental benefits, adsorbent regeneration attracts the attention of investors and researchers. Multiple use cycles would decrease the cost of adsorbent purchase and transportation, reduce the demand of raw materials, and save energy. Thermal regeneration for instance is widely used for activated carbon. During the general manufacturing process, activated carbon experiences carbonization and activation, both of which are treatments at a temperature of approximately 1000°C. The difference between the two processes is in the presence or absence of oxygen. Activated carbon can tolerate the high temperature created by thermal regeneration. During this regeneration, an electrically-heated or gas-fired furnace gasifies and desorbs any attached substance on the activated carbon at temperatures up to 900°C (Wen, et al., 2011). This conventional treatment consumes massive amounts of energy and loses carbon due to oxidization and attrition (Koo and Hameed, 2012). Another regeneration choice is sorbent regeneration or chemical regeneration, which use a specific agent to extract or react with the adsorbate. An organic solvent was used to remove phenol from activated carbon (Cooney, et al, 1983). Oxygen was injected to regenerate H₂S loaded zinc oxide by oxidizing zinc sulfide at high temperatures (300°~800°C) (Samokhvalov and Tatarchuk, 2011).

The regeneration of rubber particle material has not been investigated before. Low price is the greatest advantage of FRPM and regeneration seems

not as essential as other expensive H₂S scrubbers. However, as a potential commercial product, it could not be neglected for the purpose of maximizing use and reducing cost. In this project, two regeneration methods of FRPM were proposed and tested for reliability: zinc chloride solution and thermal regeneration.

Materials and Methods

Breakthrough Curve

The H₂S adsorption capacities on FRPM were calculated based on breakthrough curves, which represented the relationship between outlet H₂S concentration and elapsed time. In this research, the breakthrough curves were obtained by continuously monitoring the concentration of the effluent H₂S flow through a water jacketed metal column packed with FRPM until a concentration of 200 ppmv was reached, which is the recommended accuracy limit of the sensor (with less than 5% error).

Zinc solution regeneration

After the breakthrough curve tests, spent FRPM was regenerated by washing with different concentrations of ZnCl₂ solutions (distilled water, 0.5 g ZnCl₂/L and 1g ZnCl₂/L) and filtered. Then, the treated FRPM was placed at room temperature for 48 hr for moisture balance before repacking in the column for adsorption capacity. This procedure was repeated three times for each solution to quantify the stability of the sequential regeneration. The adsorption

capacity recovery percentage was obtained by comparing the regenerated and original FRPM.

An evaporation process of water-saturated FRPM versus time under room temperature was investigated to eliminate the effect of moisture content after filtering. Around 200g water-filtered FRPM was set on a clean foil paper evenly at room temperature. The moisture content was measured and recorded each day, which was obtained with a weight balance method. Empty beakers were heated at 105 °C for 4 h and then placed in desiccators at room temperature. The beakers were cooled down and weighed. This procedure was repeated until the empty beakers' weight change was less than 0.1 g to avoid moisture leftover. An amount of 10 g FPRM was transferred into the beakers separately, which were weighed and transferred to the oven at 105°C for 8 h. Then, the samples were cooled to room temperature and weighed again. The weight differences before and after drying were considered as the mass of water in FPRM. The moisture content was calculated with the water mass divided by the sample mass.

Thermal regeneration

Spent FRPM from capacity adsorption tests was immediately transferred to clean beakers and heated in the oven at 100°C for 8 hours. The regenerated rubber materials were placed at room temperature for 48 hours in order to cool down and balance the moisture content before adsorption capacity tests were conducted. The process was repeated six times to investigate the feasibility and

stability of this regeneration method. In addition, to minimize the influence of moisture content, the moisture variation of heated FRPM was monitored.

To compare with the effect of thermal regeneration, room temperature repacking tests were conducted with FRPM. Instead of heating, spent FRPM was placed at room temperature and processed by the regeneration procedure mentioned above.

Results and Discussion

Distilled water was used as the regenerate agent for the control group. As shown in Figure 4-1, the adsorption capacities diminished during three consecutive regenerations, which suggested that water would not be sufficient as a regenerating agent. For the residual removal ability of H_2S after each wash, two reasons might be considered: the FRPM redistribution and clean particle surface. Due to the considerable surface area among the rubber particles, not all FRPM had the opportunity to contact with H_2S during one treatment, which means there must be some unsaturated adsorbent even in the lower part of the reactor. After washing, some un-spent particles were redistributed to the flow path of H_2S and participated in the removal process. Meanwhile, some particles deposited on the surface of FRPM were also cleaned during the solution regeneration process and uncovered active sites for H_2S molecules. In contrast to distilled water, adsorption capacity recovery of FRPM following washing with a zinc solution (1g $ZnCl_2/L$) yielded an adsorption capacity of 115~120% of the original, and it remained constant through all three regeneration tests. This result

indicated that 1g/L $ZnCl_2$ solution served as a suitable regeneration agent for FPRM, while a half-strength solution (0.5g $ZnCl_2$ /L) recovered approximately 110% of the adsorption capacity after the first wash and 80% after the second wash. This shows, to some extent, unstable recovery ability at this concentration. The higher regeneration after the very first washing was attributed to the reasons discussed above when washed with distilled water. However, with subsequent washing, these advantages were not enough to offset the loss of the active component of FPRM. Complex mechanisms including ion adsorption and particle redistribution might affect the efficiency of regeneration. Particle redistribution might take effect during the first several rounds of washing, however, the influence diminished as the regeneration process was repeated. Zinc ions were believed to play the more important role. It has been confirmed that zinc ions could be adsorbed on the FPRM through the reaction between zinc oxide and H_2S (Wang, et al, 2010). In this case, there was not enough time for the equilibrium of zinc ions transferred from solution onto FPRM during the short washing period.

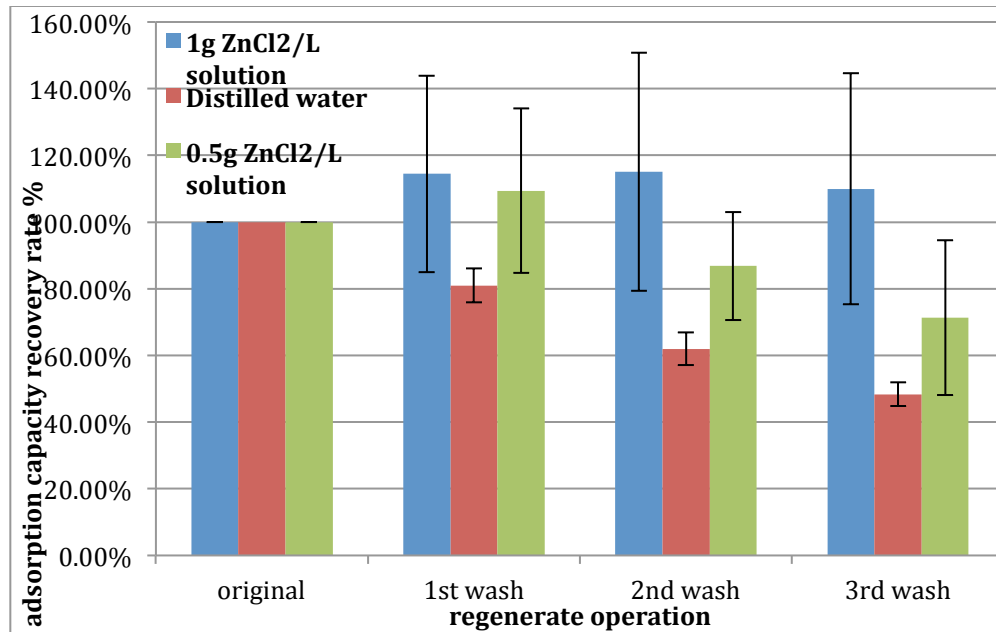


Figure 5-1 H₂S adsorption capacity regeneration by ZnCl₂ solutions

The moisture content of FRPM has significant effect on the H₂S adsorption (Wang, et al., 2010), which is approximately 0.6%. The values of regenerated materials should be comparable with the regenerated ones for better test accuracy. Figure 5-2 shows the moisture content change of rinsed-filtered FRPM versus elapsed time. In the short time after filtering, FRPM could retain water up to approximately 25%. Then, it sharply decreased to the average level of original FRPM with two days. Although there are few specific tests focusing on the moisture content of rubber particles, for crumb rubber used as a construction additive, it is controlled to less than 1% by weight (Sunthonpagasit and Duffey, 2004). Moisture content is primarily a function of the humidity and temperature of the storage area. Most artificial rubber is made from polymer, carbon black and other small amounts of additives (Siddique and Naik, 2004). Although different

brands of rubber contain various kinds of polymers, such as styrene-butadiene and methyl isoprene, these are all nonpolar substances that repel water and resist moisture uptake. Another key component, carbon black, comprising approximately 30% of tire rubber, contains 0.5% of water under normal conditions (Mezgebe, et al., 2012). This water content is close to that observed with FRPM. The moisture content in synthetic rubber products is less affected by the shape of the particles because of lower surface area and less opportunity to contact with vapor in air. For instance, the weight of water in new tire rubber was less than 0.01% (Amari, et al., 1999). The trace water adsorption gives the stronger structure and resistance of rubber for vehicle tires. However, moisture contents of rubber stoppers were relatively higher, 0.2%~0.4% (Corveleyn, et al., 1997). The difference may be caused by different rubber formulations and manufacturing procedure and protocols. The results recommend that the samples regenerated with zinc solutions should be balanced moisture at room temperature for at least two days, to make sure all the H₂S adsorption capacity tests are free of the influences of abnormal moisture contents.

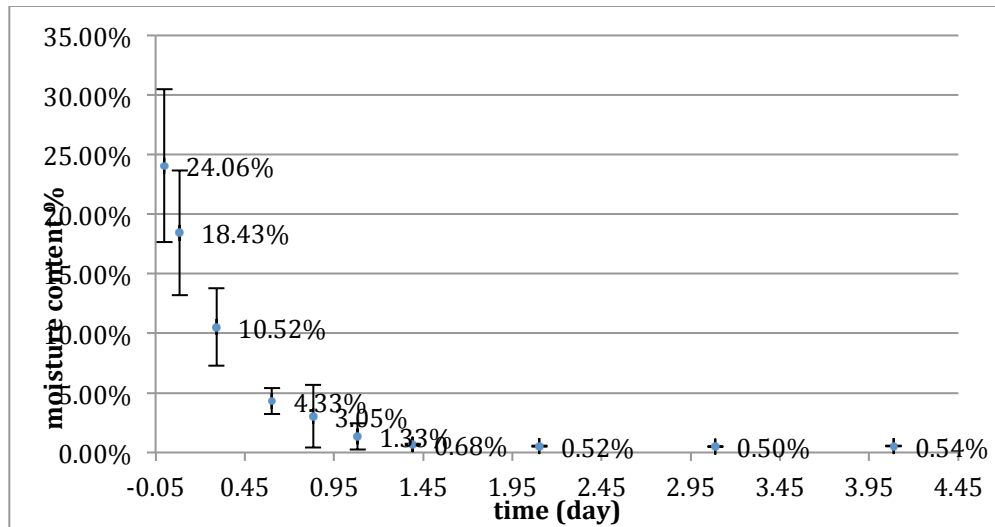


Figure 5-2 FRPM moisture balance trend after filtration

According to the previous research, higher temperatures can significantly increase the adsorption capacity of H_2S on FRPM (Wang, 2012). Higher temperature can accelerate the diffusion of H_2S molecules and facilitate the chemical reaction between H_2S and active sites. Zinc oxide was found to play an important role in the H_2S adsorption on FRPM (Wang, 2010). Higher temperature could improve the saturation adsorption capacity of H_2S on zinc oxide because of the increase in diffusivity (Haimour, et al, 2005). Another H_2S -adsorbing compound, black carbon may also uptake more H_2S since higher temperature assists the formation of water film on carbonaceous material surface under $100^\circ C$ and, consequently, enhance the contact between H_2S and functionality groups (Li, 2008). At lower temperature, the bonds between sulfur species and carbon are weaker because physical adsorption dominates the adsorption process (Yang, et al, 2002). The room temperature repacking test

results, shown in Figure 5-3, partially supported this theory. Without exterior heat, FRPM partially recovered adsorption capacity at room temperature after 24-hr exposure to air. This suggests that the deposition energy of H_2S was lower and the physical adsorption participated in the removal process. Unfortunately, since the adsorption capacity was low, it was hard to measure the escaped gas molecules. The recovery percentage remained at approximately 30~35% except for the first repacking. This difference resulted in the unsaturated breakthrough of the first adsorption capacity test limited by short contact time and voids between rubber particles. H_2S may escape from the voids before diffusing and contacting with other rubber particles. When repacked repeatedly, rubber particles redistribute through the reactor and minimize this effect.

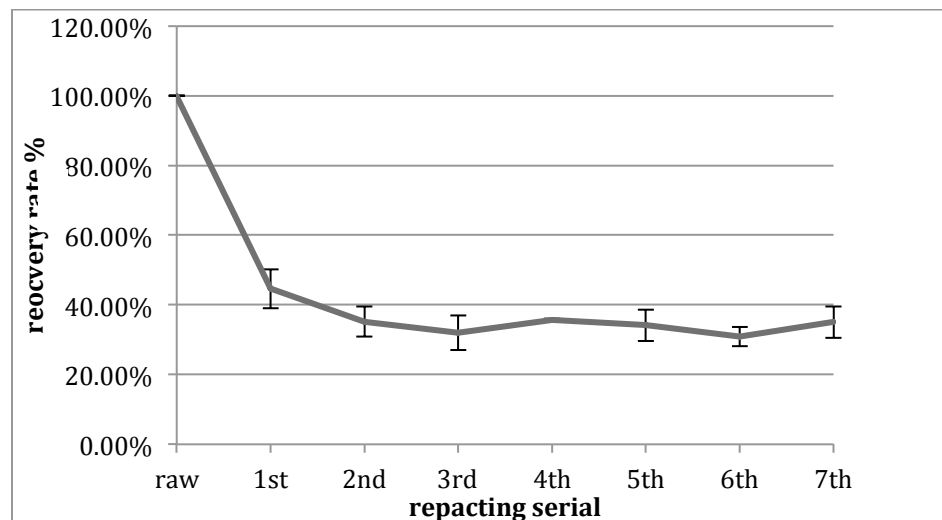


Figure 5-3 FRPM repacking tests at room temperature

According to the positive performance of H_2S adsorption at higher temperature ($30^{\circ}C \sim 80^{\circ}C$), FRPM was tested for the possibility of thermal regeneration. Since previous tests showed that over $100^{\circ}C$ had caused the

clogging of FRPM in beakers, a lower temperature (80°C) was chosen for thermal regeneration and the results are shown in Figure 5-4.

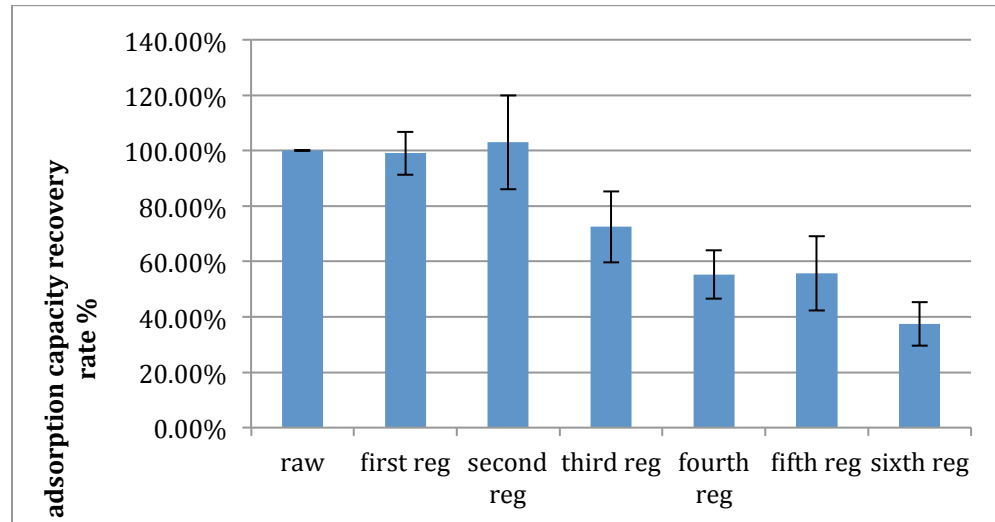


Figure 5-4 Adsorption capacity recovery following thermal regeneration at 80°C

As Figure 5-4 shows, the spent FRPM recovery percentage reached approximately 100% in the first and second regeneration operation. However, recovery significantly decreased from the third regeneration. With the increase of regeneration times, adsorption capacity was close to 35%, which was viewed as physical adsorption. The temperature is not high enough to reverse the chemisorption of FRPM. This supported the theory that the adsorption mechanism is a combination of chemisorption and physical adsorption. The reason that the first two regenerations were successful might be due to desorption of carbon dioxide and other volatile gases attached on the surface of FRPM at higher temperature. Consequently, new adsorption active sites were made available for the adsorption of H₂S. Figure 5-5 shows that the adsorption

capacity of raw FRPM was enhanced by 30% after experiencing the same heat treatment as the through thermal regeneration. This phenomenon may also be attributed to desorption of gases on FRPM.

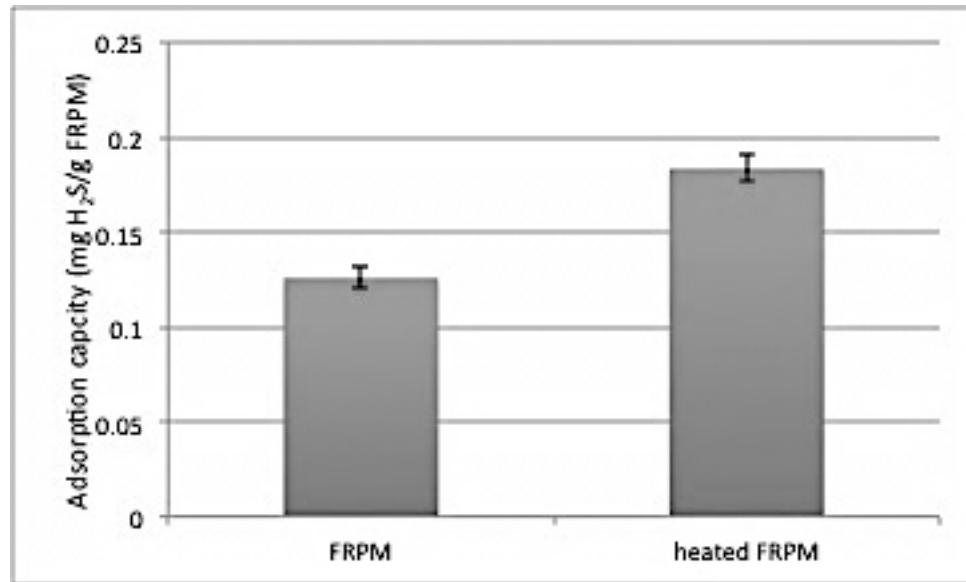


Figure 5-5 Adsorption capacity difference before raw FRPM and heated FRPM

Conclusions

About 30% of bonded H₂S on FRPM escaped at room temperature. This indicated that physical adsorption should not be neglected during the process. However, thermal regeneration just temporarily recovered the adsorption capacity of spent FRPM. With multiple adsorption-regeneration cycles, the recovery percentage kept declining until physical adsorption dominated the process. ZnCl₂ solution regeneration showed significant regeneration capacity. Due to the ability of FRPM to capture metal ions in solution, more zinc ion was

made available on the surface while exhausted ZnS was likely washed out. By adjusting the concentrations of the solution, spent FRPM could fully regain its adsorption capacity.

References

- Amari, T.; Themelis, N.J.; Wernick, I.K. (1999) Resource recovery from used rubber tires. *Resources Policy*, **25**:179-188
- Chiang, H.L.; Tsai, J.H.; Tsai, C.L.; Hsu, Y.C. (2000) Adsorption characteristics of alkaline activated carbon exemplified by water vapor, H₂S, and CH₃SH gas. *Sci. Technol.*, **35**: 903-918
- Cooney, D.O.; Nagerl, A.; Hines, A.L. (1983) Solvent regeneration of activated carbon. *Water Res*, **17**: 403-410
- Corveleyn, S.; Smedt, S.D.; Remon, J.P. (1997) Moisture absorption and desorption of different rubber lyophilisation closures. *International Journal of Pharmaceutics*, **159**:57-65
- Foo, K.Y.; Hameed, B.H. (2012) Microwave-assisted regeneration of activated carbon. *Bioresource Technology*, **119**: 234-24
- Haimour, N.; E1-Bishtawi, R.; Ail-Wahbi, A. (2005) Equilibrium adsorption of hydrogen sulfide onto CuO and ZnO. *Desalination*, **181**:145-152
- Leuch, L.M.L.; Subrenat, A.; Cloirec, P.L. (2003) Hydrogen sulfide adsorption and oxidation onto activated carbon cloths: applications to odorous gaseous emission treatments. *Langmuir*, **19**: 10869-10877
- Li, H. (2008) Selective catalytic oxidation of hydrogen sulfide from syngas, *Master's Thesis*, University of Pittsburgh.
- Mezgebe, M.; Shen, Q.; Zhang, J.; Zhao, Y. (2012) Liquid adsorption behavior and surface properties of carbon blacks *Colloids and Surfaces A: Physicochem. Eng. Aspects*, **403**:25-28
- Samokhvalov, A. and Tatarchuk B.J. (2011) Characterization of active sites, determination of mechanisms of H₂S, CO₂ and CS₂ sorption and

regeneration of ZnO low-temperature sorbents: past, current and perspectives. *Chem. Phys*, **13**: 3197-3209

Shakya, P.R.; Shrestha, P.; Tamrakar, C.S.; Bhattarai, P.K. (2008) Studies on potential emission of hazardous gases due to uncontrolled open-air burning of waste vehicle tyres and their possible impacts on the environment *Atmos. Environ*, **42**: 6555-6559

Siddique, R.; Naik, T.R. (2004) Properties of concrete containing scrap-tire rubber – an overview. *Waste Management*, **24** (6): 563-569

Smolders, E. and Degryse F. (2002) Fate and effect of zinc from tire debris in soil. *Environ Sci Technol*, **36**: 3706-3710

Sunthonpagasit, N.; Duffey M.R. (2003) Scrap tires to crumb rubber: feasibility analysis for processing facilities *Resources. Conservation and Recycling*, **40** (4): 281-299

Troca-Torrado, C.; Alexandre-Franco, M.; Fernández-González, C.; Alfaro-Domínguez, M.; Gómez-Serrano, V. (2011) Development of adsorbents from used tire rubber: Their use in the adsorption of organic and inorganic solutes in aqueous solution. *Fuel Processing Technology*, **92**, (2): 206-212

Wang, H.; Davidson, M.; Zuo, Y.; Ren, Z. (2011) Recycled tire crumb rubber anodes for sustainable power production in microbial fuel cells. *Journal of Power Sources*, **196** (14): 5863-5866

Wang, N.; Evans, E.A.; Ellis, T. G. (2010) Biogas Hydrogen Sulfide Adsorption using Waste Tire Media Products, *WEFTEC 2010: Session 1 through Session 10*, (20): 39-58

Wang, X.H.; Sun, T.H.; Yang, J.; Zhao, L.; Jia, J.P. (2008) Low-temperature H₂S removal from gas streams with SBA-15 supported ZnO nanoparticles. *Chem. Eng. J.*, **142**: 48-55

Wen, Q.B.; Li, C.T.; Cai, Z.H.; Zhang, W.; Gao, H.L.; Chen, L.J.; Zeng, G.M.; Shu, X.; Zhao, Y.P. (2011) Study on activated carbon derived from sewage sludge for adsorption of gaseous formaldehyde. *Bioresour. Technol.*, **102**: 942-947

Yan, R.; Liang, D.T.; Tsen, L.; Tay, J.H. (2002) Kinetics and mechanisms of H₂S adsorption by alkaline activated carbon. *Environmental Science and Technology*, **36**:4460

CHAPTER 6 CONCLUSIONS

Through the investigation of properties and surface characterization of FRPM some observations were made. Micropores do not dominate the surface of FRPM. Consequently, the specific surface is much lower than activated carbon and other porous materials. The rubber particle materials are more particulate in nature rather than porous. This suggests that physical adsorption may not work alone to remove H_2S . The pH of FRPM is greater than 7, which is advantageous for H_2S adsorbing. Based on the pH, acid functionalities may not dominate on the surface of FRPM. Metal oxides may exist on the surface and increase the surface pH. Metal concentrations, especially zinc, are relatively high in FRPM, which benefits the adsorption by reacting metal oxides and H_2S . Carbon black comprises approximately 30% of the weight of the rubber particle material, on which the functionality groups also capture H_2S molecules. Chemisorption may be the primary adsorption mechanism, and both zinc oxide and carbon black could be active components. This theory is supported by the moisture content effect test, which shows that higher moisture content enhances the adsorption capacity and water is a favorable environment for acid-base reactions and carbon black adsorption. Meanwhile, the room temperature repacking test demonstrated that at least 30% of the adsorption capacity was due to physical processes because of the lower desorption energy. Generally speaking, the adsorption mechanism of H_2S on FRPM is a complex combination of physical adsorption and chemisorption.

To improve the adsorption capacity of FRPM, it is important to provide more opportunity for interaction between absorbent and gas molecules. A larger packing quantity, higher operation temperature, and smaller rubber particle size resulted in better H₂S removal efficiency in the project. These factors focus on improving the interaction by extending contacting time, accelerating molecular diffusion, or increasing interaction area. Another method is to alter the active components in FRPM. In this research, oxidizing the surface of carbon black and impregnating the surface with zinc ions both worked to raise the adsorption capacity.

FRPM could be a sustainable H₂S scrubber media if regenerated with zinc solutions. Adjusting the concentration and contact time of the washing solution would establish a cost-effective regeneration method. Although the rubber material can resist heat up to 200°C as shown in TGA test, the operating temperature is suggested to be no more than 100°C due to potential for clogging. Thermal regeneration at low range temperatures does not work well in conjunction with the wash regeneration cycles.

FRPM shows relatively lower adsorption capacity, compared with current commercial adsorbents, such as activated carbon or metal oxides. However, the lower cost of the raw material, i.e., waste tires, makes it a potentially cost-effective H₂S scrubber.

Engineering Significance

Since 1980s, the energy crisis made biogas an important fuel in internal combustion engines for electricity. In 2003, the United States consumed biogas as much as approximately 0.6% of the total U.S. natural gas consumption.

However, due to the corrosion concerns, it is required to scrub H_2S (approximately 500~3000 ppmv in biogas) before entering biogas-fueled engines. Adsorption, absorption and biological conversion are traditional treatments. In adsorption, metal oxide (e.g. iron sponge) and activated carbon are popularly used in scrubbers in industries. Although the removal efficiency satisfies the requirement, the high cost of the adsorbents provides motivation to find more cost-effective alternatives.

A cash flow analysis has been performed between FRPM and activated carbon system as an example of determining the future cost of a system. Displayed in Table 6-1 are the parameters of two dry-scrubbing systems proposed for installation in a municipal wastewater treatment plant of a town with a population of 5,000.

Table 6-1 Parameters for cash flow analysis: dry-scrubbing systems

Biogas flow (m ³ /day)	300
H ₂ S Conc. (ppmv)	1000
Activated Carbon System	
Initial cost:	\$ 50,000
Media life (Month):	12
adsorption capacity mg/g	10
Media cost (/kg)	\$ 2
FRPM System	
Initial cost:	\$ 500,000
Media life (Month):	6
adsorption capacity mg/g	1
Media cost (/kg)	\$ 0.01

Since there is no commercial FRPM system, the initial cost was estimated with the inverse ratio of the adsorption capacity. This may overestimate the cost. The adsorption capacity of FRPM was acquired from a pilot test rather than lab-scale test because the parameter used for activated carbon came from commercial product introduction. Table 6-2 and 5-3 show cash flow in 20 years for both systems.

Table 6-2 Cash flow analysis for FRPM system

Year	Inflation (5%)	Initial Cost	Media Replacement	Regeneration cost	Accumulated cost
0	1.05	500,000			500,000
1	1.10		146.88	1762.56	502,105
2	2.05		146.88	1762.56	506,020
3	2.15		146.88	1762.56	510,130
4	3.05		146.88	1762.56	515,953
5	3.20		146.88	1762.56	522,068
6	4.05		146.88	1762.56	529,802
7	4.25		146.88	1762.56	537,921
8	5.05		146.88	1762.56	547,564
9	5.30		146.88	1762.56	557,689
10	6.05		146.88	1762.56	569,241
11	6.35		146.88	1762.56	581,371
12	7.05		146.88	1762.56	594,832
13	7.40		146.88	1762.56	608,967
14	8.05		146.88	1762.56	624,338
15	8.45		146.88	1762.56	640,478
16	9.05		146.88	1762.56	657,758
17	9.50		146.88	1762.56	675,902
18	10.05		146.88	1762.56	695,092
19	10.55		146.88	1762.56	715,242
20	11.05		146.88	1762.56	736,341

Table 6-3 Cash flow analysis for activated carbon system.

Year	Inflation (5%)	Initial Cost &	Media Replacement	Regeneration cost	Accumulated cost
0	1.05	50,000			50,000
1	1.10		2937.6	8812.8	62,955
2	2.05		2937.6	8812.8	87,043
3	2.15		2937.6	8812.8	112,336
4	3.05		2937.6	8812.8	148,175
5	3.20		2937.6	8812.8	185,805
6	4.05		2937.6	8812.8	233,394
7	4.25		2937.6	8812.8	283,363
8	5.05		2937.6	8812.8	342,702
9	5.30		2937.6	8812.8	405,009
10	6.05		2937.6	8812.8	476,099
11	6.35		2937.6	8812.8	550,743
12	7.05		2937.6	8812.8	633,584
13	7.40		2937.6	8812.8	720,566
14	8.05		2937.6	8812.8	815,157
15	8.45		2937.6	8812.8	914,477
16	9.05		2937.6	8812.8	1,020,818
17	9.50		2937.6	8812.8	1,132,476
18	10.05		2937.6	8812.8	1,250,568
19	10.55		2937.6	8812.8	1,374,564
20	11.05		2937.6	8812.8	1,504,406

From the tables, it is easy to see that the advantage of FRPM is the lower cost of replacement and regeneration while the disadvantage is the high initial investment cost. The problem is that the lower adsorption capacity requires larger amount of adsorbent to satisfy the requirement of removal. It means a larger higher initial cost reactor must be installed. However, if the adsorption capacity of FRPM were improved, the initial cost would decrease dramatically. Compared with commercial adsorbents on an industrial scale, there is still room for FRPM to improve its performance for H₂S adsorption.

FRPM made from waste rubber products results in lower production and procurement costs. With the increase in waste tires, the cost advantage is more obvious compared with the traditional H₂S adsorbents, such as activated carbon. The biggest challenge is increasing the adsorption capacity. By investigating the H₂S adsorption mechanisms, this research suggests some ways to improve the performance of FRPM. First of all, the research showed that a higher moisture content could increase the adsorption capacity dramatically. This is a practical application for H₂S removal in a wastewater treatment plant or other industry. Considering some applications of biogas use require low H₂S and water concentrations, a water removal column (dehumidifier) could be installed after the FRPM H₂S removal column. Secondly, the particle size of FRPM was shown to influence the adsorption capacity. This suggests that the FRPM could be processed to provide a high surface area to improve adsorption capacity. Finally, the zinc or other metal concentrations in FRPM also increased the H₂S adsorption capacity. This suggests the loss of metal should be avoided during the production process.

The fundamental information about FRPM characteristics and properties can also be used for practical applications. The packing and particle density are useful to calculate the porosity and packing volume during the engineering application of H₂S removal. The TGA results show the thermal stability of FRPM was reliable for temperatures less than 200 °C. This suggests that FRPM can be used for H₂S removal at higher temperatures, but the effect of temperature on adsorption capacity at higher temperatures requires further study. Other

information, such as pH and surface area, can help engineers understand FRPM adsorption mechanisms for practical application of H₂S removal.

Understanding the properties and H₂S adsorption capacity of FRPM not only provides useful information for industrial H₂S removal, but also helps identify potential applications for other gaseous pollutants which have similar properties to H₂S. For example, if the gas can react with zinc or if functional groups can oxidize the gas, it is possible that FRPM would be a suitable adsorbent.

FRPM could be a potential solution for another major challenge to the use of biogas generated by municipal digesters – siloxanes, which result from silica containing compounds that are widely used in personal care products because of their useful properties (high compressibility, low flammability, low surface tension, water repellent, and high thermal stability) (Dewil et al., 2006). However, it is a type of trace contamination in wastewater system since it volatilizes in anaerobic digestion into the gas phase. When biogas is combusted for energy, siloxanes are converted to silicon dioxide, a glass-like substance that causes reduced engine efficiency, reduced heat transfer, increased scour and abrasion, acceleration of equipment deterioration, possible air permit violations, and poisoning of catalysts (Ajhar et al., 2010). It is required to reduce the concentration from approximately 100 mg/m³ to less than 0.1 mg/m³ and 5~28 mg/m³ before entering microturbines and cogeneration engines, respectively. The worldwide production of siloxanes is estimated to be in excess of one million tons per year and growing at an estimated rate of 17,000 tons per year of siloxanes in wastewater in the U.S. (Hagmann et al., 1999). Molecular sieves

and activated carbon are commonly used as scrubbers. Activated carbon costs vary; but in most cases, the cost falls in the range from \$15 to \$100 per kilogram. Therefore, it is advantageous to find a more economical adsorbent. FRPM would be a potential choice due to the lower cost (less than \$1 per kilogram). A preliminary test has presented the capacity of FRPM to clean siloxanes from biogas (Siefers, et al., 2010) with removal efficiencies between 90 and 99%.

REFERENCES

- Adib, F.; Bagreev, A.; Bandosz, T. (1999) Effect of Surface Characteristics of Wood-Based Activated Carbons on Adsorption of Hydrogen Sulfide. *Journal of colloid and interface science*, **214** (2), 407-415.
- Ajhar, M.; Travesset, M.; Yüce, S.; Melin, T. (2010) Siloxane removal from landfill and digester gas – A technology overview. *Bioresource Technology*, **101**, 2913-2923.
- Bagreev, A.; Bandosz, T. (2000) Study of Hydrogen Sulfide Adsorption on Activated Carbons Using Inverse Gas Chromatography at Infinite Dilution. *J. Phys. Chem. B*, **104** (37), 8841-8847.
- Bagreev, A.; Bandosz, T. (2001) H₂S Adsorption/Oxidation on Unmodified Activated Carbons: Importance of Prehumidification. *Carbon*, **39** (15), 2303-2311.
- Bandosz, T. (1999) Effect of Pore Structure and Surface Chemistry of Virgin Activated Carbons on Removal of Hydrogen Sulfide. *Carbon*, **37** (3), 483-491.
- Chatterjee, G.; Houde, A.; Stern, S. (1997) Poly (Ether Urethane) and Poly (Ether Urethane Urea) Membranes with High H₂S/CH₄ Selectivity. *Journal of Membrane Science*, **135** (1), 99-106.
- Dewil, R.; Appels, L.; Baeyens, J. (2006) Energy use of biogas hampered by the presence of siloxanes. *Energy Conversion and Management*, **47**, 1711-1722.
- Entezari, M.; Ghows, N.; Chamsaz, M. (2005) Combination of Ultrasound and Discarded Tire Rubber: Removal of Cr (Iii) from Aqueous Solution. *Journal of Physical Chemistry A*, **109** (20), 4638-4642.
- Garcia, C.; Lercher, J. (1992) Adsorption of Hydrogen Sulfide on Zsm 5 Zeolites. *The Journal of Physical Chemistry*, **96** (5), 2230-2235.
- Haimour, N.; El-Bishtawi, R.; Ail-Wahbi, A. (2005) Equilibrium Adsorption of Hydrogen Sulfide onto CuO and ZnO. *Desalination*, **181** (1-3), 145-152.
- Hagmann, M.; Heimand, E.; Hentschel, P. (1999) Determination of siloxanes in biogas from landfills and sewage treatment plants. *Proceedings Sardinia 99, seventh international waste management and landfill symposium*, Cagliari, Italy, Oct. 4-8, 1999.
- Hao, J.; Rice, P.; Stern, S. (2002) Upgrading Low-Quality Natural Gas with H₂S- and CO₂-Selective Polymer Membranes Part I. Process Design and Economics of Membrane Stages without Recycle Streams. *Journal of Membrane Science*, **209** (1), 177-206.

- Kapdi, S.; Vijay, V.; Rajesh, S.; Prasad, R. (2005) Biogas Scrubbing, Compression and Storage: Perspective and Prospectus in Indian Context. *Renewable energy*, **30** (8), 1195-1202.
- Kim, J.; Park, J.; Edil, T. (1997) Sorption of Organic Compounds in the Aqueous Phase onto Tire Rubber. *Journal of Environmental Engineering*, **123** (9), 827-835.
- Lehmann, C.; Rostam-Abadi, M.; Rood, M.; Sun, J. (1998) Reprocessing and Reuse of Waste Tire Rubber to Solve Air-Quality Related Problems. *Energy Fuels*, **12** (6), 1095-1099.
- Leung, D.; Yin, X.; Zhao, Z.; Xu, B.; Chen, Y. (2002) Pyrolysis of Tire Powder: Influence of Operation Variables on the Composition and Yields of Gaseous Product. *Fuel Processing Technology*, **79** (2), 141-155.
- Li, G.; Stubblefield, M.; Garrick, G.; Eggers, J.; Abadie, C.; Huang, B. (2004) Development of Waste Tire Modified Concrete. *Cement and Concrete Research*, **34** (12), 2283-2289.
- Lin, C.; Huang, C.; Shern, C. (2008) Recycling Waste Tire Powder for the Recovery of Oil Spills. *Resources, Conservation & Recycling*, **52** (10), 1162-1166.
- Lisi, R.; Park, J.; Stier, J. (2004) Mitigating Nutrient Leaching with a Sub-Surface Drainage Layer of Granulated Tires. *Waste Management*, **24** (8), 831-839.
- Mbah, J.; Krakow, B.; Stefanakos, E.; Wolan, J. (2008) Electrolytic Splitting of H₂s Using Cshso Membrane. *Journal of The Electrochemical Society*, **155**, 166-170.
- Meng, X.; Hua, Z.; Dermatas, D.; Wang, W.; Kuo, H. (1998) Immobilization of Mercury (II) in Contaminated Soil with Used Tire Rubber. *Journal of Hazardous Materials*, **57** (1-3), 231-241.
- Novochinskii, I.; Song, C.; Ma, X.; Liu, X.; Shore, L.; Lampert, J.; Farrauto, R. (2004) Low-Temperature H₂s Removal from Steam-Containing Gas Mixtures with ZnO for Fuel Cell Application. 1. ZnO Particles and Extrudates. *Energy and Fuels*, **18** (2), 576-583.
- Park, J. (2004) Effectiveness of Scrap Tire Chips as Sorptive Drainage Material. *Journal of Environmental Engineering*, **130**, 824.
- Potivichayanon, S.; Pokethitiyook, P.; Kruatrachue, M. (2006) Hydrogen Sulfide Removal by a Novel Fixed-Film Bioscrubber System. *Process Biochemistry*, **41** (3), 708-715.
- Purakayastha, P.; Pal, A.; Bandyopadhyay, M. (2002) Adsorption of Anionic Surfactant by a Low-Cost Adsorbent. *Journal of environmental science and health. Part A, Toxic/hazardous substances & environmental engineering*, **37** (5), 925-938.

- Purakayastha, P.; Pal, A.; Bandyopadhyay, M. (2005) Sorption Kinetics of Anionic Surfactant on to Waste Tire Rubber Granules. *Separation and Purification Technology*, **46** (3), 129-135.
- Putman, B.; Amir Khanian, S. (2004) Utilization of Waste Fibers in Stone Matrix Asphalt Mixtures. *Resources, Conservation & Recycling*, **42** (3), 265-274.
- Ranade, D.; Dighe, A.; Bhirangi, S.; Panhalkar, V.; Yeole, T. (1999) Evaluation of the Use of Sodium Molybdate to Inhibit Sulphate Reduction During Anaerobic Digestion of Distillery Waste. *Bioresource technology*, **68** (3), 287-291.
- Segre, N.; Joekes, I.; Galves, A.; Rodrigues, J. (2004) Rubber-Mortar Composites: Effect of Composition on Properties. *Journal of Materials Science*, **39** (10), 3319-3327.
- Seredych, M.; Strydom, C.; Badosz, T. (2008) Effect of Fly Ash Addition on the Removal of Hydrogen Sulfide from Biogas and Air on Sewage Sludge-Based Composite Adsorbents. *Waste Management*, **28** (10), 1983-1992.
- Siddique, R.; Naik, T. (2004) Properties of Concrete Containing Scrap-Tire Rubber—an Overview. *Waste Management*, **24** (6), 563-569.
- Siefers, A.; Wang, N.; Sindt, A.; Dunn, J.; McElvogue, J.; Evans, E.; Ellis, T. (2010) A Novel and Cost-Effective Hydrogen Sulfide Removal Technology Using Tire Derived Rubber Particles, WEFTEC 2010: Session 61 through Session 70 , pp. 4597-4622 (Soreano, G.; Béland, M.; Falletta, P.; Edmonson, K.; Seto, P. (2008) Laboratory Pilot Scale Study for H₂S Removal from Biogas in an Anoxic Biotrickling Filter. *Water Science and Technology*, **57** (2), 201-208.
- Sugio, T.; White, K.J.; Shute, E.; Choate, D.; Blake II, R.C. (1992) Existence of a Hydrogen Sulfide: Ferric Ion Oxidoreductase in Iron-Oxidizing Bacteria. *Appl. Environ. Microbiol.* **58** (1), 431-433.
- Truong, L.; Abatzoglou, N. (2005) A H₂S Reactive Adsorption Process for the Purification of Biogas Prior to Its Use as a Bioenergy Vector. *Biomass and Bioenergy*, **29** (2), 142-151.
- Tsai, J.; Jeng, F.; Chiang, H. (2001) Removal of H₂S from Exhaust Gas by Use of Alkaline Activated Carbon. *Adsorption*, **7** (4), 357-366.
- Ucar, S.; Karagoz, S.; Ozkan, A.; Yanik, J. (2005) Evaluation of Two Different Scrap Tires as Hydrocarbon Source by Pyrolysis. *Fuel*, **84** (14-15), 1884-1892.
- Van der Zee, F.; Villaverde, S.; Garcia, P.; Fdz.-Polanco, F. (2007) Sulfide Removal by Moderate Oxygenation of Anaerobic Sludge Environments. *Bioresource technology*, **98** (3), 518-524.
- Xiao, Y.; Wang, S.; Wu, D.; Yuan, Q. (2008) Experimental and Simulation Study of Hydrogen Sulfide Adsorption on Impregnated Activated Carbon under

Anaerobic Conditions. *Journal of Hazardous Materials*, **153** (3), 1193-1200.

Yuan, W.; Bandosz, T. (2007) Removal of Hydrogen Sulfide from Biogas on Sludge-Derived Adsorbents. *Fuel*, **86** (17-18), 2736-2746.

APPENDICES

Appendix A. Calculation of the adsorption capacity

The adsorption capacity of H₂S on FRPM was calculated based on breakthrough curves generated by Origin 7.0 software shown in Figure 1a. The Y axis presents outlet H₂S concentration monitored and recorded with a JEROME 860 sensor while the X axis is shown in two second intervals. After being transferred from the sensor into Excel on a PC, the data was imported and used to generate the breakthrough curve.

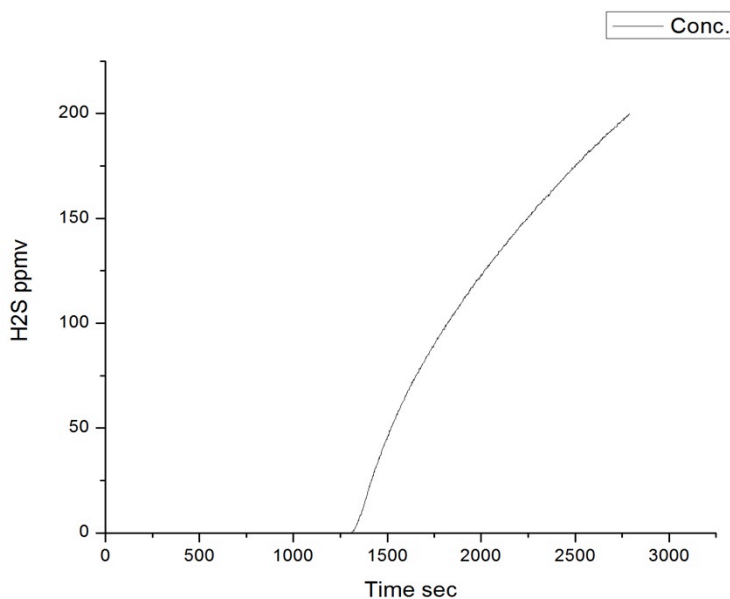


Figure 1a An example of a breakthrough curve

Calculations were run based on the a curve so as to get the area of the shading in Figure 2a, which stood for the total portion of H₂S escaping from the scrubber before the experiment was stopped at 200 ppmv.

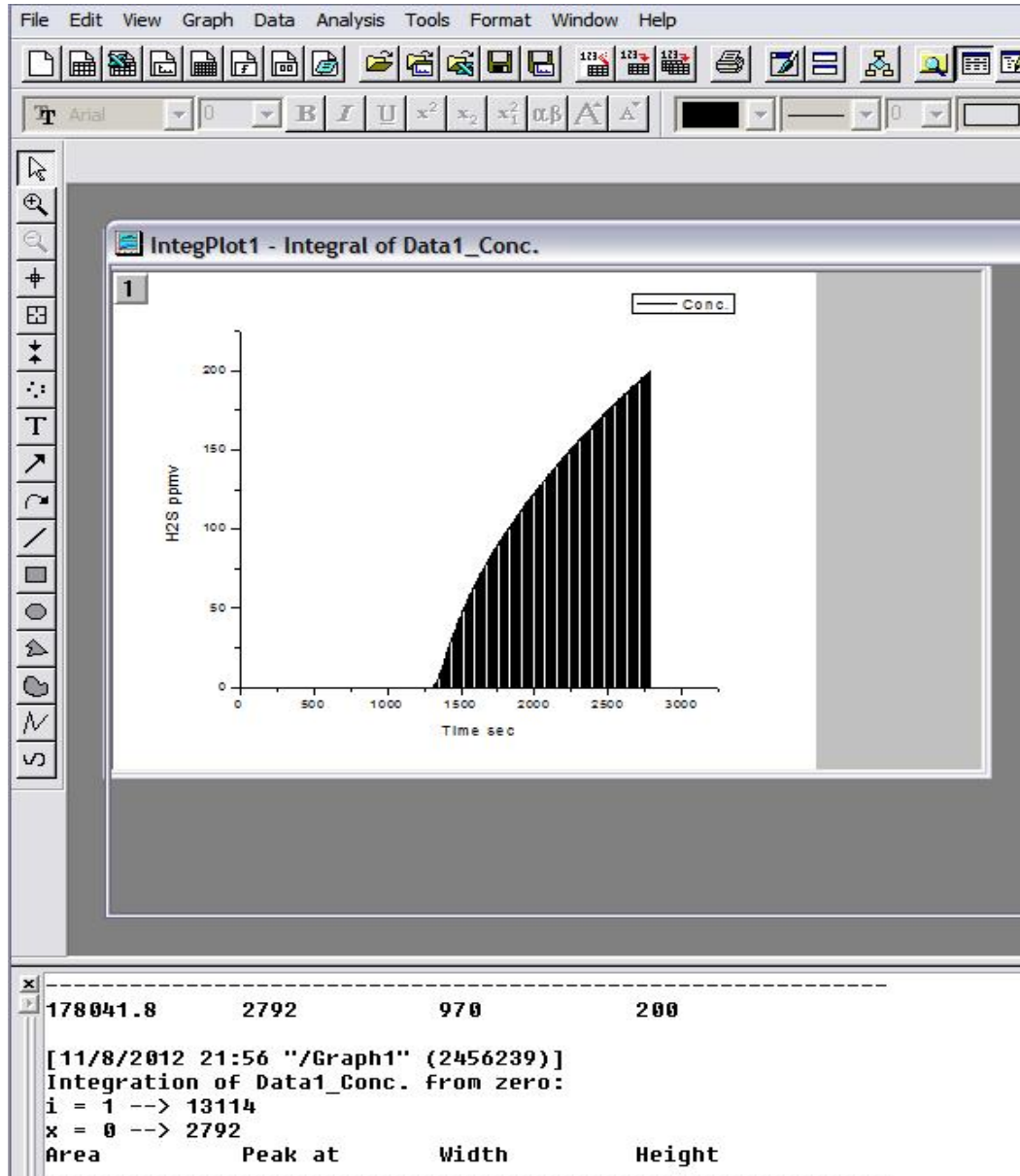


Figure 2a Calculus of the breakthrough curve

The inlet H₂S concentration is 250 ppmv (diluted into half by air before entering the sensor), which could be an imaginary line in the figure. The total area, multiplying 250 ppmv with time, presents the portion of H₂S passing through the reactor during the experiment. Then, the proportion of H₂S captured on FRPM would be calculated with equation 1a

$$\text{Percentage of adsorbed H}_2\text{S} = \frac{\text{Total area} - \text{Shade area}}{\text{Total area}}$$

Since the concentrations, flow rate, and operation time are known for the inlet H₂S, the total amount passing the reaction could be obtained with equation 2a.

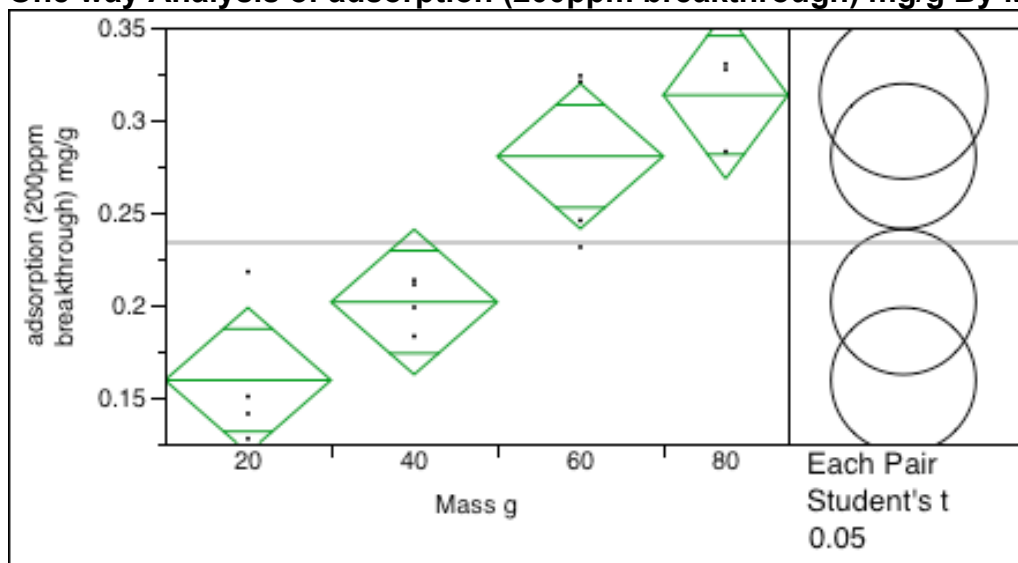
$$\text{Total H}_2\text{S} = \text{Flowrate} \times \text{Conc.} \times \text{Time}$$

Finally, the amount of adsorbed H₂S is the product of “Total H₂S” and “percentage of adsorbed H₂S”.

Appendix B. JMP 10.0 results

Packing quantity

One way Analysis of adsorption (200ppm breakthrough) mg/g By Mass g



Oneway Anova Summary of Fit

Rsquare	0.794689
Adj Rsquare	0.738696
Root Mean Square Error	0.035626
Mean of Response	0.233753
Observations (or Sum Wgts)	15

Analysis of Variance

Source	DF	Sum of Squares	Mean Square	F Ratio	Prob > F
Mass g	3	0.05403920	0.018013	14.1925	0.0004*
Error	11	0.01396120	0.001269		
C. Total	14	0.06800040			

Means for Oneway Anova

Level	Number	Mean	Std Error	Lower 95%	Upper 95%
20	4	0.159387	0.01781	0.12018	0.19859
40	4	0.201637	0.01781	0.16243	0.24084
60	4	0.280430	0.01781	0.24122	0.31964
80	3	0.313496	0.02057	0.26822	0.35877

Std Error uses a pooled estimate of error variance

Means Comparisons

Comparisons for each pair using Student's t Confidence Quantile

t	Alpha
2.20099	0.05

LSD Threshold Matrix

Abs(Dif)-LSD	80	60	40	20
80	-0.06402	-0.02682	0.05197	0.09422
60	-0.02682	-0.05545	0.02335	0.06560
40	0.05197	0.02335	-0.05545	-0.01320
20	0.09422	0.06560	-0.01320	-0.05545

Positive values show pairs of means that are significantly different.

Connecting Letters Report

Level		Mean
80	A	0.31349602
60	A	0.28043025
40	B	0.20163674
20	B	0.15938656

Levels not connected by same letter are significantly different.

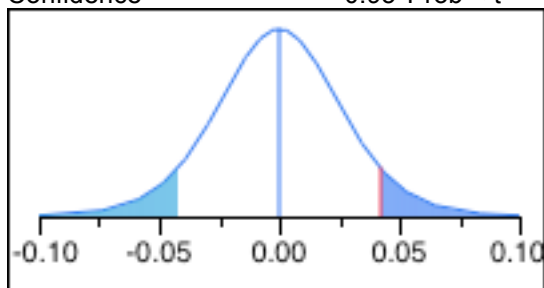
Ordered Differences Report

Level	- Level	Difference	Std Err Dif	Lower CL	Upper CL	p-Value
80	20	0.1541095	0.0272097	0.094221	0.2139976	0.0001*
60	20	0.1210437	0.0251913	0.065598	0.1764893	0.0005*
80	40	0.1118593	0.0272097	0.051971	0.1717474	0.0017*
60	40	0.0787935	0.0251913	0.023348	0.1342391	0.0096*
40	20	0.0422502	0.0251913	-0.013195	0.0976958	0.1217
80	60	0.0330658	0.0272097	-0.026822	0.0929539	0.2497

Detailed Comparisons Report

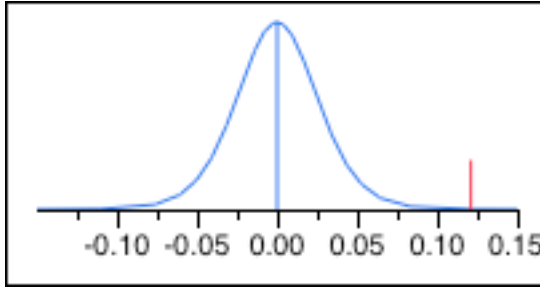
Comparing 40 with 20

Difference	0.04225	t Ratio	1.677175
Std Err Dif	0.02519	DF	11
Upper CL Dif	0.09770	Prob > t	0.1217
Lower CL Dif	-0.01320	Prob > t	0.0608
Confidence	0.95	Prob < t	0.9392



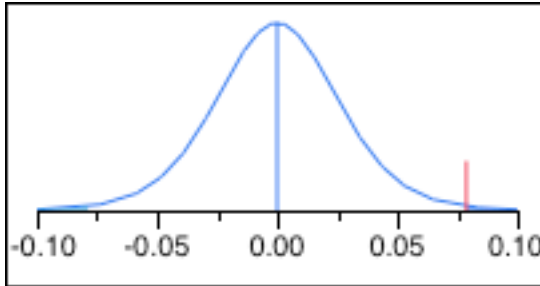
Comparing 60 with 20

Difference	0.121044	t Ratio	4.804986
Std Err Dif	0.025191	DF	11
Upper CL Dif	0.176489	Prob > t	0.0005*
Lower CL Dif	0.065598	Prob > t	0.0003*
Confidence	0.95	Prob < t	0.9997



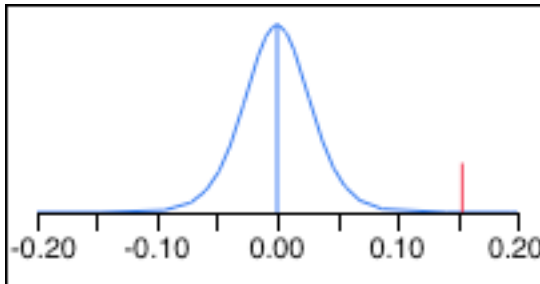
Comparing 60 with 40

Difference	0.078794	t Ratio	3.127811
Std Err Dif	0.025191	DF	11
Upper CL Dif	0.134239	Prob > t	0.0096*
Lower CL Dif	0.023348	Prob > t	0.0048*
Confidence	0.95	Prob < t	0.9952



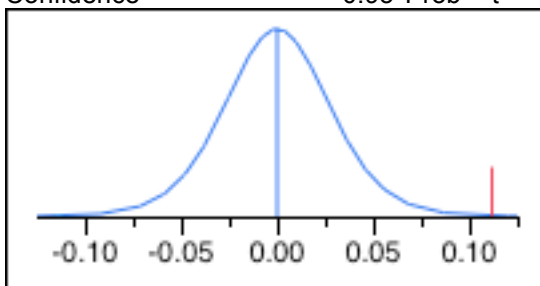
Comparing 80 with 20

Difference	0.154109	t Ratio	5.663773
Std Err Dif	0.027210	DF	11
Upper CL Dif	0.213998	Prob > t	0.0001*
Lower CL Dif	0.094221	Prob > t	<.0001*
Confidence	0.95	Prob < t	0.9999



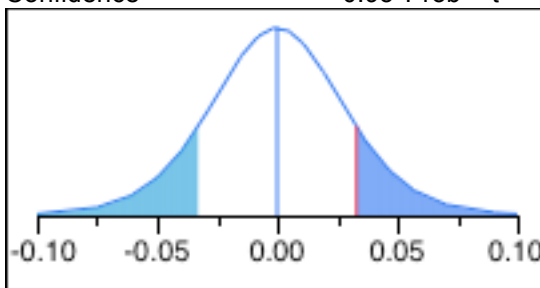
Comparing 80 with 40

Difference	0.111859	t Ratio	4.11101
Std Err Dif	0.027210	DF	11
Upper CL Dif	0.171747	Prob > t	0.0017*
Lower CL Dif	0.051971	Prob > t	0.0009*
Confidence	0.95	Prob < t	0.9991

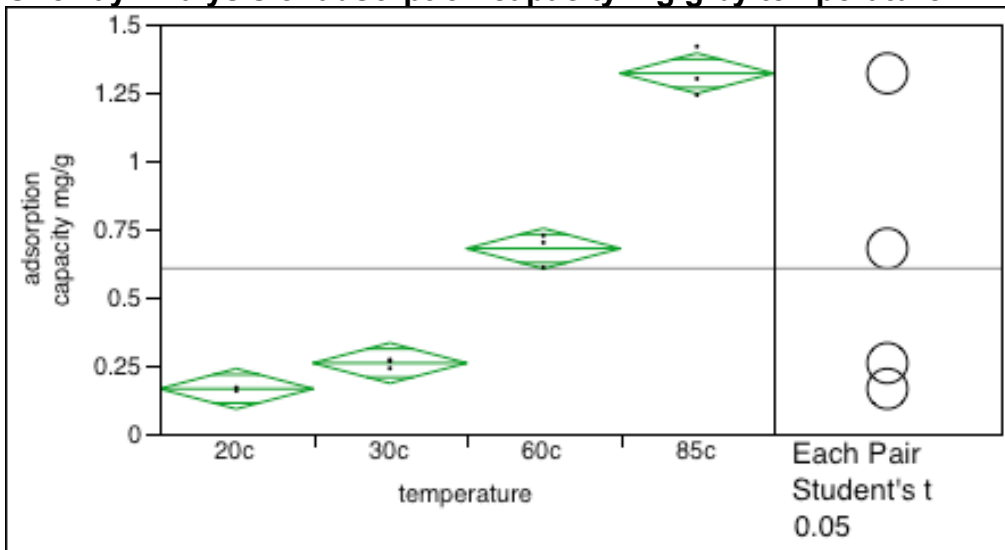


Comparing 80 with 60

Difference	0.03307	t Ratio	1.215221
Std Err Dif	0.02721	DF	11
Upper CL Dif	0.09295	Prob > t	0.2497
Lower CL Dif	-0.02682	Prob > t	0.1249
Confidence	0.95	Prob < t	0.8751



Oneway Analysis of adsorption capacity mg/g by temperature



Oneway Anova Summary of Fit

Rsquare	0.990244
Adj Rsquare	0.986586
Root Mean Square Error	0.055377
Mean of Response	0.605637
Observations (or Sum Wgts)	12

Analysis of Variance

Source	DF	Sum of Squares	Mean Square	F Ratio	Prob > F
temperature	3	2.4901499	0.830050	270.6751	<.0001*
Error	8	0.0245327	0.003067		
C. Total	11	2.5146827			

Means for Oneway Anova

Level	Number	Mean	Std Error	Lower 95%	Upper 95%
20c	3	0.16492	0.03197	0.0912	0.2386
30c	3	0.25906	0.03197	0.1853	0.3328
60c	3	0.67852	0.03197	0.6048	0.7522
85c	3	1.32005	0.03197	1.2463	1.3938

Std Error uses a pooled estimate of error variance

Means Comparisons

Comparisons for each pair using Student's t Confidence Quantile

t	Alpha
2.30600	0.05

LSD Threshold Matrix

Abs(Dif)-LSD	85c	60c	30c	20c
85c	-0.1043	0.5373	0.9567	1.0509
60c	0.5373	-0.1043	0.3152	0.4093
30c	0.9567	0.3152	-0.1043	-0.0101
20c	1.0509	0.4093	-0.0101	-0.1043

Positive values show pairs of means that are significantly different.

Connecting Letters Report

Level	Mean
85c A	1.3200531
60c B	0.6785160
30c C	0.2590637
20c C	0.1649157

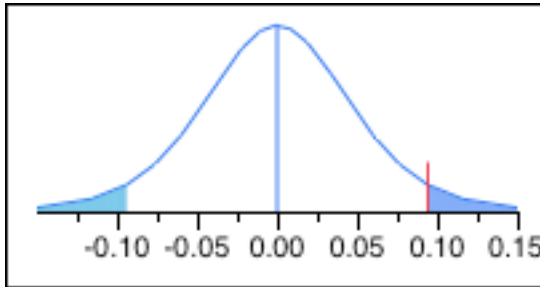
Levels not connected by same letter are significantly different.

Ordered Differences Report

Level	- Level	Difference	Std Err Dif	Lower CL	Upper CL	p-Value
85c	20c	1.155137	0.0452150	1.05087	1.259403	<.0001*
85c	30c	1.060989	0.0452150	0.95672	1.165255	<.0001*
85c	60c	0.641537	0.0452150	0.53727	0.745803	<.0001*
60c	20c	0.513600	0.0452150	0.40933	0.617866	<.0001*
60c	30c	0.419452	0.0452150	0.31519	0.523718	<.0001*
30c	20c	0.094148	0.0452150	-0.01012	0.198414	0.0709

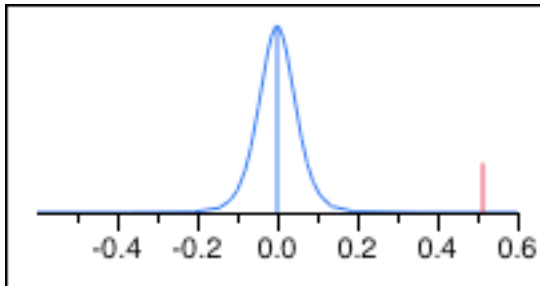
Detailed Comparisons Report Comparing 30c with 20c

Difference	0.09415	t Ratio	2.082229
Std Err Dif	0.04521	DF	8
Upper CL Dif	0.19841	Prob > t	0.0709
Lower CL Dif	-0.01012	Prob > t	0.0354*
Confidence	0.95	Prob < t	0.9646



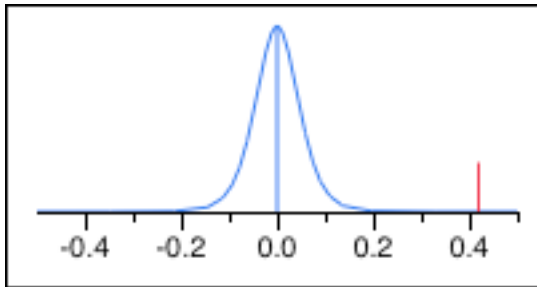
Comparing 60c with 20c

Difference	0.513600	t Ratio	11.35907
Std Err Dif	0.045215	DF	8
Upper CL Dif	0.617866	Prob > t	<.0001*
Lower CL Dif	0.409334	Prob > t	<.0001*
Confidence	0.95	Prob < t	1.0000



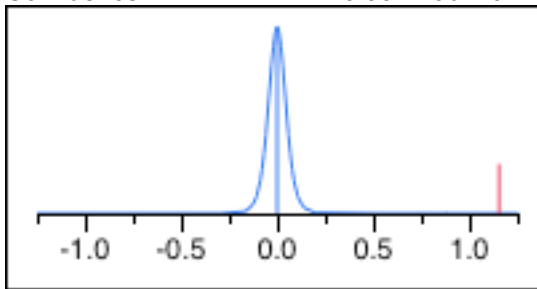
Comparing 60c with 30c

Difference	0.419452	t Ratio	9.276845
Std Err Dif	0.045215	DF	8
Upper CL Dif	0.523718	Prob > t	<.0001*
Lower CL Dif	0.315186	Prob > t	<.0001*
Confidence	0.95	Prob < t	1.0000



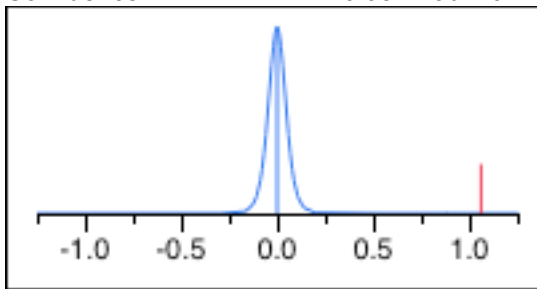
Comparing 85c with 20c

Difference	1.15514	t Ratio	25.54767
Std Err Dif	0.04521	DF	8
Upper CL Dif	1.25940	Prob > t	<.0001*
Lower CL Dif	1.05087	Prob > t	<.0001*
Confidence	0.95	Prob < t	1.0000



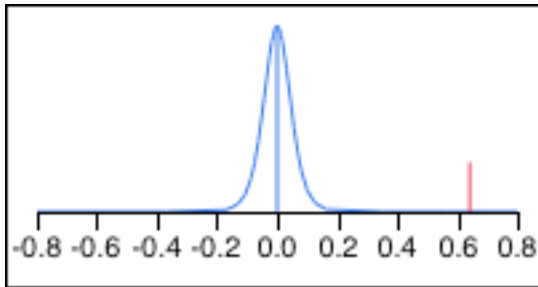
Comparing 85c with 30c

Difference	1.06099	t Ratio	23.46544
Std Err Dif	0.04521	DF	8
Upper CL Dif	1.16526	Prob > t	<.0001*
Lower CL Dif	0.95672	Prob > t	<.0001*
Confidence	0.95	Prob < t	1.0000

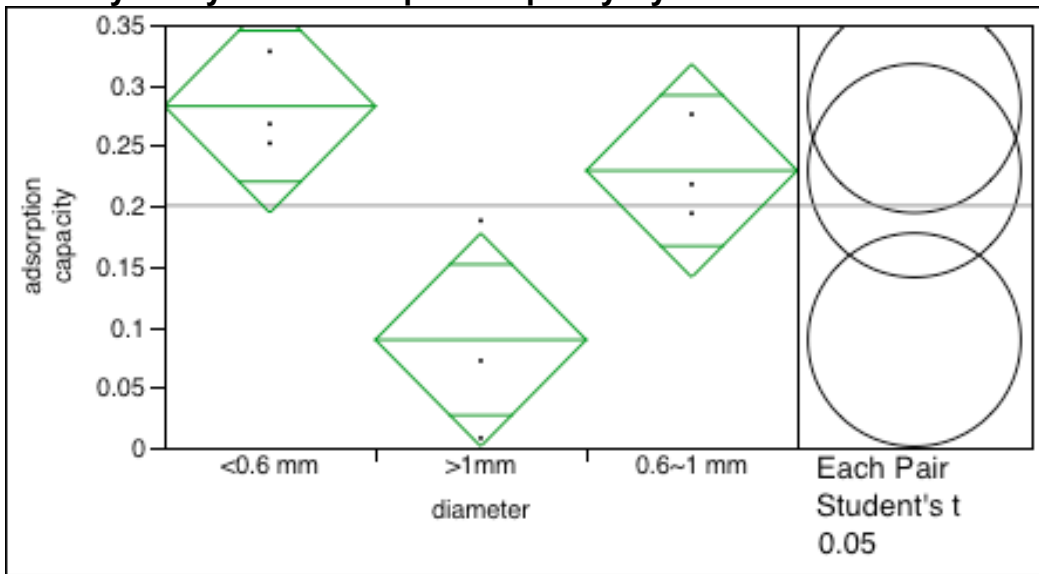


Comparing 85c with 60c

Difference	0.641537	t Ratio	14.1886
Std Err Dif	0.045215	DF	8
Upper CL Dif	0.745803	Prob > t	<.0001*
Lower CL Dif	0.537271	Prob > t	<.0001*
Confidence	0.95	Prob < t	1.0000



Oneway Analysis of adsorption capacity By diameter



**Oneway Anova
Summary of Fit**

Rsquare	0.718687
Adj Rsquare	0.624916
Root Mean Square Error	0.062471
Mean of Response	0.200444
Observations (or Sum Wgts)	9

Analysis of Variance

Source	DF	Sum of Squares	Mean Square	F Ratio	Prob > F
diameter	2	0.05982222	0.029911	7.6643	0.0223*
Error	6	0.02341600	0.003903		
C. Total	8	0.08323822			

Means for Oneway Anova

Level	Number	Mean	Std Error	Lower 95%	Upper 95%
-------	--------	------	-----------	-----------	-----------

Level	Number	Mean	Std Error	Lower 95%	Upper 95%
<0.6 mm	3	0.282667	0.03607	0.19441	0.37092
>1mm	3	0.089333	0.03607	0.00108	0.17759
0.6~1 mm	3	0.229333	0.03607	0.14108	0.31759

Std Error uses a pooled estimate of error variance

Means Comparisons

Comparisons for each pair using Student's t Confidence Quantile

t	Alpha
2.44691	0.05

LSD Threshold Matrix

Abs(Dif)-LSD	<0.6 mm	0.6~1 mm	>1mm
<0.6 mm	-0.12481	-0.07148	0.06852
0.6~1 mm	-0.07148	-0.12481	0.01519
>1mm	0.06852	0.01519	-0.12481

Positive values show pairs of means that are significantly different.

Connecting Letters Report

Level		Mean
<0.6 mm	A	0.28266667
0.6~1 mm	A	0.22933333
>1mm	B	0.08933333

Levels not connected by same letter are significantly different.

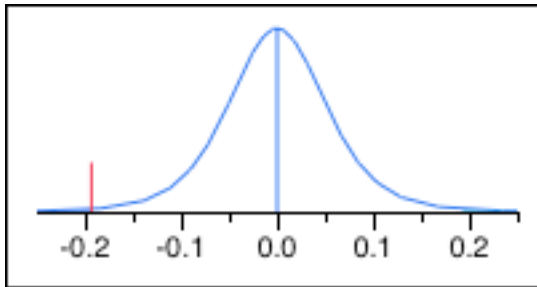
Ordered Differences Report

Level	- Level	Difference	Std Err Dif	Lower CL	Upper CL	p-Value
<0.6 mm	>1mm	0.1933333	0.0510076	0.068522	0.3181445	0.0091*
0.6~1 mm	>1mm	0.1400000	0.0510076	0.015189	0.2648112	0.0335*
<0.6 mm	0.6~1 mm	0.0533333	0.0510076	-0.071478	0.1781445	0.3360

Detailed Comparisons Report

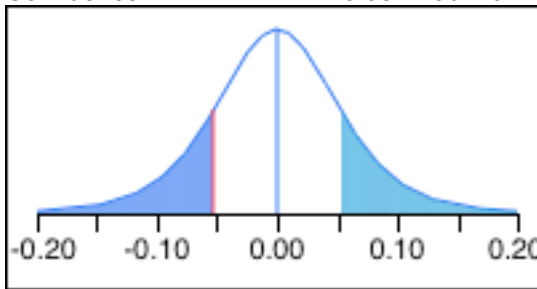
Comparing >1mm with <0.6 mm

Difference	-0.19333	t Ratio	-3.79028
Std Err Dif	0.05101	DF	6
Upper CL Dif	-0.06852	Prob > t	0.0091*
Lower CL Dif	-0.31814	Prob > t	0.9955
Confidence	0.95	Prob < t	0.0045*



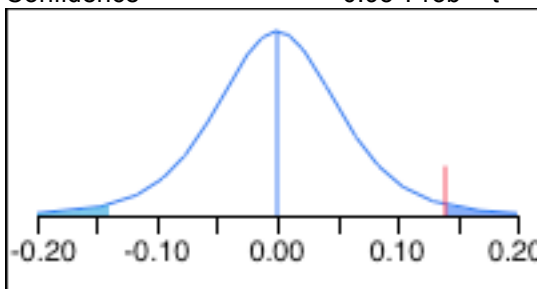
Comparing 0.6~1 mm with <0.6 mm

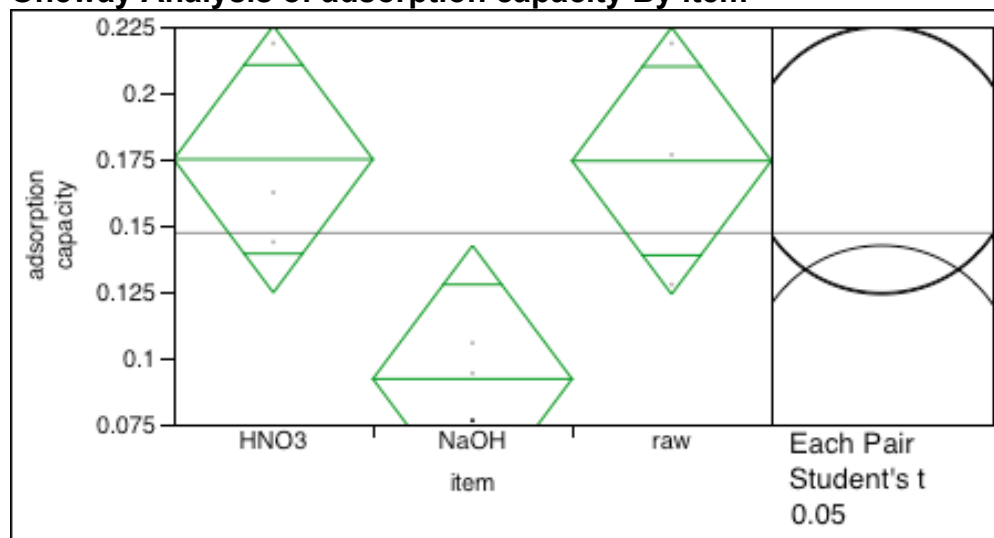
Difference	-0.05333	t Ratio	-1.0456
Std Err Dif	0.05101	DF	6
Upper CL Dif	0.07148	Prob > t	0.3360
Lower CL Dif	-0.17814	Prob > t	0.8320
Confidence	0.95	Prob < t	0.1680



Comparing 0.6~1 mm with >1mm

Difference	0.140000	t Ratio	2.744688
Std Err Dif	0.051008	DF	6
Upper CL Dif	0.264811	Prob > t	0.0335*
Lower CL Dif	0.015189	Prob > t	0.0168*
Confidence	0.95	Prob < t	0.9832



Zinc extract**Oneway Analysis of adsorption capacity By item****Oneway Anova
Summary of Fit**

Rsquare	0.641557
Adj Rsquare	0.522076
Root Mean Square Error	0.035618
Mean of Response	0.147189
Observations (or Sum Wgts)	9

Analysis of Variance

Source	DF	Sum of Squares	Mean Square	F Ratio	Prob > F
item	2	0.01362404	0.006812	5.3695	0.0461*
Error	6	0.00761187	0.001269		
C. Total	8	0.02123591			

Means for Oneway Anova

Level	Number	Mean	Std Error	Lower 95%	Upper 95%
HNO3	3	0.175000	0.02056	0.12468	0.22532
NaOH	3	0.092167	0.02056	0.04185	0.14249
raw	3	0.174400	0.02056	0.12408	0.22472

Std Error uses a pooled estimate of error variance

Means Comparisons**Comparisons for each pair using Student's t
Confidence Quantile**

t Alpha

t	Alpha
2.44691	0.05

LSD Threshold Matrix

Abs(Dif)-LSD	HNO3	raw	NaOH
HNO3	-0.07116	-0.07056	0.01167
raw	-0.07056	-0.07116	0.01107
NaOH	0.01167	0.01107	-0.07116

Positive values show pairs of means that are significantly different.

Connecting Letters Report

Level		Mean
HNO3	A	0.17500000
raw	A	0.17440000
NaOH	B	0.09216667

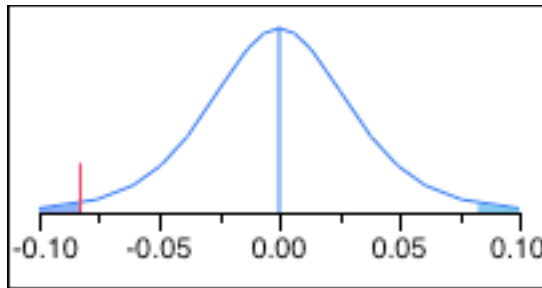
Levels not connected by same letter are significantly different.

Ordered Differences Report

Level	- Level	Difference	Std Err Dif	Lower CL	Upper CL	p-Value
HNO3	NaOH	0.0828333	0.0290820	0.011672	0.1539944	0.0292*
raw	NaOH	0.0822333	0.0290820	0.011072	0.1533944	0.0301*
HNO3	raw	0.0006000	0.0290820	-0.070561	0.0717611	0.9842

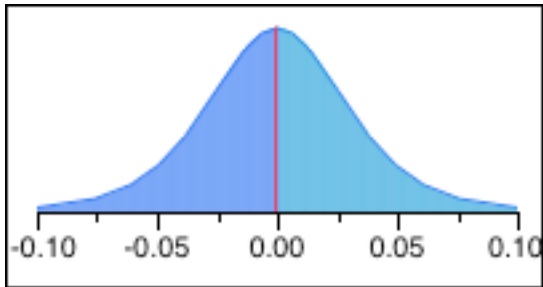
Detailed Comparisons Report Comparing NaOH with HNO3

Difference	-0.08283	t Ratio	-2.84827
Std Err Dif	0.02908	DF	6
Upper CL Dif	-0.01167	Prob > t	0.0292*
Lower CL Dif	-0.15399	Prob > t	0.9854
Confidence	0.95	Prob < t	0.0146*



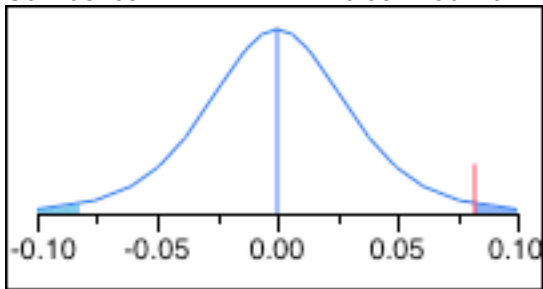
Comparing raw with HNO3

Difference	-0.00060	t Ratio	-0.02063
Std Err Dif	0.02908	DF	6
Upper CL Dif	0.07056	Prob > t	0.9842
Lower CL Dif	-0.07176	Prob > t	0.5079
Confidence	0.95	Prob < t	0.4921



Comparing raw with NaOH

Difference	0.082233	t Ratio	2.827636
Std Err Dif	0.029082	DF	6
Upper CL Dif	0.153394	Prob > t	0.0301*
Lower CL Dif	0.011072	Prob > t	0.0150*
Confidence	0.95	Prob < t	0.9850



ACKNOWLEDGEMENT

I owe my gratitude and respect to a number of people helping me complete during my PhD study. I am indebted to my major professor, Dr. Tim Ellis who has been my guide through my five years study. Thanks to Dr. Eric Evans, who helped me build up the experiment instruments and give me valuable advises on my research. Special thanks are extended to Lei Gong and Shan Li who both encourage me on my final defense. Thanks to James Anderegg, who tested the samples for my research. I also want to thank to Kathy Petersen for the great help of doing university bureaucracy.

Above all, thanks to my parents for the constant encouragement. Finally thanks to the China Scholarship Council, who provided me the opportunity to study abroad.